RHEOLOGY OF
ASSOCIATIVE BIOPOLYMERS

RHEOLOGY OF
ASSOCIATIVE BIOPOLYMERS

PROEFSCHRIFT

ter verkrijging van
de graad van doctor aan de Universiteit Twente,
op gezag van de rector magnificus,
prof.dr. F.A. van Vught,
volgens besluit van het College voor Promoties
in het openbaar te verdedigen
op vrijdag 2 maart 2001 te 16:45 uur.

door

Roland Hendrikus Wilhelm Wientjes

geboren op 5 Augustus 1971
te Enschede

Wetenschap is de titanische poging van het menselijk intellect
zich uit zijn kosmische isolement te verlossen door te begrijpen.
W.F. Hermans

Contents

Chapter 1

Introduction

1.1 General Introduction

Rheology studies the relation between the deformation of materials and the applied forces. This relation is important during the processing and applications of many agricultural and industrial products such as paints, food and cosmetic products. The macroscopic flow properties (like the viscosity) of these products are related to the microscopic properties of the ingredients (like the molecular weight). Understanding this relation for Guar gum solutions is the main goal in this thesis.

One of the ingredients which is often used as a thickener in food and cosmetic products is Guar gum. By adding only a small amount of Guar gum in water a drastic increase in the solution viscosity is caused. Guar gum belongs to the class of Galactomannan biopolymers. These polymers consist of a Mannose backbone partially covered with Galactose side groups.
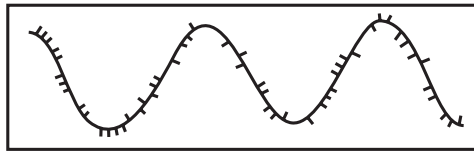
Figure 1.1: Impression of a Guar gum chain

In the case of Guar the mannose/galactose ratio is 1.6 to 1. Other Galactomannans are for example Tara gum, Locust bean gum and Fenugreek. In the case of Locust bean gum, which has a mannose/galactose ratio of 3.9 to 1, it is possible to form a solid gel from the viscous fluid via a freeze-thaw process. With Guar gum solutions, this is not possible. In industry, the above mentioned effects are used to improve the properties of the products. This is mostly done via a trial and error process, since the relation between macroscopic and microscopic properties is not yet understood. By understanding this relation, further improvement of industrial products like ice-creams, salad dressings and dairy products would be possible. Therefore, Guar gum was investigated intensively in order to find out more about this relation. The results of this investigation are presented in this thesis. In order to understand the relation between macroscopic and microscopic properties, these results are compared with microrheological model predictions. From this comparison it follows that no quantitative model predicts the observed rheological behavior. Besides these quantitative models there are also undeveloped model concepts that might provide insight in the rheological behavior of Guar gum solutions. As a part of this work, one of these concepts (a transient network model with chain connectivity) was developed in order to check the capabilities of this concept in describing the relation between macroscopic rheological and microscopic properties of Guar gum.

1.2 Previous work

Although investigations on Galactomannans can be dated back to the sixties, the research that forms the basis for this work started in the later seventies. In this section an overview of this literature is given. This overview is split up into a number of different areas:

'Hyperentanglements' in Guar gum solutions
Semi-rigidity of Guar chains
Galactose distribution along Guar chains
Microrheological models
Enzymatic modifications
Gel formation of Locust bean gum solutions
Other experimental work on Guar gum

The first three areas deal with the polymer properties of Guar gum. In subsection four, some previous work is presented with was done in order to relate the macroscopic behavior to a mesoscopic model concept. Subsection number five contains the work that is already done on enzymatic modifications. Since it is possible to change the mannose/galactose ratio via enzymatic modifications to the ratio of Locust bean gum, a subsection with previous work on Locust bean gum is also given.

An overview of the important theoretical models is not given here, since in chapter 4, the relevant models will be already discussed in more detail.

1.2.1   'Hyperentanglements' in Guar gum solutions

Doublier and Launay[2] started in 1976 to investigate the rheological properties of Guar gum solutions and noticed a strong concentration dependence. In 1981 they compared Locust bean gum with Guar gum solutions[3]. From the fact that the zero shear viscosity depends mainly on the reduced concentration $c[\eta]$ and not on the mannose/galactose ratio, they suggested that entanglements play a dominant role in concentrated solutions. Remaining differences in the relaxation time of the Ree-Eyring model fits between Guar and locust bean gum solutions were attributed to the difference in the mean branching degree.

Morris *et al.*[4] continued this investigation of the rheological properties and they found that Locust bean gum and Guar gum did not follow the empirical rule $c^*\eta = 4$. Also the Cox-Merz rule did not hold. They pointed out that more specific intermolecular associations ('hyperentanglements') might cause these deviations. Also, the extremely strong dependence of the specific viscosity upon polymer concentration (investigated by Robinson *et al.*[5]) was attributed to the existence of specific polymer-polymer interactions.

Still, Richardson and Ross-Murphy[9] concluded from non linear rheological mea-
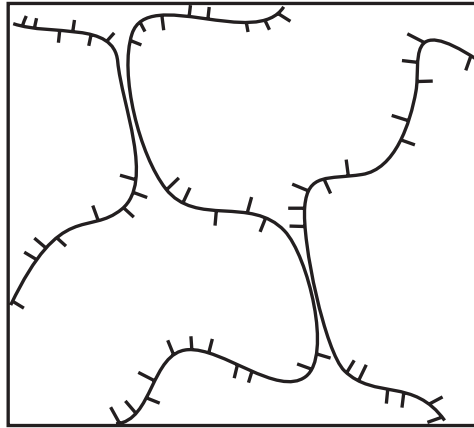
Figure 1.2: Impression of specific polymer-polymer interactions. The larger Galactose free backbone parts are believed to form hydrophobic bonds with each other.

surements that Guar gum solutions behaved as ideal reptating polymers[10,11]. Ross-Murphy even repeated this conclusion in an overview article in 1995[20].

New evidence for 'hyperentanglements' was presented in 1995 by Goycoolea *et al.*[21]. They compared the difference in viscosity, caused by a difference in pH, in concentrated and diluted solutions. From the fact that the relative difference in concentrated solutions was much higher, they concluded that 'hyperentanglements' exist in Guar gum solutions. These 'hyperentanglements' or specific polymer-polymer interactions are then in fact physical bonds between the larger Galactose free hydrophobic backbone parts. These parts will attract to each other, thereby forming physical bonds. Recently, Gittings *et al.* presented even more evidence for physical bonds between Guar gum polymer chains. They studied the structure of Guar gum in water via ultra small angle light scattering[23] and found the presence of large aggregates of 10 μm.

1.2.2   Semi rigidity of Guar chains

A detailed study about the influence of the solvent on the specific viscosity versus reduced concentration curve was presented by Launay *et al.*[26]. They reported three different concentration dependence regimes (two critical concentrations). Richardson *et al.*[27] concluded from an analous study where also three concentration regimes were found, that Galactomannans are semi-rigid polymers.

1.2.3   Galactose distribution along Guar chains

McCleary[1] analyzed the fine structure of Guar gum. Using the results of chromatography experiments of different enzymatically hydrolyzed modified Guar gums, Mc-

Cleary found first indications for a non random Galactose distribution. Also he proposed that long sections of unsubstituted Mannose groups are required for strong interactions of Galactomannan polymers with Xanthan gum. McCleary *et al.*[6] continued to investigate these interactions and proved that the interaction of Galactomannan samples with Xanthan increased as the D-Galactose content decreased. In 1985, McCleary *et al.*[7] published new results about the fine structure of Guar gum. By comparing the amounts of different oligosaccharides released on hydrolysis of the polymer with predictions from several computer models, they showed that the Galactose sidegroup distribution in Guar seed indeed is non-regular. They found indications that the Galactose side groups are arranged mainly in pairs and triplets. In 1986, evidence was published[8] for the fact that the Galactose substitution pattern effects the interaction properties of Galactomannans.

1.2.4 Microrheological models

In 1994, Kokini and Surmay[14] reported a study of the first normal stress difference. From the concentration dependence of $\sigma_{11} - \sigma_{22}$ they concluded that interchain relaxation processes play a dominant role in Guar gum solutions. After investigating the linear rheological behavior of Guar gum, Kokini[15] compared model predictions of four different models (the Rouse model[16], the Zimm model[17], the Bird-Carreau model[18] and the reptation model[10,11]). His conclusion was that the Bird-Carreau model was able to predict the linear rheological behavior (storage and loss modulus as a function of frequency) of concentrated Guar gum solutions. However, Kokini based his conclusion upon the data of one Guar gum solution, so no concentration and molecular weight dependencies were taken into account.

1.2.5 Enzymatic modifications

A new branch in the field of Guar gum research was the development of an enzymatic modification process which was used for changing the interaction properties[12]. This modification process was used to investigate the yield behavior of Xanthan and enzyme modified Galactomannans[19]. It turned out, that this yield behavior depends strongly on the Galactose content.
Besides this, Tayal *et al.*[28] reported a study on a different modification: The enzymatic degradation of Guar gum (enzymatically lowering of the molecular weight). They found that the zero shear viscosity was sensitive (a decrease of several orders of magnitude) to the extent of degradation.

1.2.6   Gel formation of locust bean gum solutions

Work that does not deal directly with the microstructure of Guar, is the studies of the gelation behavior of Locust bean gum. However since it is possible to modify the mannose/galactose ratio of Guar gum to the ratio of Locust bean gum, this work is also related to our work. Tanaka *et al.*[24] reported the gel formation of Locust bean gum via a freezing-thawing process. Richardson and Norton[25] studied this gelation behavior in more detail as a function of Sucrose concentration and temperature. They found a maximum in gelation rate close to -5 ^{o}C and a large temperature hysteresis. According to the authors this indicates that the process of cross-linking of the polymers (which causes the gel formation) is controlled by nucleation and growth processes instead of reversible pairwise cross-linking. Recently, another paper that deals with Galactomannan gelation was presented[30]. Richardson *et al.* reported that the gel properties of locust bean gum gels depended on the Galactose content, gelling temperature and concentration. Also a large temperature hysteresis between gelation temperature and gel melting was observed which was interpreted as an indication that the gelation mechanism is under kinetic control. The presented gels melted at a temperature of 44 ^{o}C.

1.2.7   Other experimental work on Guar gum

Besides from the work mentioned above, some research was done in related areas.
For example, Carnali[13] published in 1992, a paper in which the gelation of Guar gum with borate is described. This was not of much interest for the in this thesis presented research, but it is an important fact to know that Guar gum gels with borate.
Work from a completely different field is the x-ray diffraction study, done by Kapoor *et al.*[22]. Their results indicate that Galactomannans of low and high Galactose content have a related crystal structure.
In 1999, a study was done on the degradation of Guar gum due to high temperature processing[29]. It was found that degradation of Guar gum occurred, caused by high temperatures of up to 120 ^{o}C. This degradation also caused a decrease in viscosity.

1.3   Outline of the thesis

From the overview, it becomes clear that, although Guar gum was investigated intensively, the relation between rheological macroscopic and microscopic properties is still not clear. Also, a systematic study on the influence of the macroscopic variables on the linear rheological behavior has not been performed yet. Further on, microrheological modeling of associative polymers is still an under developed area, although it has been receiving increased interest in the last few years. Also, only few studies

have been aimed at analyzing experimental rheological data with such models. Especially, the field of models based on entanglements and physical bonds is still open.

Since the previous work shows that both entanglements and physical bonds ('hyperentanglements') might play a role in the rheology of Guar, we developed a new model in which the relaxation processes are related directly to the breakup of physical bonds but influenced indirectly by entanglements. They cause the chain connectivity effect: Each chain segment that is located directly or via other segments between two physical bonds carries stress due to the presence of entanglements. This model is presented in chapter two.

In chapter three the model assumption that chain segments carry stress if they are located between two physical bonds was changed to the assumption that chain segments carry only stress if they are located between two physical bonds and never have lost their stress in the past. The difference of these two assumptions can be understood by thinking of a G(t) experiment. If a step strain is performed, the active segments (segments that are located directly or via other segments between two physical bonds) start to carry stress. Due to the breakup of bonds these segments will become inactive (not located between two physical bonds) and therefore they will loose their stress. But due to the forming of bonds some inactive segments will also become active. In the first of the two assumptions, these segments will not only become active, but they will also carry new stress. In the second assumption, they only become active and remain free of stress.

Besides this difference in assumptions, also the model was extended so that different types of physical bonds (strong and weak ones) can be taken into account.

In chapter four a systematic study is presented on the rheological macroscopic properties of Guar gum as a function of several different variables like molecular weight, temperature and polymer concentration. Also a comparison of this behavior with predictions from different microrheological models is made. The best overall predictions were obtained with the in chapter three presented model.

In order to obtain more evidence, three important model assumptions (the occurrence of weak bonds, strong bonds and thermodynamic equilibrium) were investigated in chapter five by changing the solvent quality and the mannose/galactose ratio via enzymatic modifications. The results of this study show that the assumption of thermodynamic equilibrium and the assumption of having weak bonds do not hold. Therefore no developed model is able to describe the rheological behavior of Guar gum solutions correctly. However strong indications were found that the two observed relaxation mechanisms are caused by hydrophobic bonds between polymer chains (that cause large structures) and by a diffusion process which is not reptation.

1.4   References

[1]   McCleary B.V.; *Carbohydrate Research* **1979**, 71, 205-230.

[2]   Doublier J.L., Launay B.; *Proceedings of the VIIth international congress on rheology*, **1976**, 532-533.

[3]   Doublier J.L., Launay B.; *Journal of Texture Studies*, **1981**, 12, 151-172.

[4]   Morris E.R., Cutler A.N., Ross-Murphy S.B., Rees D.A., Price J.; *Carbohydr. Polym.*, **1981**, 1, 5-21.

[5]   Robinson G., Ross-Murphy S.B., Morris E.R., *Carbohydr. Res.*, **1982**, 107, 17-32.

[6]   McCleary B.V., Dea I.C.M., Windust J., Cooke D.; *Carbohydr. Polym.*, **1984**, 4, 253-270.

[7]   McCleary B.V., Clark A.H., Dea I.C.M., Rees D.A.; *Carbohydr. Res.*, **1985**, 139, 237-260.

[8]   Dea I.C.M., Clark A.H., McCleary B.V.; *Carbohydr. Res.*, **1986**, 147, 275-294.

[9]   Richardson R.K., Ross-Murphy S.B.; *Int. J. Biol. Macromol.*, **1987**, 9, 250-256.

[10]   de Gennes P.G; *J. Chem. Phys.*, **1971**, 55, 572.

[11]   Doi M., Edwards S.F.; *J. Chem. Soc. Faraday Trans. II*, **1978**, 74, 1789, 1802, 1818.

[12]   Bulpin P.V., Gidley M.J., Jeffcoat R., Underwood D.R.; *Carbohydr. Polym.*, **1990**, 12, 155-168.

[13]   Carnali J.O.; *Rheol Acta*, **1992**, 31, 399-412.

[14]   Kokini J.L., Surmay K.; *Carbohydr. Polym.*, **1994**, 23, 27-33.

[15]   Kokini J.L.; *Carbohydr. Polym.*, **1994**, 25, 319-329.

[16]   Rouse P.E.; *J. Chem. Phys.*, **1953**, 21, 1272.

[17]   Zimm B.H.; *J. Chem. Phys.*, **1956**, 24, 269.

[18]   Leppard W.R.; *Viscoelasticity: strress measurements and constitutive theory*, PhD Thesis, **1975**, University of Utah.

[19]   Luyten H., Kloek W., van Vliet T.; *Food Hydrocolloids*, **1994**, 8, 431-440.

[20]   Ross-Murphy S.B.; *J. Rheol.*, **1995**, 39, 1451-1463.

[21]   Goycoolea F.M., Morris E.R., Gidley M.J.; *Carbohydr. Polym.*, **1995**, 27, 69-71.

[22]   Kapoor V.P., Chanzy H., Taravel F.R.; *Carbohydr. Polym.*, **1995**, 27, 229-233.

[23]   Gittings M.R., Cipelletti L., Trappe V., Weitz D.A., In M., Marques C.; *J. Phys. Chem.*, **2000**, 104, 4381-4386.

[24]   Tanaka R., Hatakeyama T., Hatakeyama H.; *Polymer Int.*, **1998**, 45, 118-126.

[25]   Richardson P.H., Norton I.T.; *Macromolecules*, **1998**, 31, 1575-1583.

[26]   Launay B., Cuvelier G., Martinez-Reyes S.; *Carbohydr. Polym.*, **1997**, 34, 385-395.

[27]   Richardson P.H., Willmer J., Foster T.J.; *Food Hydrocolloids*, **1998**, 12, 339-348.

[28]   Tayal A., Kelly R.M., Khan S.A.; *Macromolecules*, **1999**, 32, 294-300.

[29]   Kök M.S., Hill S.E., Mitchell J.R.; *Food Hydrocolloids*, **1999**, 13, 535-542.

[30]   Richardson P.H., Clark A.H., Russell A.L., Aymard P., Norton I.T., *Macromolecules*, **1999**, 32, 1519-1527.

Chapter 2

A New Transient Network Model for Associative Polymer Networks

2.1 Synopsis

A new model for the linear viscoelastic behaviour of polymer networks is developed. In this model the polymer system is described as a network of spring segments connected via sticky points (as in the Lodge model). An important extension (with respect to previous models) is that chain connectivity is taken into account. All segments that are located in between connected stickers are supposed to carry stress. The attachment and detachment of stickers is described with kinetic equations in which activation energies play a role. Simultaneous transitions involving groups of stickers are allowed.

The model shows a strong dependence upon the number of segments per chain. Broad relaxation spectra can be obtained. The storage modulus can have more then one plateau corresponding with the fact that stress relaxation may need the breakup of several bonds.

2.2   Introduction

Several models have been developed so far to describe the rheological behaviour of polymer melts and solutions. We can distinguish between three model types. First there are the bead spring models like the Rouse model[18]. Secondly we have the reptation models in which the polymer chain moves back and forth along a tube which represents the constraints imposed by the other polymers[6].

The third class is formed by the transient network models, first proposed by Green and Tobolsky[11], Lodge[14] and Yamamoto[25]. In these models a polymer system is described as a network of spring segments in which segments are annihilated and created during flow. The stress is the sum of the contributions of all network segments.

Many improvements have been made later on the transient network model to describe non linear flow phenomena[1,16,17]. More recently a lot of work was done considering linear and non linear visco-elasticity of physically cross-linked networks[20−23]. Simulations have also become an important tool for the investigation of transient networks[3,5,8,12].

Despite their success to describe the rheology of particular systems, there is still much to be desired. No analytical models have so far been able to describe broad relaxation spectra (without using the *ad-hoc* concept of a 'segment complexity'[14]) and the same holds for the molecular weight dependence. A recent approach to deal with these limitations was given by González[9,10] and Leibler *et al.*[13] who modeled stress relaxation, combining transient network and reptation elements.

In the present chapter, we develop a new transient network model for linear visco-elasticity, following a different approach in the sense that several relaxations are all explained from a single origin, being intermolecular bonding. The polymer system is described as a network of polymer chains, consisting of spring segments connected via sticky points. The connectivity of the whole polymer chain is taken into account by assuming many sticky points on the polymer chain (at which the chain can be connected to the network). As a result, the model predicts a chain length (molecular weight) dependence and broad relaxation spectra. The model may also be a good starting point for developing a transient network model for the non linear behaviour. Transient networks have also been the subject of a number of recent experimental studies[2,7,15]. A first confrontation of our new model with experiments from literature will be made in section 2.6.5.

The outline of this chapter is as follows. In section 2.3 we present the model concept and in section 2.4 we derive the constitutive equation. Comparison with the Lodge model was made in section 2.5. The model results are presented and discussed in section 2.6. In section 2.7 the assumptions made, and the scope of the model are treated in more depth. Section 2.8 contains the conclusions of this chapter.

2.3   General Model Concept

It is assumed that a polymer chain can be modeled as a series of segments permanently linked to each other in a linear (i.e. unbranched) configuration. At the joints, whereabout free rotation is possible, there are sticky points via which the polymer chain can be connected to the network. Here, the network is defined as a collection of chains connected to each other via stickers, and which can resist stress via a deformation of its segments.

We focus upon the state of a whole chain instead of individual segments. This is similar to the reptation model[6]. In the chain each sticky point can exist in two states: either connected or free. The state of a chain is defined by the states of all its sticky points. Transitions between the states of the chain are possible via various processes involving one or more sticky points.

One should notice here that we distinguish between the state and the configuration of a chain. The state of a chain designates the state of its sticky points. The configuration of the chain is given by the orientations and magnitudes of its segment-vectors.

We consider in our model two types of segments: Segments belonging to the network and segments not belonging to it. We assume that the network will deform affinely with the macroscopic flow. Because of this deformation, segments belonging to the network will carry stress. Therefore they are called *active* segments. Segments which are part of either a loose end or a free chain will not carry stress. They are called *inactive* segments. In figure 2.1 active and inactive segments are shown. Note that for *active* segments one or both segment ends may also be *indirectly* connected to the network via other segments of the same chain.
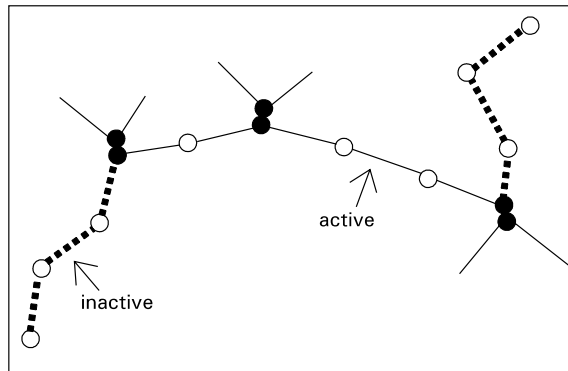
Figure 2.1: A polymer with active and inactive segments.

When transitions take place, chain-segments may change from active to inactive and vice versa. If a segment becomes inactive, the stress in that segment is lost. As in the original Lodge model[14] the distribution function for the parts of the chain consisting

of inactive segments is assumed to be the Gaussian equilibrium distribution function. For the active segments we assume confinement in a tube, similar to the reptation model[6], where the tube represents the topological constraints for a strand imposed by the other chains in a network. This idea is shown in figure 2.2.
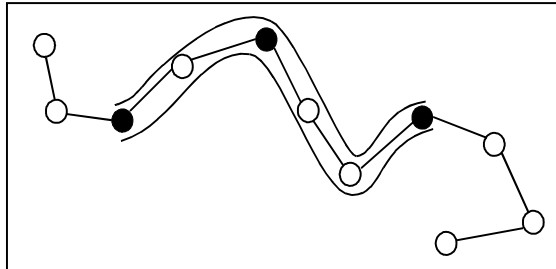
Figure 2.2: A polymer chain with the active segments confined in a tube representing the topological constraints.

Note that the tube concept is only used as a constraint on the sticker positions; we do not consider diffusive motion along the tube. In the present paper we restrict ourselves to the linear viscoelastic regime.

2.4   The constitutive equation

We consider an incompressible fluid with a concentration of c macromolecules per unit volume. It is assumed that every chain contains the same number of segments and all segments have identical properties. With N sticky points per chain, the number of segments is $N-1$.

To define the state of a chain we introduce the state vector s. This is a row matrix of N elements designating for each sticker whether it is connected ($s = 1$) or not ($s_i = 0$). When a sticker is connected to the network we have a so called *bond*. Stickers that are not connected will be called *free*. So the state of a segment is either *active* or *inactive* whereas the state of a sticker is either *free* or *connected*.

We assign the vector $\mathbf{q}_i$ to the segment from sticky point i to sticky point $i+1$. We define $\psi_s(\mathbf{q}_1,...,\mathbf{q}_{N-1},t)$ as the normalized configuration-space distribution-function of the chains that are in state s. We also define a distribution function Ψ_s, normalized to N_s, as: $N_s\psi_s$ with N_s the total number of chains in state s per unit volume.

Since only the *active* segments deform affinely, they contribute to the stress and the stress tensor $\mathbf{T}$ can be written as:

$$\mathbf{T} = \sum_s \sum_{i \varepsilon A_s} N_s \kappa < \mathbf{q}_i \mathbf{q}_i >_s \equiv \sum_s \sum_{i \varepsilon A_s} \mathbf{T}_{si} \tag{2.1}$$

where A_s is the set of the indices (i) designating the active segments $\mathbf{q}_i$ of chains in state s. Here κ is the spring constant of the segments and the brackets denote an averaging with respect to the distribution function ψ_s:

$$< \mathbf{q}_i \mathbf{q}_i >_s = \int \mathbf{q}_i \mathbf{q}_i \psi_s(\mathbf{q}_i, t) d^3 \mathbf{q}_i \tag{2.2}$$

To obtain an expression for the second moment $< \mathbf{q}_i \mathbf{q}_i >_s$ we start with the balance equations that govern the time dependence of the distribution functions. For chains in state s these are of the usual form of equations of continuity for the distribution function Ψ_s in configuration space, with a convection term describing the motion, and creation and annihilation terms describing the transitions between chain states:

$$\frac{\partial \Psi_s}{\partial t} = \sum_{k=1}^{N-1} \frac{\partial}{\partial \mathbf{q}_k} \cdot \Psi_s \dot{\mathbf{q}}_k - \sum_{s \neq s'} f_{s,s'} \Psi_s + \sum_{s' \neq s} f_{s',s} \Psi_{s'} \tag{2.3}$$

In equation (2.3), the second term on the right-hand side represents the annihilation of chains in state s to all other possible states noted as s' with $f_{s,s'}$ the corresponding transition rate-constant. The third term is the creation rate of chains in state s from all other possible states s'. Since we restrict to linear viscoelastic behaviour, we assume that all $f_{s,s'}$ are independent of $\mathbf{q}_i$.

The configuration-space distribution function for the parts of the chain consisting of *inactive* segments is assumed to be the Gaussian equilibrium distribution function. Because of the tube-constraint no change in configuration takes place during the state transition unless active segments become inactive. So $< \mathbf{q}_i \mathbf{q}_i >_s$ is taken equal to $< \mathbf{q}_i \mathbf{q}_i >_{s'}$ unless active segments become inactive. To obtain an equation for the second moment $< \mathbf{q}_i \mathbf{q}_i >_s$ we multiply equation (2.3) by $\mathbf{q}_i \mathbf{q}_j$ and integrate over configuration space. This leads to:

$$\int \frac{\partial \Psi_s}{\partial t} \mathbf{q}_i \mathbf{q}_j d^3 \mathbf{q}_i = \int \sum_k \frac{\partial}{\partial \mathbf{q}_k} \cdot \Psi_s \dot{\mathbf{q}}_k \mathbf{q}_i \mathbf{q}_j d^3 \mathbf{q}_i \tag{2.4}$$

$$- \int \sum_{s \neq s'} f_{s,s'} \Psi_s \mathbf{q}_i \mathbf{q}_j d^3 \mathbf{q}_i + \int \sum_{s' \neq s} f_{s',s} \Psi_{s'} \mathbf{q}_i \mathbf{q}_j d^3 \mathbf{q}_i$$

As in the Lodge model we make the assumption that the active segments deform affinely with the macroscopic flow described by $\mathbf{L}$, the macroscopic velocity gradient tensor. So:

$$\dot{\mathbf{q}}_i = \mathbf{L} \cdot \mathbf{q}_i \tag{2.5}$$

Substituting this in the previous equation we obtain the equation for the second moment of the distribution function for segment i of a chain in state s:

$$\frac{\delta}{\delta t} N_s < \mathbf{q}_i \mathbf{q}_i >_s = - \sum_{s \neq s'} f_{s,s'} N_s < \mathbf{q}_i \mathbf{q}_i >_s + \sum_{s' \neq s} f_{s',s} N_{s'} < \mathbf{q}_i \mathbf{q}_i >_{s'} \tag{2.6}$$

where $\frac{\delta}{\delta t}$ is the so-called upper convected derivative which is defined as:

$$\frac{\delta}{\delta t}\mathbf{A} \equiv \frac{d}{dt}\mathbf{A} - \mathbf{L} \cdot \mathbf{A} - \mathbf{A} \cdot \mathbf{L}^T \tag{2.7}$$

To obtain an expression for the stress tensor we also need an expression for the number of chains per unit volume in state s, N_s. For this purpose we use the kinetic equations obtained by integrating equation (2.3) over all configurations:

$$\frac{dN_s}{dt} = - \sum_{s \neq s'} f_{s,s'} N_s + \sum_{s' \neq s} f_{s',s} N_{s'} \tag{2.8}$$

An Arrhenius equation is assumed to relate the transition rate constant $f_{s,s'}$ between two chain-states to the activation energy $E_{s,s'}$ needed for the transition and the temperature T:

$$f_{s,s'} = \alpha \cdot exp(\frac{-E_{s,s'}}{kT}) \tag{2.9}$$

Here α^{-1} is the characteristic time-scale of the process when the activation energy becomes zero and k is the Boltzmann constant.

The energy needed for a transition of a chain state is related to the energies, needed for bonds to be broken or formed. For single bonds, we define these activation energies to be E_b and E_f (see figure 2.3).
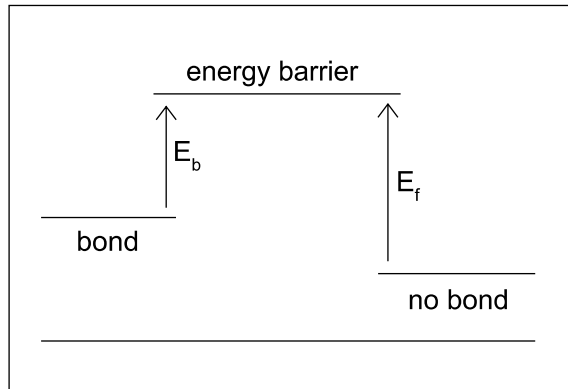

Figure 2.3: The activation energies that must be overcome for one bond (one sticky point).

By assuming that the sticky points behave independent of each other, the activation energy of a chain-state transition equals the summation of the energies needed for the formation and breakup of the single bonds:

$$E_{s,s'} = \sum_{i=1}^{N} E_{s_i,s_i'} \tag{2.10}$$

with:

$$E_{1,1} = 0, \quad E_{1,0} = E_b, \quad E_{0,1} = E_f \quad \text{and} \quad E_{0,0} = 0 \tag{2.11}$$

Using the equations (2.8) and (2.9) we obtain the following set of differential equations:

$$\frac{dN_s}{dt} = -\sum_{s \neq s'} \alpha \cdot exp(\frac{-E_{s,s'}}{kT})N_s + \sum_{s' \neq s} \alpha \cdot exp(\frac{-E_{s',s}}{kT})N_{s'} \tag{2.12}$$

Solving this set of equations leads to the following steady state solution:

$$N_s = \left(\frac{exp(-E_f)}{exp(-E_f) + exp(-E_b)}\right)^{n_s} \cdot \left(\frac{exp(-E_b)}{exp(-E_f) + exp(-E_b)}\right)^{N-n_s} \cdot c \tag{2.13}$$

with n_s the number of connected sticky points for the chains in state s:

$$n_s = \sum_{i=1}^{N} s_i \tag{2.14}$$

This solution can also be obtained by using statistics (and is only valid for the linear viscoelastic regime since $f_{s,s'}$ was taken independent of $\mathbf{q}_i$). We recall here that s_i is element i of the state vector s.

Returning to the calculation of the stress tensor, we can now make equation (2.6) explicit by substituting equation (2.9-2.11) and (2.13). The resulting expressions contain many summations but they are just a set of uncoupled first order differential equations as we will explain now.

Since we assumed that the distribution function for a part of the chain consisting of inactive segments equals the Gaussian equilibrium distribution function, the second moment for these inactive segments is given by $\frac{kT}{\kappa}\mathbf{1}$. This means that $< \mathbf{q}_i\mathbf{q}_i >_{s'} = \frac{kT}{\kappa}\mathbf{1}$ when $\mathbf{q}_i$ in state s' is an inactive segment.

On the other hand, since we assume that the chain-part belonging to the network is enclosed in a tube and we neglect the stress relaxation due to movement relative to the tube, $< \mathbf{q}_i\mathbf{q}_i >_{s'}$ can be set equal to $< \mathbf{q}_i\mathbf{q}_i >_s$ when $\mathbf{q}_i$ in state s' is an active segment. Summarizing, $< \mathbf{q}_i\mathbf{q}_i >_{s'}$ is either set equal to $< \mathbf{q}_i\mathbf{q}_i >_s$ or set equal to $\frac{kT}{\kappa}\mathbf{1}$, depending on the state of segment i in chain state s' and therefore the differential equations are uncoupled. Using this, the summations given in equation (2.6) can be simplified because N_s and $f_{s,s'}$ are constants. Therefore the equations for the second moment for segment i in state s become of the form:

$$\frac{\delta}{\delta t} < \mathbf{q}_i\mathbf{q}_i >_s = -A_{si} \cdot < \mathbf{q}_i\mathbf{q}_i >_s + B_{si}\mathbf{1} \tag{2.15}$$

with A_{si} and B_{si} depending only on the state of the chain s, the number of the segments i, the energies E_f and E_b, the temperature T, the chain concentration c, the prefactor α and the spring constant κ. This type of equations can be easily solved for $< \mathbf{q}\mathbf{q}_i >_s$.

When we multiply equation (2.15) by $N_s\kappa$ and we add to $\mathbf{T}_{si}$ (see for the definition equation (2.1)) an isotropic stress of $\frac{B_{si}}{A_{si}}N_s\kappa\mathbf{1}$, equation (2.15) can be rearranged to:

$$\frac{1}{A_{si}}\dot{\mathbf{T}}_{si} + \mathbf{T}_{si} = \frac{B_{si}}{A_{si}}N_s\kappa 2\mathbf{D} \qquad (2.16)$$

Here we used that $\mathbf{D} = \frac{1}{2}\frac{\delta}{\delta t}\mathbf{1}$ with $\mathbf{D}$ the rate-of-strain tensor and we linearized the equation. This is the equation corresponding to the Maxwell model and from which the moduli can be calculated[4]. From equation (2.1) it can be seen that the stress tensor is a summation over $\mathbf{T}_{si}$, so this model leads us to a summation of Maxwell elements. The problem is in all the summations. We have to solve equation (2.16) for each segment for each state which means that we have to solve $(N-1)\cdot 2^N$ equations. The two summations within each equation are summations over $2^N - 1$ terms so we have to determine $2\cdot(N-1)\cdot 2^N \cdot (2^N - 1)$ constants. Therefore it is not possible to give an explicit expression for the stress tensor. For small N, however, it is possible to derive and solve all the equations of $< \mathbf{q}_i\mathbf{q}_i >_s$.

2.5   Comparison to the Lodge model

We will now show that our model for the case of one segment per chain can be reduced to the Lodge equation. In the Lodge model[14] chains are not considered explicitly and only segments are distinguished. This corresponds to our model with chains consisting of one segment and two stickers. Segments can occur in four states: one of them active and the other three inactive. The state vector of the active segments is 11 and the state vectors of the free segments are 10, 01 and 00. The stress tensor, given by equation (2.1) then reduces to:

$$\mathbf{T} = N_{11}\kappa < \mathbf{q}_1\mathbf{q}_1 >_{11} \qquad (2.17)$$

When we define h as $(f_{11,10} + f_{11,01} + f_{11,00})$ and gN_0 as $(f_{10,11}N_{10} + f_{01,11}N_{01} + f_{00,11}N_{00})$ and use that the distribution functions for the inactive segments are the same we can write equation (2.6) as the relevant equation of the Lodge model:

$$\frac{\delta}{\delta t}N_1 < \mathbf{q}_1\mathbf{q}_1 >_{11} = -hN_1 < \mathbf{q}_1\mathbf{q}_1 >_{11} + gN_0 < \mathbf{q}_0\mathbf{q}_0 > \qquad (2.18)$$

Also the kinetic equation for the active segments, given by equation (2.8), becomes the kinetic equation of the Lodge model:

$$\frac{d}{dt}N_1 = -hN_1 + gN_0 \qquad (2.19)$$

2.6   Results

For small N it is still tractable to derive all the equations for the second moment of the distribution function for a segment q_i in state s and hence calculate the dynamic moduli. The largest number of sticky points per chain used was 8. This number was used in all calculations unless stated otherwise. To explore the capabilities of the model we have varied the activation energies, the temperature and the number of sticky points and calculated the dynamic moduli for a very broad frequency range. The moduli G' and G'' are expressed in units of kT and the frequency f is normalized to α.

2.6.1   General features of the model

We will first examine the general features of the model. Figure 2.4 shows a typical result for the dynamic moduli of a multi-segment chain. We took both activation energies equal to 6 kT.
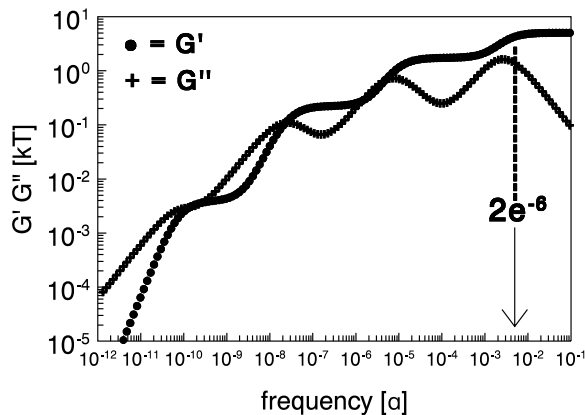
Figure 2.4: Representative result of the new transient network model. See text for details.

This leads to several plateau zones for the storage modulus. The shortest relaxation time is visible at the dimensionless frequency of $2 \cdot e^{-6}$. The factor of 2 expresses that the fastest process via which a chain can lose tension is the breakup of one of its outermost bonds, of which there are two. More generally, for any number of bonds that have to be broken (simultaneously) to get a certain stress-relaxation, there are always two chain-ends available.

The other frequencies marking the upper end of the plateaus are likewise simply obtained from equation (2.9), with the energy a multiple of the activation energy needed for one bond to break.

Although there is a clear separation between the different plateaus, the number of

relaxation times is in fact much larger than the number of plateaus. This does not show up due to a clustering of relaxation times within groups: this is illustrated in figure 2.5.
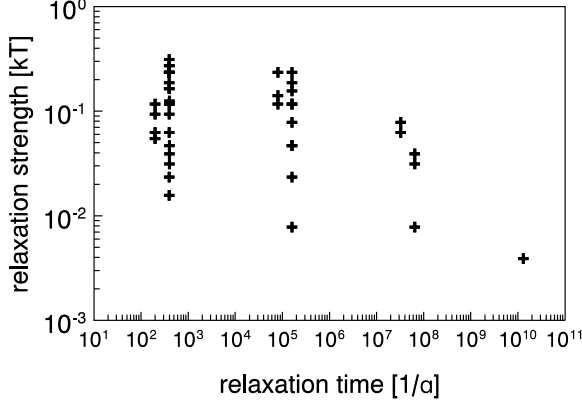
Figure 2.5: The relaxation spectrum[24] corresponding to figure 2.4.

To understand this, one should recognize that the relaxation time τ_{si}, belonging to segment i in state s results from a summation of all rate constants $f_{s,s'}$ that belong to transitions, where segment i will relax (see equation (2.6)):

$$\tau_{si} = \frac{1}{\alpha \sum_{s'_i = free} exp(-E_{s,s'}/kT)} \tag{2.20}$$

The most important contribution to this summation is given by the fastest relaxation; the other small contributions cause the clustering of relaxation times shown in figure 2.5. The distance between these clusters is e^6 as expected.

The number of the plateaus N_p can simply be obtained from the number of bonds that have to be broken to release a segment in the middle of a chain with all stickers fixed. The fastest way to achieve this stress release in a single step is simultaneous breakup of all bonds from the segment to the (nearest) chain-end. This involves:

$$\begin{array}{lll} \frac{N}{2} & stickers \quad for & N = 2, 4, 6... \\ \frac{N-1}{2} & stickers \quad for & N = 3, 5, 7... \end{array} \tag{2.21}$$

The magnitude (i.e. stress level) of the highest plateau G_{p_0} is the summation over all chain states of the number of active segments a_{s_0} multiplied with the concentration of that chain state:

$$G_{p_0} = \sum_s a_{s_0} \cdot N_s \tag{2.22}$$

We recall that G_{p_0} in (2.22) is normalized to kT.

The value of the second highest plateau can be similarly accounted by now considering all chain segments that will stay active when the most left and right bonds of the

chains are broken:

$$G_{p_1} = \sum_s a_{s_1} \cdot N_s \tag{2.23}$$

where the subscript p_1 stands for the first additional plateau and where the subscript s_1 designates segments in state s that stay active when the most right and left bonds are broken.

This analysis can be extended to the other plateaus too:

$$G_{p_{no}} = \sum_s a_{s_{no}} \cdot N_s \tag{2.24}$$

with *no* the number of bonds broken at the left and the right side of the chain.

2.6.2 Dependence upon the number of sticky points

Figure 2.6 shows the influence of the number of sticky points per chain. Both activation energies are taken 6 kT which is sufficient to observe a separation into G' plateaus, but still small enough to have a transient network behaviour. The number of sticky points per chain is varied from 2 to 8. The concentration of chain segments is set equal to 1.
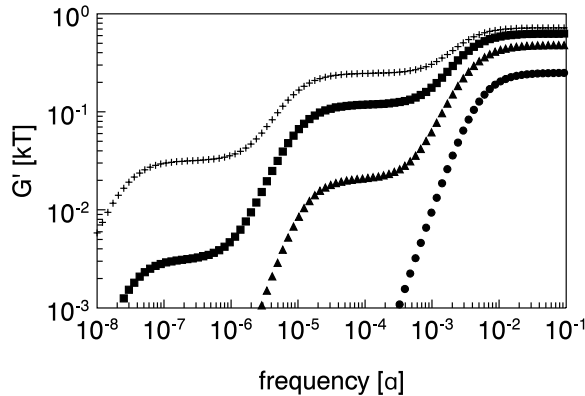
Figure 2.6: Dependence upon the number of stickers per chain. $\bullet = 2$, $\blacktriangle = 4$, $\blacksquare = 6$ *and* $+ = 8$.

Two sticky points per chain leads to the Lodge model with a relaxation time of $\frac{1}{2} \cdot e^6$. The plateau value is proportional to the concentration of active segments which in this particular case equals the concentration of active chains: 0.25 *kT* according to equation (2.13). See also figure 2.6. There is no second relaxation time here, because all chain segments are able to relax all stress when the outermost bonds are broken. To explain quantitatively the first additional plateau we will examine the result with four sticky points per chain. Here according to equation (2.21), there should be a

second plateau. The dominant relaxation times are $\frac{1}{2} \cdot e^6$ and $\frac{1}{2} \cdot e^{12}$ which correspond with the frequencies in figure 6. The highest plateau value can be determined using equation (2.22) and is equal to $\frac{23}{16} kT$. Note that in figure 2.6, G' is normalized to the number of segments per chain. The second plateau value is, using equation (2.23), equal to $\frac{1}{16} kT$ (because only the middle segment, in the chain state where every sticky point has formed a bond, is not able to relax when the outermost bonds are broken).

These examples illustrate our statement in § 2.6.1 that the dominant relaxation times and strengths can be directly related to physical processes. For a higher number of sticky points we see an increase of the levels of the G plateaus.

2.6.3 Dependence upon the activation energies

Figure 2.7 shows the storage modulus for different activation energies when the difference in the two activation energies is taken to be zero. When the activation energy is small, the bonds form and breakup easily and the storage modulus can be compared with the storage modulus from the reptation theory. When the activation energies become larger the transient network model will become more and more a rubber-like network, because the relaxation times become larger (see equation (2.20)).

Figure 2.7: Dependence upon the activation energy. The number of sticky points per chain is 8 and the activation energy of breakup is equal to the activation energy of forming. The activation energies are: ▲ = *2 kT,* ● = *4 kT,* ■ = *6 kT and* + = *8 kT.*

Now we will focus upon the moduli when the activation energy of forming a bond is taken to be different from the activation energy of breaking a bond. We will split this dependence in two parts. First the activation energy of forming a bond is taken constant (6 kT) and the energy of breaking a bond is taken equal and less ($6, 5, 4, 2$ kT). In figure 2.8 this is shown.

Figure 2.8: Difference in activation energies. The number of sticky points per chain is 8 and the activation energy of forming is 6 kT. Activation energies of breaking are: • = *6 kT*, ▲ = *5 kT*, + = *4 kT and* ■ = *2 kT.*

We see that the relaxation time decrease follows equation (2.20) with $E_{s,s'}$ the activation energy needed for the transition from chain state s to s'. Also the plateaus become less discernible and finally the second, third and fourth plateau disappear. When we look at equation (2.13) we see that the number of chains that are in state s depends on both activation energies. By taking the activation energy of forming a bond much higher than the activation energy of breaking a bond, the number of chains that are in states with many bonds is decreasing sharply. Therefore also the G' plateau levels decrease.

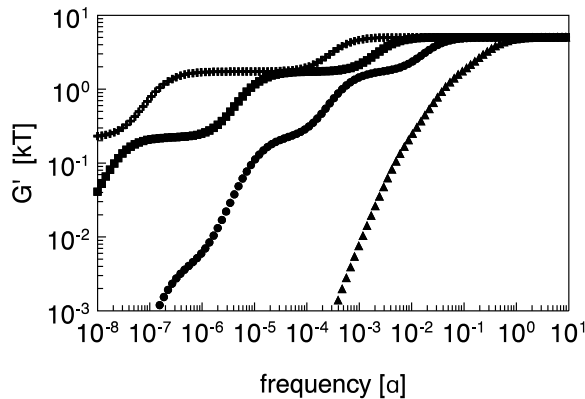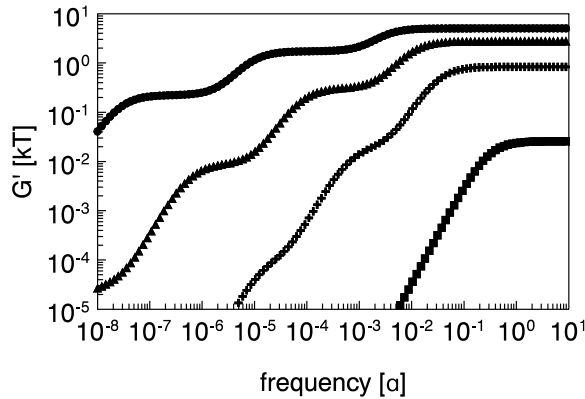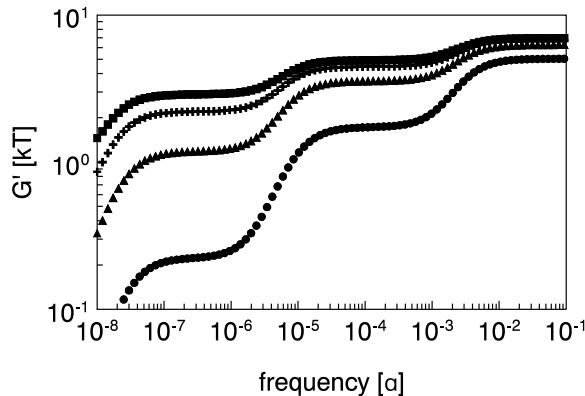**Figure 2.9:** Difference in activation energies. The number of sticky points per chain is 8 and the activation energy of breaking is 6 kT. Activation energies of forming are: • = *6 kT*, ▲ = *5 kT*, + = *4 kT and* ■ = *2 kT.*

In figure 2.9 the activation energy of breaking a bond is set constant (6 kT) and the

energy of forming a bond is varied $(6, 5, 4, 2$ kT). We now can see that when the energy of breaking a bond is much higher than the energy needed to form a bond, the storage modulus plateau levels become also much higher because most sticky points are connected and therefore only small parts of chains are able to relax their stress when one bond is broken. It can be seen in figure 2.9 that the important relaxation times do not change. These relaxation times are determined by the energy of breaking a bond and this energy is not changed.

2.6.4   Special cases

In this section we will present two interesting special cases. First, with our model reptation like moduli can be obtained. Also our model does not necessarily satisfy time temperature superposition.

Comparison with the reptation model

The key concept of reptation[6] is that a polymer chain is confined in a tube. This chain moves back or forth via a diffusion process like a reptile and is therefore able to relax stress. The tube represents the topological constraints imposed by the other chains in the network. The most important and also the longest relaxation time in the reptation model is the time needed for the innermost tube segments to relax their stress via the process of tube renewal. It is important to note that the reptation model leads to a narrow spectrum of relaxation times.

In our model, a narrow relaxation spectrum, can be achieved by taking a chain with many sticky points and weak bonds (activation energies of about 1 kT).
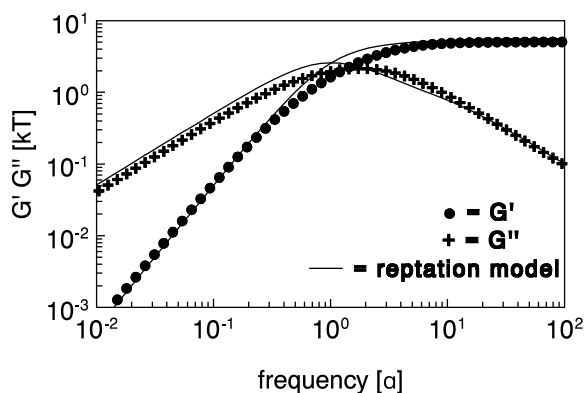
Figure 2.10: Comparison of our model and the reptation model. The longest reptation time used is 1 s. See text for details.

By taking weak bonds the activation energy for simultaneous break-up of many bonds

will still be low. As a consequence, the probability of these processes will be relatively high, whereas the longest relaxation time will not be too different from the shortest time. Hence, a fairly narrow relaxation spectrum will be generated, like for reptation. In figure 2.10 a comparison between our model and the reptation model is shown (for a chain with 8 sticky points). It can be seen that we get reptation like moduli.

Time temperature superposition

Last we will show that our model does not necessarily satisfy time temperature superposition. In other models it is possible by scaling the frequency and the moduli axes to obtain superimposed curves for the moduli. In our model there are two reasons why this is not the case.

First, the dominant relaxation times do not scale in the same way with the temperature. The first dominant relaxation time scales logarithmically with the activation energy for breakup whereas the second dominant relaxation time scales logarithmically with twice the activation energy for breakup. Therefore the ratio between these dominant relaxation times will change with the temperature and this makes it impossible to obtain superimposed moduli curves by scaling.

Secondly, when the activation energies for breakup and forming of a bond are different, the storage modulus plateau values will also scale differently with the temperature as can be seen from equations (2.13) and (2.24). An example is shown in figure 2.11, where we used relatively high activation energies to show the difference in the moduli. In this figure we scaled both axes in such a way that at the high frequencies time temperature superposition is obtained.
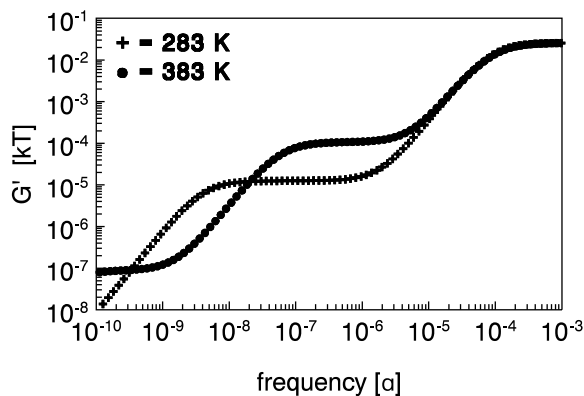
Figure 2.11: Failure of the time temperature superposition over the full frequency range. Activation energies: $E_f = 14\ kT$, $E_b = 10\ kT$.

It can be seen very clearly that time temperature superposition fails at the lower fre-

quencies.

2.6.5   Comparison of predictions with experimental data

To illustrate the potential of our new model, we present here a first comparison with experimental data. In figure 2.12 data (taken from Maerker and Sinton[15]) are shown. They measured the dynamic moduli of a 2.0 % poly (vinyl alcohol) solution in water plus sodium borate (SB). In this system the PVA-chains can form a transient network due to a reversible cross-linking reaction mediated by the borate ions[19]. Obviously, many sites along the PVA-chain are available for such a cross-linking. A peculiarity of this system (which is however irrelevant for this illustration) is that after cessation of shear the network slowly breaks down.
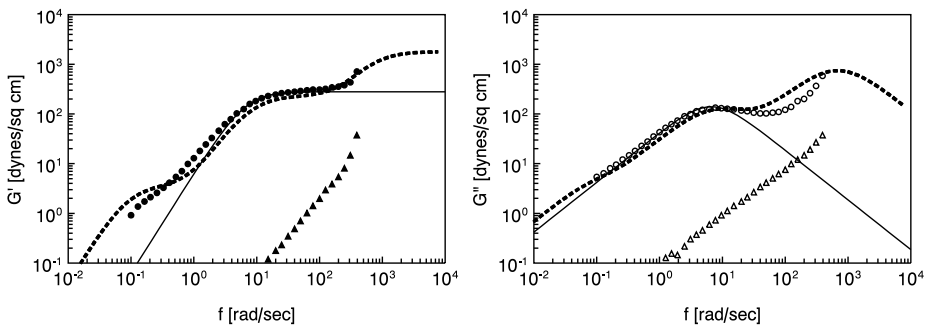
Figure 2.12: Experimental data taken from Maerker and Sinton[15]. $(\blacktriangle, \triangle) = 2\%$ PVA-SB solution measured 21 days after having a shear induced network, $(\bullet, \circ) = 2$ % PVA-SB solution measured 1day after having a shear induced network, lines are transient network model, dashed lines are new transient network model (see text for details).

A PVA solution without SB exhibits dynamic mechanical properties nearly identical to those of the 21 days old sample, showing no evidence of plateaus. When we compare the data of a sample equilibrated without shear for 21 days with a 'freshly' (1day) presheared sample, it is clear that the contribution of other relaxation mechanisms like Rouse or reptation can be neglected compared to the transient network contribution.

Looking at the moduli for the network, we see at low frequencies for the storage modulus an increase compared to low-frequency limiting behaviour. At intermediate frequencies there is a plateau zone for the storage modulus and at high frequencies there is an increase of the loss modulus. From this we can conclude that there are at least three relaxation processes due to the transient network behaviour (since other relaxation mechanisms can be neglected).

When we want to predict three relaxation processes with our model we need at least

6 sticky points per chain. The real PVA/SB system may well have more sticky points per chain, but due to computational limitations we had to take the number of sticky points per chain equal to 8. Assuming activation energies of forming and breaking of 5.05 and 4.70 kT and using 8 sticky points as explained, we obtained the model prediction shown in figure 2.12.

The qualitative improvement obtained with our model as compared to the transient network model of Lodge[14], Yamamoto[25] and Green and Tobolsky[11] is obvious, whereas the activation energies are not unreasonable.

2.7   Discussion

We will evaluate the capabilities of the model and discuss the important model assumptions.

2.7.1   Model capabilities

As explained it turned out to be intractable to calculate the moduli for more than 8 sticky points per chain. The question is to what extent the moduli curves would change if the number of sticky points would be further increased. This issue may be important in comparisons to experimental systems. The answer depends on the activation energies for breaking and forming a bond, since these are of key importance for the magnitudes of the various relaxation strengths, as can be seen from equations (2.13) and (2.24).

One can distinguish between the dominant relaxation times and the storage modulus plateaus. All dominating relaxation times can be determined using:

$$\tau = \frac{1}{\alpha}\exp(M \cdot \frac{E_b}{kT}) \qquad M = \{1, 2, ..., N_p\} \tag{2.25}$$

with N_p the number of storage modulus plateaus (equation 21). For $N >> 1$ the plateau moduli cannot be accounted, but for a finite number it can be done. In figure 2.13 the values of the highest and second highest storage modulus plateaus are plotted as a function of the number of sticky points per chain (keeping the segment concentration constant as before). This is in accordance with the usual practice that the dynamic moduli curves extend over about 4 decades in frequency and that only the first two storage modulus plateaus will be observed.

It can be seen from the figure that the highest storage modulus plateau is almost insensitive to N except when the activation energy for breakup is lower than that for formation of a bond. In that case the highest storage modulus shows a dependence on N which however becomes very weak for N>8. This can be concluded since the fraction of active segments must become 1 (unless the activation energy for breakup approaches zero) when N becomes infinite. Then a rubber-like behaviour will be
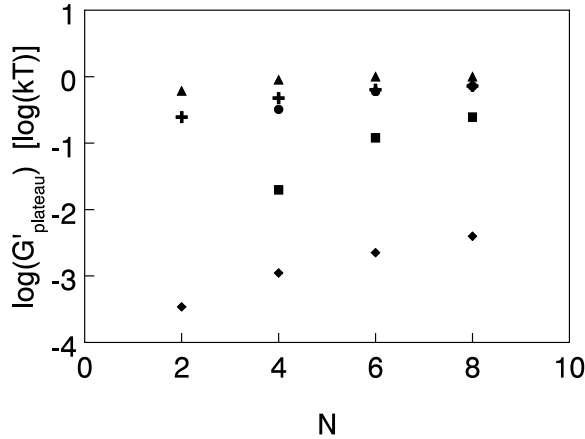
Figure 2.13: Storage modulus plateau levels as function of the number of sticky points per chain. The highest plateau levels (G_{p0}) start at N=2. The second plateau levels (G_{p1}).start at N=4. Activation energies (E_b,E_f) in units of kT, belonging to the plateaus (G_{p0},G_{p1}) are: (▲,●) = (6,2), (+,■) = (6,6), (♦,..) = (2,6).

reached which is a theoretical limit.

When the activation energy for breakup is lower than the energy for formation, there is no visible second storage modulus plateau. For the other two cases, the second storage modulus plateau levels are already relatively insensitive to *N* when the number of sticky points per chain is 8. So even if more sticky points per chain would be present in the 'real chain' the right order of magnitude should already be obtained with 8 stickers.

A second point is that the rate constants for the various transitions between chain-states were set equal to one constant α in equation (2.9). Obviously, the structure of the model (i.e. the types of equations that have to be solved) allows to make a distinction between different rate constants for different transitions. Such a distinction may be appropriate in certain cases. For instance, when the concentration of chain segments is increased, the probability for a bond to break will remain the same, whereas the formation rate of bonds could increase since there are more stickers available per unit volume.

2.7.2 The model assumptions

We made in this model three important assumptions that will now be discussed: The incorporation of the tube concept, the additivity of the activation energies (equation (2.10)) and the (re)distribution of inactive chain segments according to a Gaussian distribution function.

The tube concept was incorporated in the model via the assumption that stress relax-

ation can only occur when active segments become inactive. However, among the active segments there will be segments with one or both stickers not bonded. Still, these segments are not supposed to (be able to) relax any stress. This is a simplification and it allowed us to obtain a set of uncoupled differential equations instead of a coupled set.

This assumption, that stress relaxation can only occur when active segments become inactive, is best justified when the system is concentrated which means that the segment length is large compared to the mesh size of the network. This is the case when the polymer concentration is much higher than the critical concentration c^* were overlap starts to occur. Then there are topological constraints imposed by the other chains in the network and the chain is only able to move along its contour.

The latter movement is in our model also restricted because of the bonds and therefore active segments cannot reptate. Then however, relaxation due to Rouse motion of polymer chains is still possible. In our model we did not take into account Rouse relaxation, because we assume that Rouse relaxation becomes important at much shorter timescales than the timescale where transient network behaviour starts to occur. So our model is valid when:

$$c > c^* \qquad \text{and} \qquad \tau_r = \frac{\zeta N R_g^2}{\pi^2 kT} \quad < \quad \frac{1}{\alpha} \exp(\frac{E_b}{kT}) \qquad (2.26)$$

with τ_r the longest Rouse relaxation time[18], ζ the friction per sticky point and R_g the radius of gyration.

Secondly we assumed that the activation energy needed for a chain transition simply equals the sum of the activation energies needed for all the sticky points involved in the transition. This is a first order approximation, but it is clear that the energy needed for the breakup of two bonds simultaneously is more than the energy needed for the breakup of one bond.

Last we will discuss the assumption that inactive segments are distributed in a Gaussian equilibrium distribution. When the system is concentrated the distribution function of segments that become inactive will not instantaneously transform into the equilibrium distribution. This equilibrium distribution will be reached via a diffusion process. We did not take this diffusion process into account, but when the characteristic diffusion time is small compared to the shortest relaxation time of the network processes, this is justified. The time during which the segments are free is then much larger compared to the time scale of the diffusion process.

2.8   Conclusions

We think that our new model opens interesting possibilities for describing and understanding the linear visco-elasticity of polymers that form a transient network via

associative sites. Varying only three model variables (the activation energies of break-ing and forming a bond and the number of sticky points per chain), the model can predict moduli functions resembling those of known models, as well as various new cases. Reptation like moduli can be obtained with our model by taking chains with many weak bonds of 1 kT. Rubber-like behaviour occurs when the activation energy for breaking a bond becomes large. The larger the number of segments, the lower the activation energy that is needed for this behaviour.

The number of equations that have to be solved becomes very large when the number of sticky points per chain becomes large.
However, provided that the activation energy for breakup of a single sticker is large enough (say greater than 3 kT), the essential features of the relaxation behaviour i.e. the number of storage modulus plateaus, the stress-levels of these plateaus and the dominant relaxation times can be easily predicted in terms of activation energies of forming and breakup of bonds and the number of sticky points per chain.

The dependence upon the activation energy of breaking a bond is clear. Raising this energy leads to higher relaxation times according to the Arrhenius equation and also the number of chains in certain states depends strongly upon this energy following equation (2.13).

The activation energy of forming a bond does not have any influence upon the re-laxation times, but like the activation energy of breaking a bond it determines the number-distribution of chains in state *s* and therefore the plateau-values.

This model is also the first transient network model that predicts a clear dependence upon the number of sticky points per chain, which can be seen as a kind of depen-dence upon the molecular weight. Not only the number of plateaus depends upon this number, also the plateau magnitudes depend upon it.

In our model the temperature only appears in normalizations of the energies of springs and bonds. However time-temperature superposition does *not* necessarily hold in such a way that relaxation spectra belonging to different temperatures can be fully laid over each other.

2.9   References

[1]   Acierno, D.; La Mantia, F.P.; Marrucci, G.; Titomanlio, G. *J. Non-Newtonian Fluid Mech.* **1976**, 1, 125-146.

[2]   Annable, T.; Buscall, R.; Ettelaie R.; Whittlestone D. *J. Rheol.* **1993**, 37, 695-

726.

[3]   Biller, P.; Petruccione, F. *J. Chem. Phys.* **1990**, 92, 6322-6326.

[4]   Bird, R.B.; Amstrong, R.C.; Hassager, O. In *Dynamics of Polymeric Liquids, volume 1*, Wiley, New York, 1987.

[5]   Brule, B.H.A.A. van den; Hoogerbrugge, P.J. *J. Non-Newtonian Fluid Mech.* **1995**, 60, 303-334.

[6]   Doi, M.; Edwards, S.F. In *The theory of polymer dynamics*, Clarendon, Oxford, 1986.

[7]   English, R.J.; Gulati, H.S.; Jenkins, R.D.; Khan, S.A. *J. Rheol.* **1996**, 41, 427-444.

[8]   Geurts, K.R.; Wedgewood, L.E.; *J. Chem. Phys.* **1997**, 106, 339-346.

[9]   González, A.E. *Polymer* **1983**, 24, 77-80.

[10]   González, A.E. *Polymer* **1984**, 25, 1469-1474.

[11]   Green, M.S.; Tobolsky, A.V. *J. Chem. Phys.* **1946**, 14, 80-89.

[12]   Groot, R.D.; Agterof, W.G.M. *J. Chem. Phys.* **1993**, 100, 1657-1664.

[13]   Leibler, L.; Rubinstein, M.; Colby, R.H. *Macromolecules* **1991**, 24, 4701-4707.

[14]   Lodge, A.S. *Trans. Faraday Soc.* **1956**, 52, 120-130.

[15]   Maerker, J.M.; Sinton, S.W. *J. Rheol.* **1986**, 30, 77-99.

[16]   Phan-Thien, N.; Tanner, R.I. *J. Non-Newtonian Fluid Mech.* **1977**, 2, 353-365.

[17]   Phan-Thien, N. *J. Rheol.* **1978**, 22, 259-283.

[18]   Rouse, P.E. *J. Chem. Phys.* **1953**, 21, 1272-1280.

[19]   Schultz, R.K.; Myers, R.R. *Macromolecules* **1969**, 2, 281-285.

[20]   Tanaka, F.; Edwards, S.F. *Macromolecules* **1992**, 25, 1516-1523.

[21]   Tanaka, F.; Edwards, S.F. *J. Non-Newtonian Fluid Mech.* **1992**, 43, 247-271.

[22]   Tanaka, F.; Edwards, S.F. *J. Non-Newtonian Fluid Mech.* **1992**, 43, 273-288.

[23]   Tanaka, F.; Edwards, S.F. *J. Non-Newtonian Fluid Mech.* **1992**, 43, 289-309.

[24]   Tschoegl, N.W. In *The phenomenological theory of linear viscoelastic behavior, an introduction*, Springer verlag, Berlin, 1989.

[25]   Yamamoto, M. *J. Phys. Soc. Jpn.* **1956**, 11, 413-421.

Chapter 3

A generalized transient network model for associative polymer networks

3.1   Synopsis

A transient network model is described for a polymeric system consisting of linear chains, connected with temporary cross-links. The model is a reformulation and extension of a similar model which was presented recently [Wientjes, R. H. W.; Jongschaap, R. J. J.; Duits, M. H. G.; and Mellema, J. A new transient network model for associative polymer networks. *J. Rheol.*, 43(2):375–391, 1999].
Contrary to common transient network models the interconnection between segments is explicitly taken into account. The dynamics of the system is also described by the state of a whole chain, instead of separate segments. As a result a prediction of the shape of relaxation spectra is possible. The model predicts broad spectra with long relaxation times, in particular for chains with many stickers. In the present formulation also systems with multiple types of stickers is can be treated. In that case plateau regions in dynamic moduli may appear.

3.2 Introduction

Transient network models are an important class of models, developed to describe the rheological behavior of polymer melts and solutions. The transient network concept was first proposed by Green and Tobolsky[3], put in a tensorial format by Lodge[8] and Yamamoto[16] and developed further by many others (see the book[1] for a review). Lately, there are a number of new developments in transient network models. First, improvements in order to describe nonlinear flow behavior.[10], further on simulations, which have become an important tool for the investigation of transient networks.[13,4] and finally a combined transient network and reptation theory in the sticky reptation models of of Rubinstein et al. [6,11,12]

Although the transient network concept was primarily developed to model entanglement in polymeric systems, the model may also be used to model the dynamics of weak gels, consisting of a network of chains with reversible crosslinks. In the present paper we propose a new transient network model for this type of systems.

A special feature of this model is that the network segments are not treated as independent. Instead, the interconnection of segments in a chain is taken into account explicitly. As a result the present theory allows the prediction of relaxation spectra. This is fundamentally different from ordinary transient network models, where relaxation spectra are introduced by using the ad-hoc concept of complexity of segments. Although a general constitutive equation is derived (eq 3.19 below), we will concentrate here on the linear viscoelastic behavior. In a recent paper,[14] we published a model based upon the same principles. In our present paper the mathematical analysis, however, is reformulated and extended. We improve an assumption in our earlier paper about the stress contribution of newly created segments. As a result we now obtain different predictions. In the new formulation, we are able to treat also the case of multiple types of stickers. This turns out to be of significant influence.

3.3 Model

We consider a system of linear flexible polymer chains with on each chain (see figure 3.1) a finite number of *stickers* that can associate to form reversible crosslinks. As a result the whole system acts as a reversible gel of multiple connected chains. The stickers can exist in one of two states: *free* and *fixed*. The connection state of the whole chain will be specified by a variable s which determines the states of all stickers along a chain. The parts of a chain between stickers are called segments. All segments are equal and modeled by linear entropic springs. Segments which carry stress are called *active*.

In order to specify the state of a segment i in a chain in state s we use a parameter v_s^i
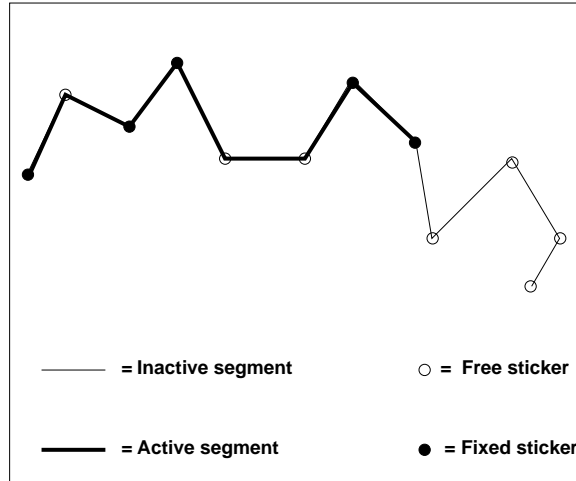
Figure 3.1: Chain with free and fixed stickers and active and inactive segments.

defined as

$$v_s^i = 1 \Longleftrightarrow \text{segment i active in state s}$$
$$v_s^i = 0 \Longleftrightarrow \text{segment i inactive in state s} \qquad (3.1)$$

This is not a dynamic variable, but a constant which determines unambiguously the state of all segments for any value of the state variable *s*.

The environment of a chain is treated for the active segments as a tube, which prevents motions perpendicular to it. This tube-constraint is similar to the one used in reptation dynamics.[2] In the present model, contrary to the so called sticky reptation models[6] however, there is no motion of the chain along the tube. The main purpose of the tube is to retain the direction of active segments as long as they remain active, even when adjacent stickers are free. A transition of a sticker from fixed to free results only in a loss of tension in an adjacent segment if in that transition the segment becomes inactive. If, for example the sticker in the middle of the chain in the 5th state displayed in figure 3.2 becomes free, no change of stress takes place in the adjacent segments. If this occurs in the 6th state of the same figure the stress in the segment left to that sticker will be released. This is a cooperative effect which is specific for our model and results in relatively long times in the stress relaxation spectrum.

The non-active segments are assumed to be always in their equilibrium distribution. This is similar to the common assumption of transient network theories,[7] that segments are created in the equilibrium distribution. This assumption which is obviously an oversimplification is retained to keep the analysis relatively simple. If a non-active segment becomes active, its contribution to the stress is determined by its subsequent motion. The total contribution of active segments *i* in a state *s* is determined by the
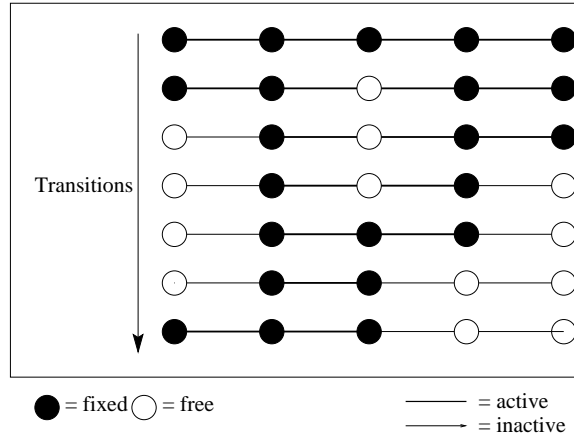
Figure 3.2: Change of state of segments due to changes of the state of stickers along the chain. A transition of a sticker from fixed to free results only in a loss of tension segment if that sticker defines the terminus of a succession of active segments.

distribution function ψ_s^i. In the next section the coupled set of evolution equations by which the segment distribution functions are determined will be discussed. This is an improvement on our earlier paper[14] where it was assumed that the distribution function of active segments was dependent only of the state s.

3.4   Evolution equations

Like in classical transient network theory[7,16] the rheological properties of the system are determined by the creation, loss and motion of segments. Of primary interest are the evolution in time of the density $\Psi_s^i(\mathbf{q}_i, t)$ of chain-segments number i of a chain in state s in an infinitesimal three-dimensional volume element $d^3\mathbf{q}_i$ in the segment-configuration space, and the number density n_s of chains in state s. We also define a one-chain probability density ψ_s^i by

$$\Psi_s^i(\mathbf{q}_i, t) = n_s \psi_s^i(\mathbf{q}_i, t) \tag{3.2}$$

The evolution equation of segments is assumed to be

$$\frac{\partial \Psi_s^i}{\partial t} = -\nu_s^i \frac{\partial}{\partial \mathbf{q}_i} \cdot (\Psi_s^i \dot{\mathbf{q}}_i) + \sum_{s' \neq s} (A_{ss'} \Psi_{s'}^i - A_{s's} \Psi_s^i) \tag{3.3}$$

The first term in the right hand side is the convective part. Due to the factor ν_s^i this term is non-zero only for active segments, in accordance with the assumption that the

inactive segments are always in equilibrium. The motion $\dot{\mathbf{q}}$ of the active segments is assumed to be affine, so

$$\dot{\mathbf{q}}_i = \mathbf{L} \cdot \mathbf{q}_i \tag{3.4}$$

where $\mathbf{L} = (\nabla \mathbf{v})^T$ the velocity gradient tensor.

The last term in eq 3.3 defines the kinetic contributions. $A_{s's}$ is the transition rate of a chain for transition from state s to state s'.

By integration of eq 3.3 a rate equation for n_s, the density of chains in state s, is obtained:

$$\dot{n}_s = \sum_{s' \neq s} A_{ss'} n_{s'} + A_{s',s} n_s \tag{3.5}$$

This kind of gain-loss equation is called a Master equation.[5] For the transition probabilities it can be proved [9] that

$$A_{s,s} = -\sum_{s' \neq s} A_{s's} \tag{3.6}$$

This allows us to write eq 3.5 in a more compact form:

$$\dot{n}_s = \sum_{s'} A_{ss'} n_{s'} \tag{3.7}$$

Where the summation over s' extends the whole range of states including $s' = s$.

From equations 3.2, 3.3 and 3.5 we obtain for the one-chain distribution function ψ_s^i

$$\frac{\partial \psi_s^i}{\partial t} = -\nu_s^i \frac{\partial}{\partial \mathbf{q}_i} \cdot (\psi_s^i \dot{\mathbf{q}}_i) + \sum_{s'} \frac{n_{s'}}{n_s} A_{ss'} (\psi_{s'}^i - \psi_s^i) \tag{3.8}$$

and by multiplication with ν_s^i, using the identity $\nu_s^i \nu_s^i = \nu_s^i$ (no summation) and separating in the last term contributions with segment i active and contributions with segment i inactive in the state s' and using our model assumption that free segments are always in the equilibrium distribution ψ^0, after some rearrangement the following evolution equation for ψ_s^i:

$$\nu_s^i \frac{\partial \psi_s^i}{\partial t} = -\nu_s^i \frac{\partial}{\partial \mathbf{q}_i} \cdot (\psi_s^i \dot{\mathbf{q}}_i) + \sum_{s'} \frac{n_{s'}}{n_s} A_{ss'} \nu_s^i (1 - \nu_{s'}^i)(\psi^0 - \psi_s^i) + \sum_{s'} \frac{n_{s'}}{n_s} A_{ss'} \nu_s^i \nu_{s'}^i (\psi_{s'}^i - \psi_s^i) \tag{3.9}$$

The first summation are transitions from *inactive* to *active*, the second summation transitions from *active* to *active* segments.

3.5 Constitutive equation

The macroscopic stress tensor $\mathbf{T}$ is the sum of contributions of the active segments, so

$$\mathbf{T} = \sum_s \sum_i \nu_s^i \mathbf{T}_s^i \tag{3.10}$$

where

$$\mathbf{T}_s^i = n_s \kappa (\mathbf{S}_s^i - \mathbf{S}^0) \tag{3.11}$$

with κ the segments-spring constant,

$$\mathbf{S}_s^i = \langle \mathbf{qq} \rangle_s^i = \int \mathbf{qq} \psi_s^i d^3\mathbf{q} \tag{3.12}$$

the second moment of the segment distribution function ψ_s^i and $\mathbf{S}^0$ the equilibrium value

$$\mathbf{S}^0 = \langle \mathbf{qq} \rangle^0 = \frac{kT}{\kappa}\mathbf{1} \tag{3.13}$$

This is essentially the so called *Kramers form*[1] of the polymer contribution to the stress tensor.

In order to obtain this result, the force in an active segment with a segment vector $\mathbf{q}$ of a chain in state s has been taken to be

$$\mathbf{f}_s^i = \kappa \mathbf{q}_i \tag{3.14}$$

This is an approximation. In fact, for a series of connected active segments, with free stickers at the interconnections, due to equilibration of forces, the force in all segments will be the same. This force will depend upon the total extension of these segments. Moreover, the free stickers will also move from the positions determined by the assumption of affine motion and no longer coincide with the connections between the tube elements. To include this in an analytical formulation of our model, if possible, would be very cumbersome. We expect, however, that eq 3.14 can be used as an approximation for the spring forces and that the free stickers always follow the positions, determined by the assumed affine motion. At least, in a treatment of linear viscoelastic behavior, which is the main issue of our present paper, these approximations are expected to be sufficient.

From eq 3.9, eq 3.12 and eq 3.13 the following evolution equation for $\mathbf{S}_s^i$ is obtained.

$$\frac{\delta}{\delta t}(\mathbf{S}_s^i - \mathbf{S}^0) + \sum_{s'} \beta_{ss'}^i (\mathbf{S}_{s'}^i - \mathbf{S}^0) = 2\frac{kT}{\kappa}\mathbf{D} \tag{3.15}$$

where $\frac{\delta}{\delta t}$ is an upper convective derivative (so $\frac{\delta}{\delta t}\mathbf{S^0} = -2\frac{kT}{\kappa}\mathbf{D}$) and

$$\beta_{ss'}^i = \frac{\dot{n}_s}{n_s}\nu_s^i \delta_{ss'} + \frac{n_{s'}}{n_s}B_{ss'}^i \tag{3.16}$$

with

$$B_{ss'}^i = -A_{ss'}\nu_s^i \nu_{s'}^i \tag{3.17}$$

We refer to appendix A for details of the derivation of these results.

From eq 3.11 and eq 3.15 the following differential equation for $\mathbf{T}_s^i$ is obtained:

$$\frac{\delta}{\delta t}\left(\frac{\mathbf{T}_s^i}{n_s}\right) + \sum_{s'} \beta_{ss'}^i \frac{\mathbf{T}_{s'}^i}{n_{s'}} = 2kT\mathbf{D} \tag{3.18}$$

With eq 3.16 and eq 3.17 this may also be written as

$$\frac{\delta}{\delta t}\mathbf{T}_s^i + \sum_{s'} B_{ss'}^i \mathbf{T}_{s'}^i = 2n_s kT\mathbf{D} \tag{3.19}$$

The equations eq 3.7, eq 3.10 and eq 3.18 or eq 3.19 provide a complete set of constitutive equations of the model. We see that the constitutive behavior is determined mainly by the matrix $A_{ss'}$ of transition rate coefficients which determines by eq 3.7 the rate of change of number densities of the states n_s of the chains and the matrices $\beta_{ss'}^i$ or $B_{ss'}^i$ occurring in the stress tensor expressions. The matrices $\beta_{ss'}^i$ or $B_{ss'}^i$ also contain information about the chain connectivity in the matrix v_s^i. Due to these features the present model is able to give more detailed predictions about, in particular the linear viscoelastic behavior of the system than the common transient network models. In the next section we will discuss in some detail how in our model the relaxation spectra are predicted explicitly.

3.6 Linear viscoelastic behavior

For the analysis of linear viscoelastic response we use a linearized version of eq 3.19 with an ordinary time derivative and for all n_s the equilibrium values: n_s^0 and instead of the whole stress tensor we only consider the shear stress component $\tau = T_{12}$. In a one-dimensional representation, the differential equation for the contributions τ_s^i to the stress $\tau = \sum_s \sum_i v_s^i \tau_s^i$ then becomes:

$$\dot{\tau}_s^i + \sum_{s'} B_{ss'}^i \tau_{s'}^i = n_s^0 kT\dot{\gamma} \tag{3.20}$$

If all eigenvalues of the matrix $[B^i]$ are distinct the following transformations can be used to decouple the equations eq 3.20

$$\tilde{B}_{ss'}^i = P_{st}^{i-1} B_{tu}^i P_{us'}^i = diag(b_1^i, b_2^i, \ldots,) \tag{3.21}$$

$$\tilde{\tau}_s^i = P_{ss'}^{i-1} \tau_{s'}^i \tag{3.22}$$

Then eq 3.20 becomes

$$\dot{\tilde{\tau}}_s^i + b_s^i \tilde{\tau}_s^i = \sum_{s'} P_{ss'}^{i-1} n_{s'}^0 kT\dot{\gamma} \tag{3.23}$$

Fourier transformation gives:

$$\widehat{\widetilde{\tau}}_s^i = \frac{\lambda_s^i}{1 + i\omega\lambda_s^i} \sum_{s''} P_{ss''}^{i\,-1} n_{s''}^0 kT\widehat{\gamma} \tag{3.24}$$

with the relaxation times

$$\lambda_s^i = \frac{1}{b_s^i} \tag{3.25}$$

After transformation to the original variables we finally obtain:

$$\widehat{\widetilde{\tau}}_s^i = G_{s'}^i \frac{\lambda_{s'}^i}{1 + i\omega\lambda_{s'}^i}\widehat{\gamma} \tag{3.26}$$

with

$$G_{s'}^i = kT \sum_s \sum_{s''} v_s^i P_{ss'}^i P_{s's''}^{i\,-1} n_{s''}^0 \tag{3.27}$$

The corresponding storage and loss moduli are

$$G'(\omega) = \sum_i \sum_s G_s^i \frac{\omega^2 \lambda_s^{i\,2}}{1 + \omega^2 \lambda_s^{i\,2}} \tag{3.28}$$

$$G''(\omega) = \sum_i \sum_s G_s^i \frac{\omega \lambda_s^i}{1 + \omega^2 \lambda_s^{i\,2}} \tag{3.29}$$

3.6.1   The matrices A and nu

In order to apply the results derived in the previous section we need explicit expressions for the elements of the matrices $A_{ss'}$ and v_s^i. To that end a consistent numbering of stickers, segments and states is needed and we use a scheme, based upon the binary representation of numbers. The state number s will be chosen such that the digits 1 in its binary representation correspond to fixed and digits 0 to free stickers. In figure 3.3 this is illustrated for eight states of a chain of three segments.

In accordance with this numbering, we will also number the segments from right to left so for a state with state number s such that $2^{k+1} < s < 2^k$ the highest value of the number of a fixed sticker is k. Noting that for states with an odd value of the state number s the right-end sticker is fixed and that multiplication of s by a factor 2^j corresponds to shift of the pattern of free and fixed stickers with j steps to the left we see that for states with $2^{k+1} < s$ and $s = m2^j$ where m is an odd number, the segments with numbers between j and k are active. In this way the the non-zero values of the matrix v_s^i are readily obtained.

Next, the transition matrix $A_{ss'}$ has to be constructed. To that end we define a matrix

$$K = \begin{bmatrix} 1 & g \\ h & 1 \end{bmatrix} \tag{3.30}$$

Chain states	Binary	Decimal
○——○——○——○	0000	0
○——○——○——●	0001	1
○——○——●——○	0010	2
○——○——●——●	0011	3
○——●——○——○	0100	4
○——●——○——●	0101	5
○——●——●——○	0110	6
○——●——●——●	0111	7
●——○——○——○	1000	8

Figure 3.3: The state numbers *s* of states for the case of a chain with three segments.

where g is the transition rate for transition of a sticker from free to fixed and h the transition rate for transition of a sticker from fixed to free.

For the two states of a 'chain' consisting of one sticker, by using eq 3.6, we obtain for the transition matrix

$$A^{(1)} = \begin{bmatrix} -h & g \\ h & -g \end{bmatrix} \tag{3.31}$$

By making use of the Kronecker product

$$K \otimes K = \begin{bmatrix} 1 & g & g & g^2 \\ h & 1 & gh & g \\ h & gh & 1 & g \\ h^2 & h & h & 1 \end{bmatrix} \tag{3.32}$$

the *A* matrix for the case of two stickers is obtained in a similar manner:

$$A^{(2)} = \begin{bmatrix} -2h - h^2 & g & g & g^2 \\ h & -g - h - gh & gh & g \\ h & gh & -g - h - gh & g \\ h^2 & h & h & -2g - g^2 \end{bmatrix} \tag{3.33}$$

In general

$$A_{ij}^{(N)} = K^{\otimes N} + (1 - \sum_k K_{ik}^{\otimes N})\delta_{ij} \tag{3.34}$$

where $K^{\otimes N}$ denotes an n-fold Kronecker product. Expressions for higher order ν and *A* matrices are readily constructed numerically with algorithms based upon these rules.

A similar procedure is possible for systems with *different types of stickers* if they are arranged in some regular pattern which is repeated along the chain. In that case the same procedure is valid, with the only difference that instead of the 2×2 matrix K a bigger matrix has to be used as building blocks for the A.

3.6.2   Examples

We will show now some examples of predictions of linear viscoelastic behavior according to the present model. A drawback of the method, outlined above is that the number of states increases rapidly with the number of stickers and a considerable amount of computer time and memory is required for the analysis. This may be reduced eventually by making use of special algorithms, but at present we only performed calculations for relatively few stickers. This, however is sufficient to illustrate some characteristic features of the model.
We use a chain with up to eight stickers. First the case of equal stickers will be discussed and after that also the case of a chain with two types of stickers. Finally, we also use a different method, namely a straightforward simulation of the creation, loss and deformation according to the present model for an ensemble of chains. In this way also results for larger numbers of stickers can be obtained.
For the creation and loss rates g and h we use an Arrhenius type of equation:

$$g, h \sim \alpha e^{\frac{E_t}{kT}} \tag{3.35}$$

were α^{-1} is a characteristic time, k is the Boltzmann constant, T the absolute temperature and the index $t = g$ for creation and $t = h$ for loss processes. For the calculations we take $\alpha = 1$ and express the activation energies E_t in units kT. The results shown here are renormalized to the number of segments per chain.
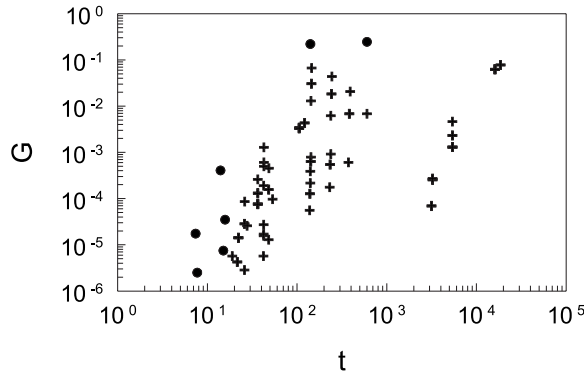

Figure 3.4: Relaxation spectra $E_g = 3$, $E_h = 5$, $\bullet$: $N = 5$, $+$: $N = 8$

In figure 3.4 the relaxation spectrum is given for the cases of 5 and 8 stickers with

$E_g = 3$ and $E_h = 5$ as calculated with eq 3.21, 3.25 and 3.27. We see that the spectrum is relatively wide and we also note the rapid growth of the number of relaxation times with increasing N. Especially for the case of 8 stickers it is visible that the relaxation times can be divided in two groups of relaxation processes. The largest relaxation times are about $2 \ 10^4$ which correspond to relaxation process where 2 bonds breakup simultaneously. The second group is the group around $1 \ 10^2$ which is the breakup time of one sticker. This group consist of many different relaxation times, divided in two subgroups. First, there is the relaxation process were chain segments relax after a process of breakup of several stickers in succession. The corresponding relaxation time grows roughly in a linear way with the number of bonds that have to break for such a process. Secondly, there are often various ways for the same number of bonds to break (either simultaneously or in succession). This will cause the relaxation time to be proportional to the number of possible ways of breaking.
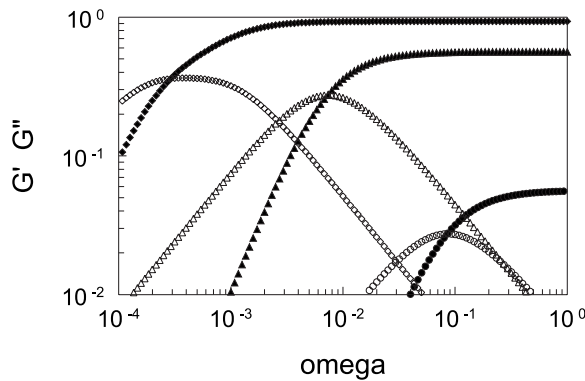
Figure 3.5: Viscoelastic moduli for 5 stickers per chain and $E_g = 5$, open symbols designate G'', closed symbols G', $E_h = 3 : \circ$, $E_h = 5 : \triangle$, $E_h = 7 : \Diamond$

In figure 3.5 the moduli G' and G'' are given for a chain of five stickers, a creation energy of $E_g = 5$ and three different values of the loss energy $E_h = 3, 5, 7$. We note (in particular for high values of E_h) the relatively flat slope in the low frequency region of the moduli curves, which is an indication of a broad spectrum. We see that the value of the plateau modulus increases for higher values of E_h. This is also what should be expected, since a high value of E_h implies a longer average lifetime of the chains, which means higher stresses. For higher values of E_h we also see a shift of the curves to the left, which corresponds to longer relaxation times. This is also in accordance with the longer lifetimes of the chains.

In figure 3.6 the viscoelastic moduli are presented for the case that $E_g = E_h = 5$ and three different values of N: $N = 3, 5, 7$. We see a strong increase of the moduli values with the number of stickers. This is characteristic of the present model where the connectivity of the chains is taken into account. If a sticker becomes free, this
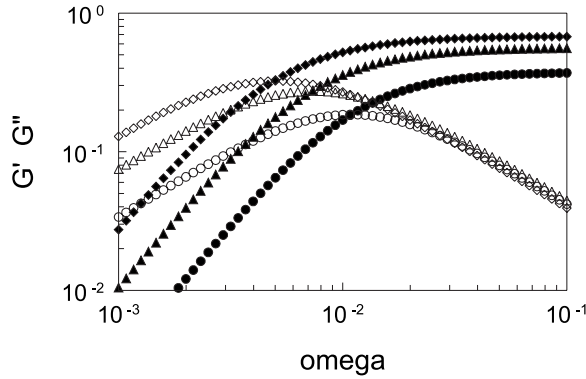
Figure 3.6: Viscoelastic moduli for $E_g = 5$ and $E_h = 5$, open symbols designate G'', closed symbols G', $\circ : N = 3$, $\triangle : N = 5$, $\Diamond : N = 7$

will not always mean a loss of stress. Only for stickers that terminate a succession of active segments such is the case. The probability of such an occurrence does not depend on N, but for larger N the fraction of such stickers is simply smaller. This increase in the number of multi-connected states for higher N also contributes to shift the relaxation spectrum to larger times; this causes the shift of curves to the left. Roughly the mean relaxation time scales with the number of stickers.
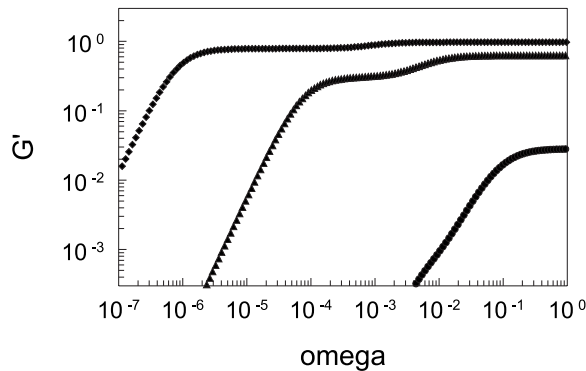
Figure 3.7: 2 types of stickers: $N = 6$, $E_{g\,weak} = 5$, $E_{g\,strong} = 10$, $\bullet : E_{h\,weak} = 3$, $E_{h\,strong} = 6$, $\blacktriangle : E_{h\,weak} = 5$, $E_{h\,strong} = 10$, $\blacklozenge : E_{h\,weak} = 7$, $E_{h\,strong} = 14$

In figure 3.7 the effect of different types of stickers is illustrated. Here we consider the viscoelastic moduli for the case of two type of stickers: strong $E_g = 10$ $E_h = 2$ and weak $E_g = 5$ $E_h = 1$ for the cases $E_h = 3, 5, 7$. We see that in this manner it is possible to obtain G' curves with different plateau's and G'' curves with multiple maxima.

Although the example here is given to show some features of our model, it should

be noted that application for the case of two types of stickers is part of our current research on the rheological behavior of Guar gum solutions [15].

Again, we see for higher values of E_h larger moduli and a shift of the curves to longer time ranges.
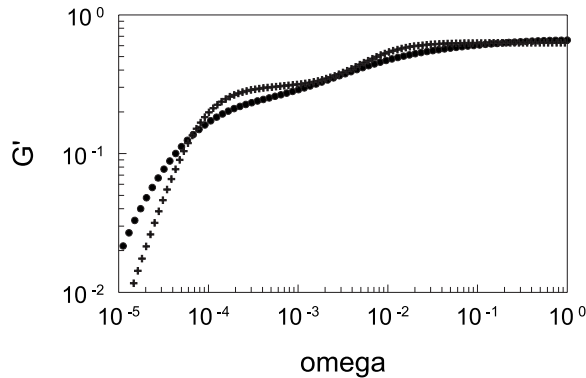
Figure 3.8: Comparison of simulation and analytical results: $N = 6, E_g = 5, E_h = 5,$
$+ : \ analytical, \bullet : \ simulation$

In figure 3.8 the results of direct simulations are compared with the results obtained with the analytical method discussed above. In this simulation the relaxation spectrum is obtained from single chain simulations. During these simulations the lengths and orientations of chain segments are kept constant. This is allowed, since the linear relaxation behavior is determined only by the breakup and formation of bonds. A step strain experiment is simulated: a chain, randomly placed in a given state performs a virtual step strain. As a consequence all active chain-segments obtain a given extension and orientation and a given stress.

During a simulation timestep, the stickers have a given probability, determined by the activation energies, to change their state (free, fixed). By this process particular chain-segments become inactive and loose their preferred orientation and stress. When chain segments become inactive the corresponding relaxation time and number of segments that becomes inactive is stored. In the stress relaxation experiment inactive segments will not contribute to the stress any more, even if they become active again. The process of changing states of stickers is repeated until all stress contributions are lost. The simulation is repeated for many randomly chosen chains and the time values and stress losses of the various chains are collected. In this way the relaxation spectrum is obtained.

We see significant differences with the analytical results, in particular in long time range. These difference are caused by errors, due to the relatively small number (typically 100) of chains used in the simulations. On the other hand the simulation results still give a reasonable approximation of the magnitude and shape of G.
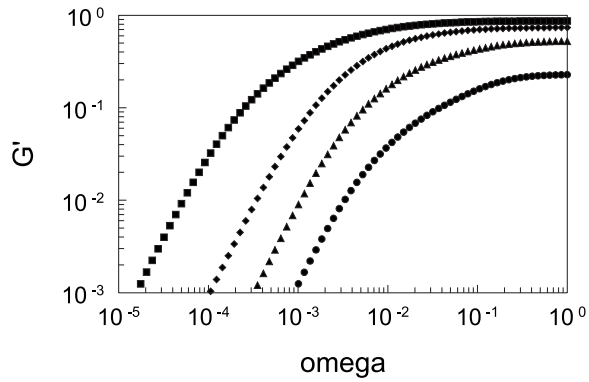
Figure 3.9: Simulation results for one type of stickers: $E_g = 5$, $E_h = 5$, $\bullet$: $N = 2$, $\blacktriangle$: $N = 4$, $\blacklozenge$: $N = 8$, $\lozenge$: $N = 16$
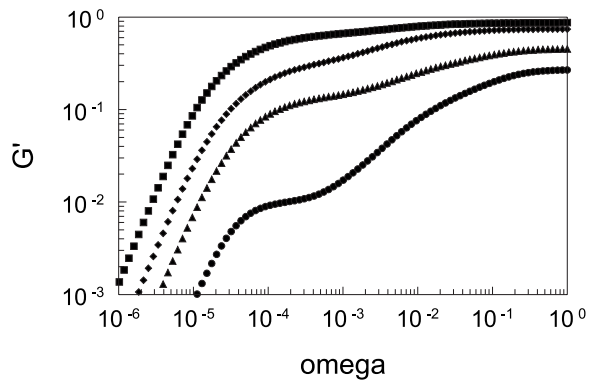
Figure 3.10: Simulation results for two type of stickers, random placement of strong and weak stickers (1:1): $E_{g\,weak} = 5$, $E_{h\,weak} = 5$, $E_{g\,strong} = 10$ $E_{h\,strong} = 10$, $\bullet$: $N = 2$, $\blacktriangle$: $N = 4$, $\blacklozenge$: $N = 8$, $\lozenge$: $N = 16$

This offers the possibility to extend the range of *N* values. This is illustrated in the figures 9 and 10 for the storage modulus G for the cases of one and two types of stickers and $N = 2, 4, 8, 16$.

Note that in figure 3.10 two plateaus are visible for the case of 2 stickers. This is a result of the random placement of strong and weak stickers. Sometimes a chain with two strong stickers is simulated and then the relaxation time becomes large. In the analytical solution the plateau at low frequencies would not be present here. For a large number of stickers the difference between the one and two type sticker behavior becomes less. However the behavior in the case of one sticker remains smooth compared to the case of two stickers.

3.7 Concluding remarks

In this chapter a network model is presented which is essentially different from common transient network models in the sense that the stress release in segments is treated as a cooperative process. If a sticker becomes free, the stress in the adjacent segments is not always released, this will happen only for segments which become free in the sense indicated in figure 3.1 In other cases the stress in the segment will remain the same. Physically this leads to broad spectra with long relaxation times, in particular for chains with many segments. This is qualitatively in accordance with the observed behavior of polymer gels.

Formally, the dynamics of the system is primarily described by the state *s* of the whole chain, and not, like in ordinary transient network models, by the state of independent segments. A drawback of this representation is that the number of states, increases rapidly with the number of stickers, so with modest computing resources, only chains with relatively few stickers can be analyzed. For that case, as has been shown in the previous section, the main features of the model can already be be demonstrated adequately. We have discussed the linear viscoelastic behavior of the chain with up to eight stickers for a few values for the creation and loss rates. It has been shown that the model predicts a wide relaxation spectrum with a shape, determined by the underlying kinetics. This is essentially different from ordinary transient network models, where shape of the relaxation spectrum is introduced *ad hoc* by the concept of complexity[7] of segments.

The shape of the spectrum alters if different types of stickers are introduced. We have seen how in that case plateau regions in the dynamic viscoelastic moduli may appear. This feature may be used by the modeling of particular systems like gels of bio-polymers. In an earlier paper[14] moduli with plateau values were also obtained for the case of one type of stickers. This, however appears to be the result of the

crude approximations in the mathematical analysis which have been improved in the present formulation.

In the work of Leibler, Rubinstein and Colby[6] [LRC] the dynamics of a temporary network with reversible crosslinks is described by a sticky reptation model. In the LRC model, a repational diffusion takes place if parts of the chain become free (in an earlier treatment of Gonzalez[3] it was required for a reptation step that the whole chain was free). Stress relaxation is modeled as in classical reptation theory and takes place at a characteristic time T_d, the disengagement time of the whole chain. Two important time scales in the LRC model also are the average lifetime τ of the stickers and the disengagement time T_d. As a result the model predicts essentially two plateau regions in $G'(\omega)$.

Our model is in a sense complementary to the LRC model. We neglect reptation completely and attribute the stress relaxation is solely to the stress release in free segments at the chain ends, which is assumed to be instantaneous. We assume that in a transient gel this mechanism of stress release is far more important than the slow stress relaxation due to (sticky) reptation. and that the only fundamental process is the creation and loss of individual stickers. Interconnection of segments is taken into account and that the relaxation spectrum is derived explicitly. As a result, our model (for one type of stickers) predicts no extra plateau region in $G(\omega)$ but only a broadening for frequencies below the characteristic time of the stickers, whereas the LRC model predicts a plateau between this region and frequencies corresponding to the reptation (disengagement) time scale. The first part of the LRC-relaxation spectrum (belonging to their characteristic time τ) is independent of the molecular weight. We, on the other hand, find a relaxation spectrum which strongly depends on the number of stickers and also of the molecular weight.

It should be noted also that currently no explicit derivation of relaxation behavior based upon the sticky reptation model is available. The LRC model provides a detailed analysis of the diffusion of the chain along the tube but only a crude estimation of the of the relaxation behavior, based upon classical reptation theory and the obtained results for the characteristic time scales. A rigorous treatment should be based upon the stress contributions in the chain segments.

Finally if should be noted that contrary to LRC, our model, although based upon rather crude approximations, predicts a closed constitutive equation.

An obvious extension of our present model is an analysis of non-linear rheological behavior. This will not be undertaken, however in this paper. The advantage of

our present analysis of linear viscoelastic behavior is that some specific results are obtained, with only a few a model assumptions.

As in classical network theory the extension to the non-linear regime may proceed by introducing (rate of) strain or stress dependent creation and loss rates, non-affine motion *etc*. This is possible, in principle, but this requires the introduction of extra model parameters. On the other hand it should be noted that the fact that we are able to derive an explicit analytical constitutive equation provides at least a starting point for non-linear constitutive modeling. In approaches like the LRC-model, where no constitutive equation is derived, such is impossible.

Instead of phenomenological and empirical constitutive modeling we would prefer however to extend the numerical treatment used in connection with our figures 3.9 and 3.10. In that treatment physically realistic properties can be attributed to individual stickers and also more realistic segment force laws then our equation 3.17 can be introduced. The only price that have to be payed here is that with such modifications the model will be no longer have a closed analytical form. Such, however is an exception in rheological modeling, anyhow.

Additional refinement of the model is possible. In particular the assumption that released segments transfer instantaneously into their equilibrium state is rather artificial. It would be more realistic to introduce here some kind of reptation time for the chain ends. Although such is probably possible we did not introduce this. The assumption is in the spirit of classical transient network theory, moreover, since the main contribution to the stress is due to the active segments, we do not expect a substantial improvement of the model by this refinement.

Other modifications could be: the introduction of additional mechanisms like stress release, non-affine motion *etc.*, we still believe, however that the basis principles as outlined in this paper are the essential elements describing the linear viscoelastic behavior of weak polymer gels.

3.8   Appendix: Derivation of equation eq 3.15

By eq 3.9, 3.12 and 3.13

$$\frac{\delta}{\delta t}\mathbf{S}_s^i + \zeta_s^i(\mathbf{S}_s^i - \mathbf{S}^0) = \sum_{s'}\chi_{ss'}^i(\mathbf{S}_{s'}^i - \mathbf{S}_s^i) \tag{3.36}$$

with

$$\zeta_s^i = \sum_{s'}\frac{n_{s'}}{n_s}A_{ss'}v_s^i(1 - v_{s'}^i) \tag{3.37}$$

and

$$\chi^i_{ss'} = \frac{n_{s'}}{n_s} A_{ss'} v^i_s v^i_{s'} \qquad (3.38)$$

so

$$\frac{\delta}{\delta t}(\mathbf{S}^i_s - \mathbf{S}^0) + \zeta^i_s(\mathbf{S}^i_s - \mathbf{S}^0) + \sum_{s'}\chi^i_{ss'}(\mathbf{S}^i_s - \mathbf{S}^0) = \sum_{s'}\chi^i_{ss'}(\mathbf{S}^i_{s'} - \mathbf{S}^0) + 2\frac{kT}{\kappa}\mathbf{D}$$

$$\frac{\delta}{\delta t}(\mathbf{S}^i_s - \mathbf{S}^0) + \sum_{s'}\zeta^i_{s'}\delta_{ss'}(\mathbf{S}^i_{s'} - \mathbf{S}^0) + \sum_{s'}\sum_{s''}\chi^i_{s's''}\delta_{ss'}(\mathbf{S}^i_{s'} - \mathbf{S}^0) = \sum_{s'}\chi^i_{ss'}(\mathbf{S}^i_{s'} - \mathbf{S}^0) + 2\frac{kT}{\kappa}\mathbf{D}$$

$$\frac{\delta}{\delta t}(\mathbf{S}^i_s - \mathbf{S}_0) + \sum_{s'}\beta^i_{ss'}(\mathbf{S}^i_{s'} - \mathbf{S}^0) = 2\frac{kT}{\kappa}\mathbf{D}$$

where $\frac{\delta}{\delta t}$ is an upper convective derivative (so $\frac{\delta}{\delta t}\mathbf{S^0} = -2\frac{kT}{\kappa}\mathbf{D}$) and

$$\begin{aligned}
\beta^i_{ss'} &= (\zeta^i_{s'} + \sum_{s''}\chi^i_{s's''})\delta_{ss'} - \chi^i_{ss'} \\
&= \sum_{s''}\frac{n_{s''}}{n_{s'}}A_{s's''}\left(v^i_{s'}(1 - v^i_{s''}) + v^i_{s'}v^i_{s''}\right)\delta_{ss'} - \frac{n_{s'}}{n_s}A_{ss'}v^i_s v^i_{s'} \\
&= \sum_{s''}\frac{n_{s''}}{n_{s'}}A_{s's''}v^i_{s'}\delta_{ss'} - \frac{n_{s'}}{n_s}A_{ss'}v^i_s v^i_{s'} \\
&= \sum_{s''}\frac{n_{s''}}{n_s}A_{ss''}v^i_s\delta_{ss'} - \frac{n_{s'}}{n_s}A_{ss'}v^i_s v^i_{s'} \\
&= \frac{\dot{n}_s}{n_s}v^i_s\delta_{ss'} - \frac{n_{s'}}{n_s}B^i_{ss'}
\end{aligned}$$

3.9 References

[1]   Bird, R.B.; Curtiss, C.F.; Amstrong, R.C.; Hassager, O. In *Dynamics of Polymeric Liquids, volume 2*, Wiley, New York, 1987.

[2]   Doi, M.; Edwards, S.F. In *The theory of polymer dynamics*, Clarendon, Oxford, 1986.

[3]   González, A.E. *Polymer* **1983**, 24, 77-80.

[4]   Green, M.S.; Tobolsky, A.V. *J. Chem. Phys.* **1946**, 14, 80-89.

[5]   Groot, R.D.; Agterof, W.G.M. *J. Chem. Phys.* **1993**, 100, 1657-1664.

[6]   Kampen, N.G. van. In *Stochastic Processes in Physics and Chemistry*, North Holland, Amsterdam, 1992.

[7]   Leibler, L.; Rubinstein, M.; Colby, R.H. *Macromolecules* **1991**, 24, 4701-4707.

[8]   Lodge, A.S. *Ind. Eng. Chem. Res.* **1995**, 34, 3355-3358.

[9]   Lodge, A.S. *Trans. Faraday Soc.* **1956**, 52, 120-130.

[10]   Oppenheim, I.; Shuler, K.E.; Weis, G.H. *Advan. Relaxation Processes* **1967**, 1, 13-68.

[11]   Phan-Thien, N. *J. Rheol.* **1978**, 22, 259-283.

[12]   Rubinstein, M.; Semenov, A.N. *Macromolecules* **1998**, 31, 1386-1397.

[13]   Rubinstein, M.; Semenov, A.N. *Macromolecules* **1998**, 31, 1373-1385.

[14]   Brule, B.H.A.A. van den; Hoogerbrugge, P.J. *J. Non-Newtonian Fluid Mech.* **1995**, 60, 303-334.

[15]   Wientjes, R.H.W.; Jongschaap, R.J.J.; Duits, M.H.G.; Mellema, J. *J. Rheol.* **1999**, 43, 375-391.

[16]   Wientjes, R.H.W.; Duits, M.H.G.; Jongschaap, R.J.J.; Mellema, J. *Macromolecules* **2000**, 33.

[17]   Yamamoto, M. *J. Phys. Soc. Jpn.* **1956**, 11, 413-421.

Chapter 4

Linear Rheology of Guar Gum Solutions

4.1 Synopsis

We have investigated the linear viscoelastic behaviour of Guar gum solutions as a function of frequency, temperature, polymer concentration and molecular weight. This was done to sort out the importance of different relaxation mechanisms like reptation or the breakup of physical bonds. In the kiloHertz regime, Rouse behaviour is observed. At lower frequencies, two storage modulus plateau zones were found, indicating two additional relaxations. One is operative between 1 and 100 Hz, and gives rise to a very broad relaxation spectrum, even for monodisperse Guar. Describing the dependencies of the relaxation time and low-shear viscosity on concentration and molecular weight with power laws resulted in unusually high coefficients. The second relaxation becomes manifest below 0.01 Hertz and has not been earlier reported. Here the temperature dependence is very strong whereas all other dependencies are weak. Analyzing the experiments with existing models for transient polymer networks revealed that at best a partial decription of the experimental dependencies can be obtained. It was concluded that at least two different relaxation mechanisms must play a role, classical reptation not being one of these. Best overall predictions were obtained with a model assuming two types of associations. However, also the picture of starpolymer-like structures held together via bonds with a long lifetime could give comparable predictions. For a further distinction between these mechanisms more information about the mesoscopic structure is needed.

4.2   Introduction

Galactomannans are water-soluble polysaccharides found in the seed endosperm of a variety of legumes. They consist of a (1→4)-linked β-D-mannopyranosyl backbone partially substituted at O-6 with α-D-galactopyranosyl side-groups[6]. One Galactomannan which is widely used as an industrial hydrocolloid is Guar gum which has a Mannose : Galactose ratio of 1.55. In connection to its use as a thickener in food products, several research groups have investigated the rheology of Guar gum solutions[8,9,23,26,27].

In a rheological study of Ross-Murphy[28] where start shear behavior and the validity of the Cox-Merz rule were investigated, it was concluded that Guar gum solutions behave like an entangled solution, as described by Doi and Edwards[7]. This conclusion was drawn in spite of earlier observations of Richardson and Ross-Murphy[26] who noted the onset of a transition at low shear rates (0.01 s^{-1}), although the Newtonian low-shear plateau had already been reached. Robinson *et al.*[27] mentioned a strong nonlinear dependence of the specific viscosity upon concentration. From this it was concluded that not only purely topological entanglements, but also specific attractive polymer-polymer interactions must play a role. Indications for this were also obtained by Goycoolea *et al.*[15] and by Gidley *et al.*[13] who attributed a crucial role to the α-D-Galactose side groups in the process of network cross-linking by semi helix-helix aggregation.

From this short overview it is clear that the rheological behavior of Guar gum solutions is still incompletely understood and that specific polymer-polymer interactions might play a role in the observed rheological behavior as well as reptation phenomena. To sort out the importance of different relaxation mechanisms, we have systematically investigated the linear viscoelastic behavior as a function of frequency, concentration, temperature and molecular weight. To support interpretation we have characterized the molecular properties by using GPC, intrinsic viscosity measurements and several microscopy techniques. In this paper we will compare the linear viscoelastic behavior with predictions from existing microrheological models that take into account topological constraints and/or physical bonds.

The chapter is further organized as follows: In section 4.3 the preparation of the solutions, the microscopic characterizations and the rheological measurement techniques are discussed. In section 4.4 the experimental results are shown. These results will be compared to rheological models in section 4.5, followed by a discussion in section 4.6, after which conclusions will be drawn in section 4.7.

4.3   Experimental

4.3.1   Materials

Guar gum [Meyhall] was purified from a commercial flour using a modification of the method of McCleary *et al.*[4]. Crude Guar gum (10 g) was treated with 200 ml of boiling, aqueous 80 % ethanol for 10 min. The obtained slurry was collected on a glassfilter (no. 3) and washed successively with ethanol, acetone and ether. This material was added to 1 liter of demiwater and allowed 1 hour to hydrate. It was then stirred with a foodblender (125 W), homogenized (1 minute) and centrifuged at 2300 g for 15 min. The supernatant was precipitated in two volumes of cold acetone. After redissolving in hot water, the polymer solution was ultracentrifuged at 82000 g for 1.5 hour at room temperature. The supernatant was precipitated with two volumes of ethanol. The precipitate was collected on a glassfilter (no. 4) and washed with ethanol, acetone and ether before freeze-drying. This lead to almost monodisperse purified Guar gum. Only one batch of Guar was purified in this laborious way, to get a monodisperse system. Solutions of this material were prepared by adding known weights of the dry Guar to twice distilled water, and allowing it to hydrate for extended periods (several days) to ensure that the sample had completely dissolved. This was done at a temperature of 277 K for concentrations between 0.4 (w/w)% and 2.0 (w/w)%. We will refer to this purification and dissolving method as procedure I. For the purpose of characterization with Mark Houwink plots, three Guar gums with different molecular weights [Meyhall] were purified with a less laborious but otherwise similar procedure. Here crude Guar gum (10.0 g) was suspended in 1 liter of demiwater and stirred with a foodblender (125 W) for 1 minute. The obtained solution was placed in a refrigerator for 24 hours and then centrifuged at 22000 g for 5 hours. 800 ml of the obtained supernatant was precipitated in two volumes of cold acetone. The precipitate was collected on a glassfilter (no. 4) and washed with ethanol, acetone and ether. The so obtained purified Guar gum was freeze-dried and dissolved as described in procedure I. This procedure is called procedure II.

Using these procedures led to very long dissolving times. To shorten this, a third purification and dissolving procedure was used. In this procedure four different Guar gums [Meyhall] with different molecular weights were purified by adding 10.0 g to 400 g acetate buffer of pH 4.66 [Merck]. The slurry was homogenized for 75 seconds with a foodblender (500 W) and centrifuged at 22000 g for 5 hours at room temperature. The supernatant (typical concentration 2% w/w) was used as a stock solution from which lower concentrations were obtained via dilution. This is procedure III. Several control experiments revealed that the rheological behavior was not significantly changed on switching from procedure II to III.

4.3.2   Molecular characterization

The molecular weights of the purified Guar gums using procedure I and II were determined by GPC-MALLS-RI (multi angle laser light scattering). The Guar was dissolved in a 50 mM phosphate buffer with pH 8.0 to a concentration of 0.1 % (w/w) and filtered through a 0.45 μm filter prior to injection. At the exit of the GPC column the (instantaneous) values of M and R_g were detected on line. The results are summarized in table 4.1.

Table 4.1: Molecular weights for via procedure I and II prepared samples

Guar	M_w[kD]	M_w/M_n
HM	1048	1.02
150	1400	1.1
90	1000	1.5
30	350	1.7

The mannose/galactose ratio of Guar HM/150/90/30 was determined by HPLC after hydrolysis of the polymer to be 1.59 ± 0.05.
Molecular weights of the Guar gums, obtained via procedure II were obtained from intrinsic viscosity measurements. These experiments were done with an Ubbelohde capillary viscometer [Scott, type 532 01 / 0A].
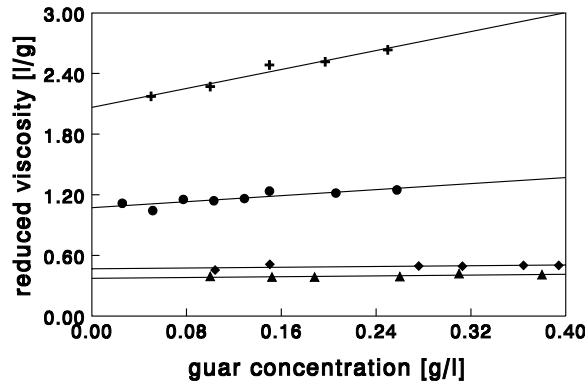
Figure 4.1: Reduced viscosity measurements. ▲ :Guar 30 ◆ :Guar 30 duplo ● :Guar 90 + :Guar 150

From the reduced viscosity measurements, intrinsic viscosities were obtained using the Huggins equation:

$$\eta_{red} = \frac{\frac{\eta}{\eta_s} - 1}{c} = [\eta] + h_c[\eta]^2 c \tag{4.1}$$

Here c is the concentration Guar gum, η_{red} is the reduced viscosity, η_s is the solvent viscosity and $[\eta]$ is the intrinsic viscosity. h_c is the so called Huggins coefficient which is a polymer constant which usually lies in the range 0.5-0.8. The Huggins coefficient was determined for all the curves and turned out to be constant within the experimental error range: 0.55 ± 0.05, which is within the expected range. With the obtained intrinsic viscosities we made a Mark-Houwink plot (figure 4.2) and found the Mark-Houwink constants k_{MH} and α to be $(6.7 \pm 1.1) \cdot 10^{-7}$ l/g and 1.05 ± 0.01. This relation was used later as a calibration curve to determine the molecular weights from intrinsic viscosity measurements for the samples made by purification procedure III.
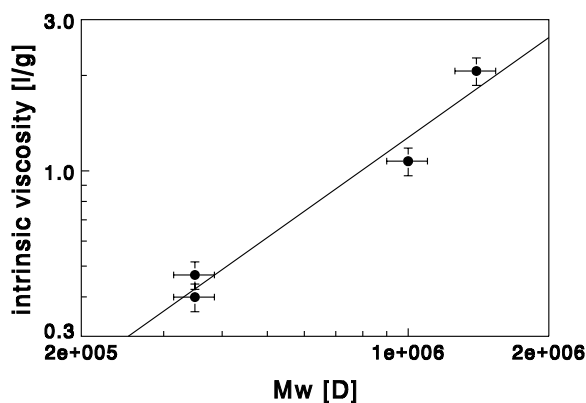
Figure 4.2: Mark Houwink plot

The critical concentration where overlap between polymer chains starts to occur (c^*) and the intrinsic viscosities for the, via preparation procedure III obtained samples, were obtained from specific viscosity measurements $(\frac{\eta}{\eta_s} - 1)$ as a function of concentration. Figure 4.3 shows a typical result. From these results we determined $c^* [\eta]$ to lie around 2 which is comparable to earlier findings of others[19].

In table 4.2, the measured intrinsic viscosities, calculated molecular weights and critical concentrations are listed.

Table 4.2: [η], M_w and c^* for the via procedure III prepared samples

Guar	[η][l/g]	M_w[kD]	c^*[g/l]
150	1.217	910	1.3
90	0.958	730	2.8
60	0.510	400	4.5
30	0.333	270	4.5
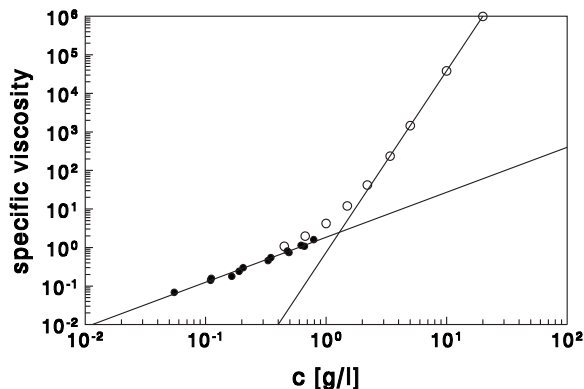
Figure 4.3: Determination of c^* of Guar 150.   • :Ubbelohde measurements
○ :Contraves Low Shear 40 measurements

All measurements other than characterizations were performed at concentrations higher than c^*. Typically, three concentrations were investigated for each Guar system, with the upper limit set by the extent to which the sample was sufficiently fluid-like to be manipulated.

4.3.3 Mesoscopic observations

To obtain information about the mesoscopic structure of the Guar gums we used three microscope methods. AFM and replica-TEM did not provide information from the bulk structure since surface and pre-treatment effects were involved.

To obtain more direct information about the mesoscopic structure as present in solution, we labeled Guar gum with RhodamineIsoThioCyanate[1,14] and observed the solution with a Confocal Scanning Laser Microscope via detection of the fluorescence of RITC. Since no inhomogeneities could be observed within the resolution of the instrument, it can be concluded that the Guar gum solutions must be homogeneous at least down to lengthscales of 1 μm.

We also attempted NMR to detect hydrogen bridges and DSC to locate a possible phase transition, but without providing conclusive evidence. Also light scattering experiments gave no useful information, since the solutions were too turbid.

4.3.4 Macroscopic rheological measurements

Linear viscoelastic moduli measurements between 10^{-3} Hz and 2 10^1 Hz and as a function of the temperature were performed using a Bohlin VOR with a cone and plate geometry (cone angle of 1° and 60 mm plate diameter). Measurements were

conducted at 6 temperatures ranging from 10 to 60 ^{0}C. To avoid effects of solvent evaporation, a home-made vapor lock filled with paraffin oil was used. A correction was made for the temperature dependence of the gap width (-1.9 $\mu m/^0$C) between cone and plate. In order to exclude inaccurate measurements, we checked the Bohlin VOR with two Newtonian fluids: water and a Baysilon oil (Bayer) with a viscosity of 300 mPas. These testsamples showed correct results, including the limiting behavior of G' and G'' for low frequencies. Further on, we ensured that all measurements resulted in data that were clearly in the range of the torque resolution (2.35 10^{-5} Nm). A 10 ml syringe was used to insert the sample. After insertion the sample was presheared at 80 1/s for 1 minute to obtain a homogeneously filled gap and to define the mechanical history of the sample. Then the sample was allowed to relaxate for 30 minutes before the measurements were started.

Linear viscoelastic measurements were also performed at high frequencies, using three torsion resonators and a nickel tube resonator. Those instruments were developed in our laboratory and details on design and principle can be found in Oosterbroek *et al.*[24], Blom and Mellema[2] and van den Ende *et al.*[10]. With those instruments, dynamic moduli of weak gels can be measured at a discrete set of frequencies between 70 Hz and 250 kHz, at ambient temperatures. To allow interpretation of the results the surface loading criterion should be satisfied[10]. This means that the shear wave generated by the torsion bar must be damped significantly before it is reflected by the walls of the container. For the in this paper presented data, this criterion was satisfied.

Measurements of the viscosity as a function of shear rate were performed at $10°C$, using a Contraves Low Shear 40. A Couette geometry was used, with inner and outer radii of respectively 5.5 and 6.0 mm.

4.4 Results

Our rheological measurements were done with the focus to distinguish between different possible relaxation mechanisms via comparison of the results with predictions from microrheological models. To get an overview we started the investigation by measuring the frequency dependence over an extended range. The results showed two storage modulus plateau zones with different temperature dependencies. These plateau's were investigated further as a function of the polymer concentration and the molecular weight.

4.4.1 Frequency behavior

To map out the frequency domain we first measured the frequency dependence of a 0.4 (w/w) % monodisperse Guar HM solution. For this system it was possible to

cover 8 decades in frequency by using the Bohlin VOR, the torsion resonators and the nickel tube resonator. As shown in figure 4.4 the data obtained from the different instruments connect well to a smooth curve.
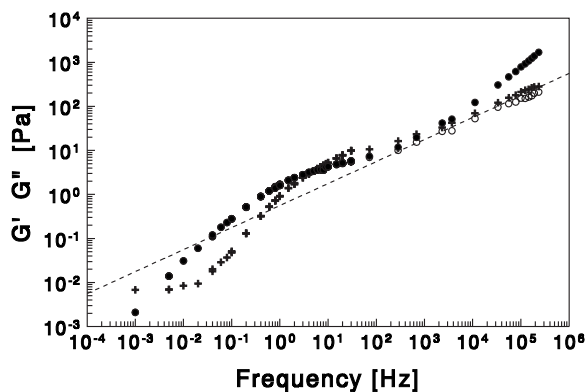
Figure 4.4: Linear viscoelastic behavior of a monodisperse 0.4 % (w/w) Guar HM solution, measured at 25 °C over an extended frequency range. The dashed line corresponds to Rouse behavior. $+$:G' $\bullet$:G" $\circ$:G"$_{guar}$

We corrected $G''(\omega)$ for the contribution of the solvent, to allow for analysis of the loss modulus of the Guar only: G''_{guar}. This correction was significant for frequencies above 10^4 Hz. The $G'(\omega)$ and the corrected $G''(\omega)$ data shown in figure 4.4, make it clear that, at high frequencies, the agreement with the frequency scaling of the Rouse model[29] is very good. Both moduli follow a slope of 0.5 in the log-log plot. At frequencies below 10^3 Hz two plateau zones for the storage modulus can be observed (at 10^{-2} and 10^1 Hz). To the best of our knowledge, this is the first time a storage modulus plateau for Guar gum solutions at very low frequencies is reported.

4.4.2   Scaling with temperature

For the temperature range studied, it turned out that all investigated samples showed a very similar frequency dependence above 0.03 Hz. Therefore it was possible to obtain temperature mastercurves by scaling the moduli curves, measured at different temperatures, along the frequency axis. Figure 4.5 shows an example of the obtained mastercurves for $G'(\omega)$ and $G''(\omega)$. Especially from these reduced plots it becomes evident that at low frequencies, the storage moduli show a different temperature dependence. A plateau is observed for $G(\omega)$, with a magnitude that increases strongly with temperature. Remarkably enough, the loss modulus $G'(\omega)$ does not show these deviations in the scaling behavior with temperature. Its slope in the log-log plot amounts 0.8 which is close to the limiting behavior. Thus it corroborates that only the onset of the low frequency relaxation is observed, and that the characteristic fre-

quency must correspond to very long timescales ($> 10^3$ s). A salient detail of the relaxation spectrum within the Hz-range is that it is rather broad. This wide range of relaxation times cannot be caused by polydispersity, since Guar HM was almost monodisperse (see table 1).
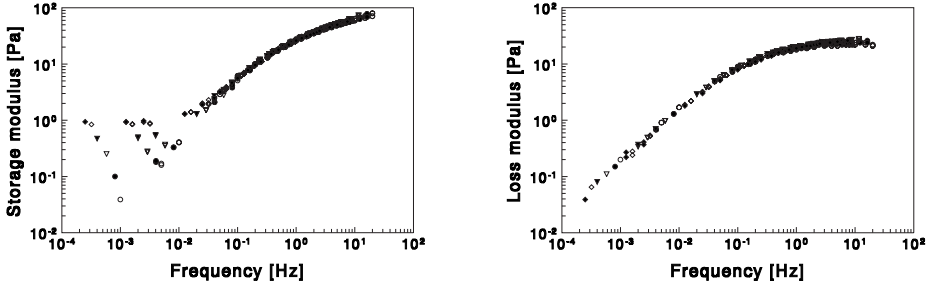
Figure 4.5: Moduli mastercurves for a 1.0 % monodisperse Guar HM solution (procedure I).Temperatures in $°C$: ♦ :60 ◇ :50 ▼ :40 ▽ :30 • :20 ∘ :10.

From the obtained frequency scaling (for frequencies above 0.03 Hz.) an Arrhenius plot was made, i.e. according to:

$$a_T = \exp(\frac{E_{ap}}{k} \left[\frac{1}{T} - \frac{1}{T_{ref}} \right])$$ (4.2)

Here a_T is the frequency multiplication factor needed to shift the moduli curves measured at temperature T to the modulicurves at temperature T_{ref}. E_{ap} is the apparent activation energy whereas k is the Boltzmann constant. Figure 4.6 shows a typical result.
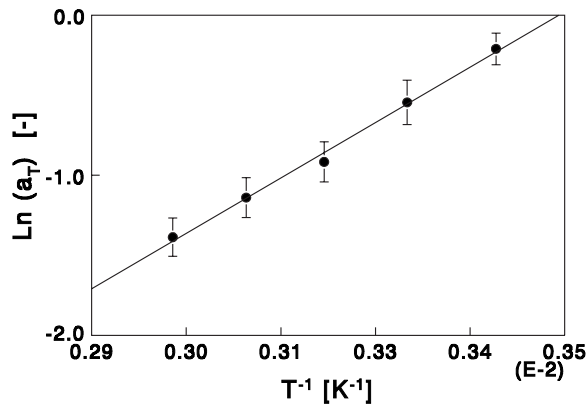
Figure 4.6: Arrhenius plot of the 1 % (w/w) monodisperse Guar HM sample.

From the slope, the apparent activation energy was obtained to be 10.0 ± 0.5 kT (at T= 283 K). It turned out that this apparent activation energy does not depend

on the molecular weight or the Guar gum concentration. Within the experimental error-range always (for all Guars listed in table 4.1 and 4.2 and all investigated concentrations) the same apparent activation energy was obtained.

4.4.3   Scaling with concentration and molar mass

To investigate the rheological behavior further so that comparison with micro-rheological models becomes possible, we studied the moduli and flowcurves as a function of concentration and molecular weight. It turned out that the shape of the moduli curves at frequencies above 0.03 Hz was independent of both. To illustrate this we scaled a 4 % Guar 30 solution on top of a 0.5 % Guar 150 solution in figure 4.7:
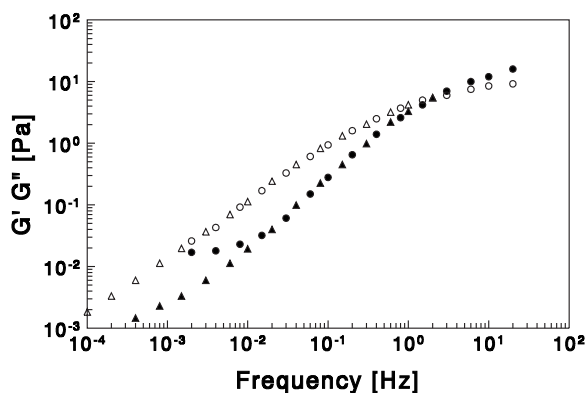
Figure 4.7: Mastercurves of 4 % (w/w) Guar 30 ($\blacktriangle, \triangle$) and 0.5 % (w/w) Guar 150 ($\bullet, \circ$) solutions. $\blacktriangle, \bullet$: storage moduli $\circ, \triangle$:loss moduli

Due to this independence, all points within a curve (except for frequencies below 0.03 Hz) can be scaled onto a mastercurve. This makes it possible to extrapolate some curves to high frequencies. Especially interesting is that it also allows for an analysis of the concentration and molar mass dependence by considering just the scale factors. The point where $G'(\omega)$ crosses $G''(\omega)$ is very suitable for both the scaling itself and for the analysis. The inverse of the crossover frequency can be seen as a characteristic time (denoted as $\tau_{G'=G''}$). The magnitude of $G'(\omega)$ at this point (denoted as $G'=G''$) can be seen as a representation of the characteristic strength of the relaxation(spectrum). It is proportional to the high frequency storage modulus in the absence of Rouse relaxations. The scaling results for $\tau_{G'=G''}$ and the relaxation strength as a function of concentration and molar mass are shown in figure 4.8 and 4.9.

Also the flow curves were measured as a function of concentration and molecular weight. An example of the flow curves of Guar 150 is shown in figure 4.10.
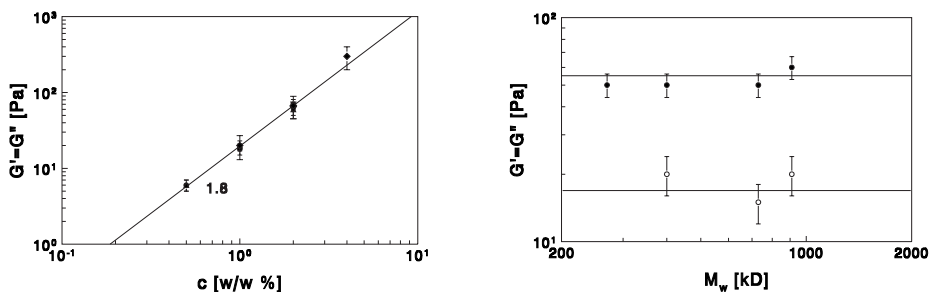
Figure 4.8: Storage modulus plateau *versus* Guar gum concentration (left) and molecular weight (right).Numbers indicate power law coefficients. left: • :Guar 150 ▲ :Guar 90 ▼ :Guar 60 ♦ :Guar 30right: • : 2 % (w/w) ∘ : 1 % (w/w)
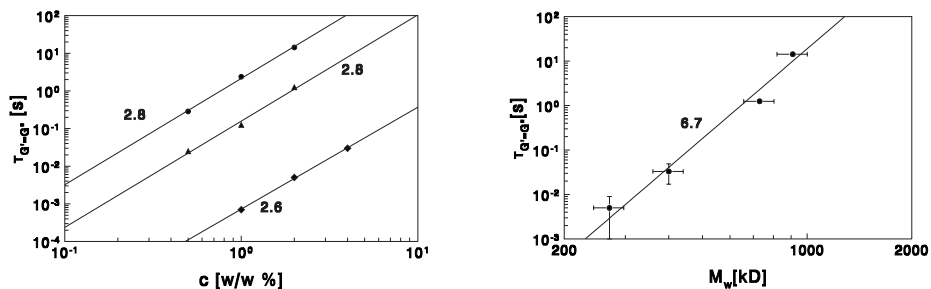
Figure 4.9: $\tau_{G'=G''}$ *versus* Guar gum concentration (left) and molecular weight (right). Numbers indicate power law coefficients. left: • :Guar 150 ▲ :Guar 90 ▼ :Guar 60 ♦ :Guar 30right: • :2 % (w/w)
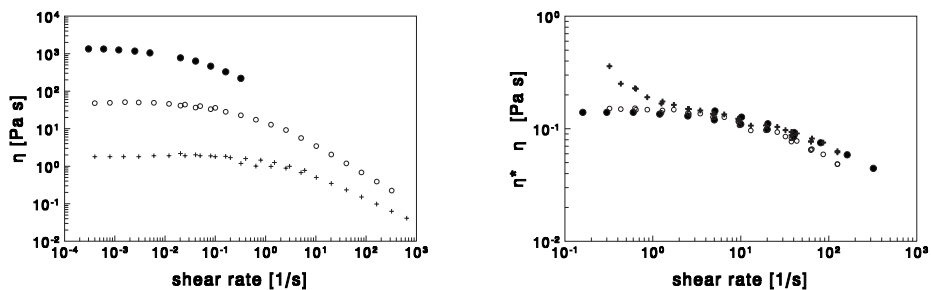
Figure 4.10: Left: Flowcurves for Guar 150 at 10 °C measured with the Contraves LS 40 (low shear rates) and the Bohlin VOR (high shear rates).• : 2.0 % (w/w) ∘ : 1.0 % (w/w) + : 0.5 % (w/w). Right: Cox-Merz rule. · : $\eta(\dot{\gamma})$ ∘ : η' + : η^*

The zero shear viscosities $\eta\,(\dot{\gamma} \to 0)$ obtained from the flow curves were found to correspond well to the low frequency limits of $\eta'(\omega \to 0)$ estimated from $G''(\omega)$ curves (figure 4.10). Such a correspondence is expected for materials that show liquid-like behavior at long timescales. It is also interesting to investigate the applicability of the Cox-Merz rule[5]. This empirical rule, stating that

$$| \eta^*(\omega) | = \sqrt{\left(\frac{G'}{\omega}\right)^2 + \left(\frac{G''}{\omega}\right)^2} = \eta\,(\dot{\gamma}) \quad for \quad \omega = \dot{\gamma} \tag{4.3}$$

does not apply to our Guar solutions. We found that $| \eta^*(\omega) | \geqslant \eta\,(\dot{\gamma})$ for $\omega = \dot{\gamma}$, which obviously is due to the contribution of $G'(\omega)$ since $G''(\omega) \approx \eta\,(\dot{\gamma})\,\omega$ as mentioned before.

The power law scaling of the zero shear viscosity with the Guar gum concentration and the molecular weight is shown in figure 4.11.
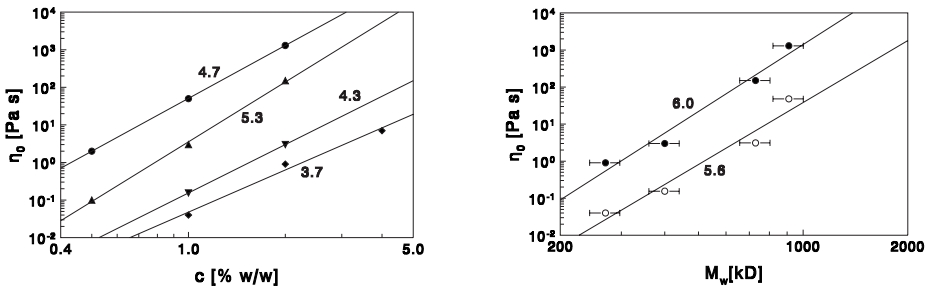
Figure 4.11: Zero shear viscosity zero shear viscosity *versus* Guar concentration (left) and molecular weight (right). Numbers indicate power law coefficients.left: • :Guar 150 ▲ :Guar 90 ▼ :Guar 60 ♦ :Guar 30right: • :2 % (w/w) ∘ :1 % (w/w)

In table 4.3 an overview of the measured scaling relations is given:

Table 4.3: Power law scaling of linear rheological quantities. Uncertainty ranges include differences between Guar batches

scaling	M_w	c
η_0	5.8 ± 0.2	4.5 ± 0.8
$G_{G'=G''}$	0	1.8 ± 0.1
$\tau_{G'=G''}$	6.7 ± 0.8	2.7 ± 0.2

4.4.4 Low frequency behavior

One of the most astonishing observations we already presented is the storage modulus plateau at low frequencies. Although differences from the limiting linear viscoelastic behavior were observed earlier by Richardson and Ross-Murphy[26], a second storage modulus plateau at low frequencies has not been reported before. It can be seen from figure 4.5 that the temperature dependence of this plateau zone is rather strong. Further investigations show that there is no clear dependence on concentration and molecular weight as can be seen in table 4.4:

Table 4.4: Storage modulus plateau at low frequencies. lmv=lowest measured G' value

Guar	Solvent	M_w [kD]	c [w/w %]	$G_{low\ plateau}$ [Pa]
HM	bidest water	1048	2.0	lmv=1
HM	bidest water	1048	1.0	0.5
HM	bidest water	1048	0.5	0.5
150	acetate buffer*	910	2.0	lmv=0.8
150	acetate buffer*	910	1.0	0.20
150	acetate buffer*	910	0.5	0.15
90	acetate buffer*	730	2.0	lmv=0.1
90	acetate buffer*	730	1.0	0.20
90	acetate buffer*	730	0.5	0.15
30	acetate buffer*	270	4.0	0.02
30r	acetate buffer*	270	4.0	0.02
30	acetate buffer*	270	2.0	0.08
30r	acetate buffer*	270	2.0	0.04
30	acetate buffer*	270	1.0	lmv=0.005
30r	acetate buffer*	270	1.0	lmv=0.005

*: acetate buffer was used to allow comparison with a future study. The buffer did not show any other influence than to optimize the performance of an enzyme to be added.

From these data we can conclude that there is only a very weak concentration dependence with a scaling power of 0.5 or less. Also, we can observe some correlation with molecular weight, but this dependence is not too clear.

4.5 Comparison with microrheological models

For the first time a low frequency plateau in G' has been observed. We have observed it for differently prepared samples (including a different purification), and at different

concentrations. The clear temperature dependence of this G' plateau demonstrates that the associated stress relaxation is one of a dynamic structure and not that of e.g. a permanent rubber like structure. In this context we also like to note that the magnitude of the elasticity is small and that a slight shearing of the fluid is sufficient to make the plateau disappear for 15 minutes. Analogous behavior was found in other associating ionomers[35]. This also indicates that this behaviour is of structural origin. We have attempted to interpret the variety of observations discussed in the previous section, in the sense of identifying relaxation processes and proposing corresponding mesoscopic structure(s). Obviously a wealth of information on the structure and relaxations is contained in the measured rheological data themselves. But the problem is how to disclose it.

Our first approach has been to obtain a focus for this, based on physical characterizations of the polymer structure at the mesoscopic level. Several microscopy techniques (CSLM, Replica-TEM and AFM) were applied but no conclusive evidence about the structure at mesoscopic lengthscales could be obtained, other than that the Guar solutions appeared to be homogeneous down to micrometer lengthscales (see section 4.3.2).

Characterizations of the chemistry of the polymer in solution can also be used to guide interpretation. Guar gum is a Galactomannan chain with free Mannose backbone parts. Combining this with the empirical relation between solubility and the galactose/mannose ratio of Galactomannans, it is implied that the free Mannose backbone parts have the tendency to form bonds when dissolved into water. Another characteristic is that all our samples were prepared above the critical overlap concentration.

Using this information we have analyzed our rheological measurements by comparing them to predictions of existing models in polymer rheology. In this comparison we have considered the dependencies on temperature, concentration as well as molar mass, to allow for a maximal distinction between the predictions according to different models. We realize that the scope of such a comparison still has its limitations. Although several models have been proposed to describe the linear rheological behavior of polymer networks, many of these contain idealizations that may not apply to a polymer solution from practice, like Guar gum. Therefore a comprehensive mapping between one of these models and our observations is not to be expected. In the following we will investigate which of the existing models gives predictions that bear the closest resemblance to our observations.

The appearance of two storage modulus plateau zones indicates the occurrence of two distinct mechanisms for relaxing the stresses imposed via the oscillatory deformation. In a polymer network, stresses are induced via distortions of the chain distribution function. This can involve both the orientation and the length of chains or chain strands. Since our polymer solutions are all above c^*, and since physical

associations between polymer chains can be expected, two mechanisms that should be considered at first are the breakup of bonds, and diffusion of chain (strands) out of confining tubes (reptation). To take into account the possibility that the two types of relaxation are independent, we will first compare our measurements with models that predict only one relaxation. Thereafter, coupled relaxations will be considered.

4.5.1 Reptation model

For fluids containing entanglements, one of the possible relaxation mechanisms to consider is the diffusion of chains along their contours. This process, called reptation has been modeled by Doi and Edwards[7]. In this model the chains do not form physical bonds with each other, but there are topological constraints which restrict the transversal motion of chains.

The reptation model predicts one storage modulus plateau and a relaxation spectrum spanning approximately 1 decade. Comparing the predictions of the Doi-Edwards model with our experimental observations for the monodisperse system (shown in figure 4.5), it is clear that the model is not able to describe the experimental high frequency relaxations, which span almost 3 decades in frequency.

Table 4.5: Predicted scaling behavior, according to reptation. Numbers between brackets indicate experimental values.

reptation scaling	M_w	c
η_0	**3** (5.8)	**3.75** (4.5)
$G_{G'=G''}$	**0** (0)	**2.25** (1.8)
$\tau_{G'=G''}$	**3** (6.7)	**1.5** (2.7)

Other discrepancies become evident from the comparison presented in table 4.5. According to the reptation model, the scaling of $\tau_{G'=G''}$ and the zero shear viscosity (with the polymer concentration and the molecular weight) would correspond to much weaker powers than observed in the experiments. An exception is the *scaling* of the magnitude of the moduli, but considering the *magnitude* of the storage modulus G_0, again a discrepancy is found. According to the model, the number of steps in a primitive chain $\frac{L}{a}$ (the number of tube segments) follows from G via :

$$G_0 = N_c \frac{L}{a} kT \tag{4.4}$$

with N_c the number of chains per unit volume. Here a is parameter which is of the order of the mesh size of the network which defines the tube. When we take for example the storage modulus of 20 Pa for the 0.5 % (w/w) Guar HM solution, we obtain a number of steps in the primitive chain equal to 2. Obviously the concept of

a confining tube, which forms a key element in the reptation model can only hold for $\frac{L}{a} >> 1$.

Considering the various discrepancies it can only be concluded that our observations for the linear rheological behavior cannot be interpreted with "simple" reptation (i.e. as described by Doi and Edwards[7]), not even when restricting to a certain part of the frequency domain (0.03-100 Hz).

4.5.2   Associative polymer solution model

Recently Bromberg[3] and English *et al.*[11,12] reported experimental studies on the rheological behavior of associative polymers. Some observations with a striking similarity to ours were made in these investigations. Bromberg[3] found an unusually strong temperature dependence for the storage modulus, comparable to the temperature dependence we found for $G'(\omega)$ at low frequencies. English *et al.*[11] found storage moduli that were not proportional to ω^2 in the low frequency regime, where this limiting behavior is usually observed. Instead they observed a slope of 0.7 in a log-log plot. Also this is in qualitative accordance with our observations. Already in the beginning of section 4.5 we have argued that chain associations are to be expected on molecular grounds. These notions make it interesting and appropriate, to consider predictions of rheological models developed for associative polymers.

In 1998 Semenov and Rubinstein presented a comprehensive modeling for associative polymer solutions, including predictions for linear viscoelastic behavior[30,31,32]. Polymers with associative sites (stickers) along the chain will form clusters in solution. Above a certain threshold concentration c_g, the clusters will connect to a space-filling network. We will discuss only the two possible regimes above this treshold concentration, since only there a storage modulus plateau zone is predicted, which can be compared to our experimental $G'(\omega)$ data above 10 Hz.

Just above the gel concentration c_g, the network consists of large clusters which are singularly connected with each other via so called 'critical bonds'. When such a bond is broken, a cluster is released from the network and will quickly relax its stress in a Rouse-like manner. The relaxation time is then determined by the time it takes to break up the critical bonds (see figure 4.12 for an illustration). At higher polymer concentrations, a strong transient network will be formed, in which each chain is multiply connected to other chains in the network. Here critical bonds do not exist anymore and the relaxation process has become the multiple breakup of bonds before chains can undergo Rouse relaxation. To investigate the applicability of the Semenov and Rubinstein (S&R) model we consider both regimes in the following.

Weak network regime

To make a comparison with the model we have assumed that for all molecular weights
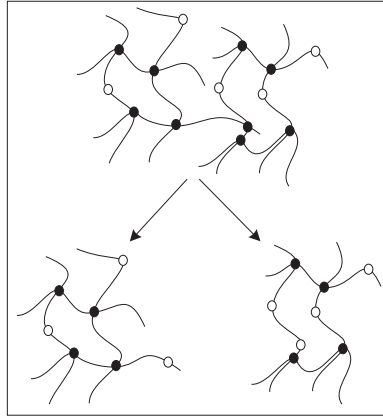
Figure 4.12: Cartoon of the breakup of a critical bond

and concentrations, our samples were just above the gelation threshold. The number of stickers per chain is expected to increase proportionally with the molecular weight. According to S&R[32], c_g is then proportional to the chainlength to the power $(1 - 3\nu)/(1 + z)$, with $\nu = 0.59$ and z depending on the solvent quality. Assuming good solvent conditions for the chain without stickers, $z = 0.225$. The scaling of the storage modulus plateau G_0 can then (using equation 3.16 of S&R[32]) be expressed as:

$$G_0 \sim \widetilde{c}\widetilde{M}^{-1} \left(\widetilde{c}\widetilde{M}^{0.63} - 1 \right)^3 \tag{4.5}$$

with $\widetilde{c} \equiv c/c_g^0$, $\widetilde{M} \equiv M/M_0$ and c_g^0 the value of c_g at reference molar mass M_0. According to equation 5, the dependence of G_0 on c or M will not show linearity in a log-log plot. However in the limiting case of $\widetilde{c}\widetilde{M}^{0.63} \gg 1$ the local slopes will be minimal, being 4 for the concentration dependence and 0.89 for the molar mass. For smaller $\widetilde{c}\widetilde{M}^{0.63}$ the local slopes will be larger. Similar arguments apply to the scalings of $\tau_{G'=G''}$ and the low shear viscosity η_0. The prediction for the relaxation time, corresponding to the breakup of 'critical bonds' is given by

$$\tau \sim \widetilde{c}\widetilde{M}^{0.63} - 1 \tag{4.6}$$

and the prediction for the zero shear viscosity is

$$\eta_0 \sim \frac{1}{\widetilde{M}^{1.63}} \left(\widetilde{c}\widetilde{M}^{0.63} - 1 \right)^4 \tag{4.7}$$

The lower bounds for the power law coefficients are listed in table 4.6.

Table 4.6: Predicted minimal scaling behavior for associative polymer solutions without entanglements. Numbers in brackets indicate experimental values. See text for further details.

associative polymer scaling	M_w	c
η_0	$\geq \mathbf{0.89}\,(5.8)$	$\geq \mathbf{4}\,(4.5)$
$G_{G'=G''}$	$\geq \mathbf{0.89}\,(0)$	$\geq \mathbf{4}\,(1.8)$
$\tau_{G'=G''}$	$\geq \mathbf{0.63}\,(6.7)$	$\geq \mathbf{1}\,(2.7)$

Except for the concentration dependence of the zero shear viscosity, the predicted power laws are not observed in our measurements and especially the minimal predicted powers for $G_0(M_w)$ and $G_0(c)$ are higher than the observed powers. Also, the shapes of the predicted scaling-curves (which are on a log-log scale steadily increasing concave functions with asymptotic power law behavior) do not agree with the observed shapes in figures 4.8, 4.9 and 4.11 which are either linear or slightly convex functions.

Therefore we can conclude that the model of Semenov and Rubinstein for the weak network (critical bonds) regime does not correspond well to our experimental data.

Strong network regime

For a strong network, the chains would have to be multiply connected to other chains and the absolute magnitude of the observed storage modulus plateaus should indicate so. From the measured values the mean number of connections per chain can be accounted, comparable to the calculation in section 4.5.1 for the number of entanglements per chain. This leads to a the mean number of connections per chain of 2 in the case of a 0.5 % (w/w) Guar HM solution, indicating that for the lower experimental polymer concentrations, the chains are on the edge of being singly or multiply connected.

According to the model of Semenov and Rubinstein, the relaxation time dependence changes for a strong network into:

$$\tau \sim \widetilde{c}^{3.2}\widetilde{M}^2 \tag{4.8}$$

Our observed molecular weight dependence of the relaxation times (belonging to the high storage modulus plateau) differs strongly from this prediction. Hence also this regime of the S&R model bears no resemblance to our observations.

4.5.3   Hindered reptation

It was already mentioned in the introduction that specific polymer-polymer interactions as well as reptation might play a role in the observed rheological behavior of

Guar gum. Therefore we will now discuss the model of hindered reptation[20] (by Leibler, Rubinstein and Colby), denoted in the following as LRC. In this model each polymer chain is supposed to contain many association sites. The chains are also entangled with each other and therefore diffusion is only possible along the chain.

To understand the relaxation processes that take place, let us consider the step-strain experiment in which polymer chains will be stretched and placed in preferred orientations. Since the chains are connected via physical bonds to the rest of the system, the whole chains will not be able to return to their equilibrium length at once. Only the *loose chain ends* can perform such a (virtually instantaneous) Rouse relaxation. The parts of the chains that belong to the network have to remain stretched until the bonds are thermally broken. These strands are only able to reach their equilibrium length after all bonds have been broken at least once. After stress has been released via this mode, there will still be residual stress, since the preferred orientations have remained. To restore the equilibrium orientation distribution, the chains have to diffuse reptation-like out of their tubes (which represent their topological constraints). This diffusion process can only take place for chainstrands that are not directly connected via bonds to the rest of the system. Since the bonds break and form continually, chain strands are only temporarily not connected to the system. In this fashion, the presence of stickers acts to slow down the diffusion process. It is via this so-called hindered reptation, that the chains will acquire random orientations and release the remaining stress.
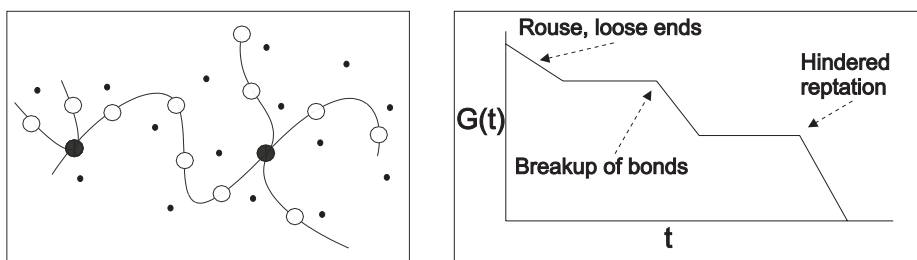
Figure 4.13: Snapshot of a polymer showing hindered reptation (left) and the corresponding predictions for the relaxation behavior (right). The dots are the surrounding polymers.

The relaxation time belonging to Rouse relaxation of the *network strands* is in the model set equal to the breakup time of a physical bond: in other words the breakup event is modeled as a trigger for these Rouse relaxations. Assuming thermal breakup as a random event, characterized only by a temperature dependent probability, the temperature dependence of the relaxation time is modeled with an Arrhenius equation. The equalization also implies that the relaxation time is predicted to be independent of the molecular weight. With respect to the dependence on concentration,

no predictions are made in the LRC model.

The second and longest relaxation time is determined by both the reptation and the breakup timescales. In the case that the relaxation times of thermal breakup and of the hindered reptation are well separated, the LRC model predicts two storage modulus plateaus as shown in figure 4.13. The magnitude of the low frequency plateau must obviously be identical to the one predicted by the Doi Edwards model, and the magnitude should scale with the polymer concentration to a power of 2.25.

When we confront these predictions with our experimental data, we see in both cases two storage modulus plateau zones. The observation that the relaxation time, corresponding to the high frequency plateau, shows an Arrhenius-like temperature dependence is explainable with the breakup of stickers involving a certain activation energy. Also this would be in accordance with the LRC model. An observation not covered by the LRC model is that the relaxation time associated with the thermal breakup, was in our experiments found to depend strongly on molecular weight.

A more serious difference between the model and the experiments becomes evident when the magnitude of the low frequency G' plateau is considered. As in the discussion of the Doi-Edwards model, again equation 4.4 can be used to estimate the number of tube segments ($\frac{L}{a}$). Applying this method now to the *low* frequency G' plateau, we find for the 0.5 % (w/w) Guar HM solution a number of only 0.05 which means that the network mesh size is large compared to the tube length. Therefore we cannot justify the attribution of the low frequency relaxation to reptation. In addition we would like to point out that it is not only the *magnitude* of the low frequency G' plateau that fits poorly. Also, its concentration dependence is much weaker than the predicted scaling with a power of 2.25. This makes the reptation of *single chains* an unlikely cause for the storage modulus plateau at low frequencies.

4.5.4   Two types of associations

Another possible reason for the occurrence of two distinct relaxations, could be a variability in the stickers present on the Guar chains. It has been suggested that a minimum number of 6 free backbone units in a row is needed to form a stable bond[15]. Following this reasoning, it is conceivable that stronger bonding is achieved for an increased number of subsequent bare backbone units. In the simplest, this situation could be represented by a two sticker model. Therefore, we will now discuss a recently developed model in which two types of physical bonds cause two different relaxation possibilities[17,34].

In these models it is assumed that the polymer chains contain regularly spaced association sites (stickers), which are available for physical bonding. In solution a transient network is formed, of which the dynamics is governed by the breakup and forming rates of the bonds. Equality between these rates (detailed balance) defines a steady state. All stickers are considered to be present in one and the same network (as illus-

trated in figure 4.14).

An important ingredient of the model (and also an improvement compared to earlier models) is that the connectivity of the chains is taken into account. All network strands that are enclosed between two bonded stickers are modeled to carry stress. Here the bonded stickers may be provided by *any* of the association sites located on the same chain. Chain strands that become part of loose ends, are supposed to release their stress instantaneously. Chain parts *not* constituting loose ends are supposed to carry stress due to their confinement in virtual tubes. Here the tubes represent the topological constraints imposed by the other chains in the network. Due to the introduction of these concepts, the predicted relaxation spectrum shows a dependency on the number of stickers per chain N_{st} (which has the molecular weight as its experimental counterpart). Both $\tau_{G'=G''}$ and the broadness of the time spectrum are predicted to increase with N_{st}.

It is now a simple matter to qualitatively explain the predicted relaxation behavior of this model. In a step-strain experiment, all chain strands that are enclosed between two bonded stickers will be stretched and will take preferred orientations. Subsequently, stress will be released via the breakup of bonds as explained above. First, stress will be released on the shortest timescale of breaking the weak bonds. What remains after this relaxation is the stress of the network held together by the strong bonds. The breakup time of these bonds is longer, and in case the two breakup times are very different, the relaxation behavior will resemble that of figure 4.14.
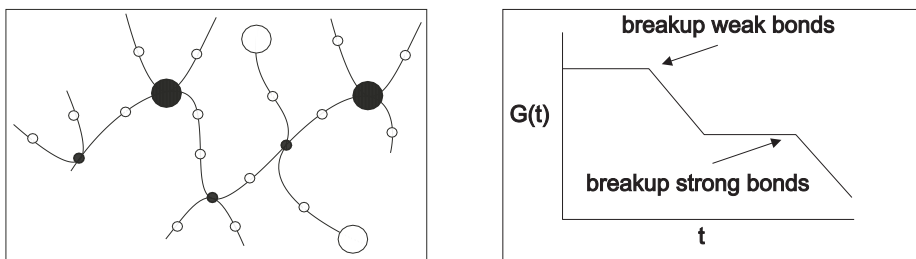
Figure 4.14: Cartoon of a transient network with strong and weak physical bonds (left), and the corresponding predictions for the relaxation behavior (right).

Two important model quantities that lend themselves to a comparison with experimental results are the breakup time(s) and the number density of bonds. The former quantity can be identified as proportional to the relaxation time whereas the latter is proportional to the storage modulus plateau. To calculate them, the breakup and forming rates (h and g) need to be specified. We would like to point out here that the dependencies of these rates on experimental variables (like the temperature and concentration) are not specified by the model itself, and hence need to be separately introduced.

A concentration dependence for h and g can be incorporated by assuming that breakup is an independent process and that the formation of a bond involves a random encounter of two stickers. In that case $h \sim n_{\bullet\bullet}$ and $g \sim n_\circ^2$ with $n_\circ$ and $n_{\bullet\bullet}$ the number densities of open stickers and closed sticker-pairs respectively. The steady state is then characterized by a chemical equilibrium constant, *i.e.*

$$\frac{n_{\bullet\bullet}}{n_\circ^2} = \frac{\frac{1}{2}Nx}{N^2\left(1-x\right)^2} = K \tag{4.9}$$

where x is the fraction of bonded stickers. N is the total number density of association sites (irrespective of whether they are bonded or not) and is proportional to the polymer concentration. Recalling that the relaxation strength G is proportional to the number density of bonds Nx, it is easily verified that $G \sim N^2$ for small K $(x \ll 1)$ whereas $G' \sim N$ for large K $(x \approx 1)$.

The temperature dependence of h and g can be modeled with Arrhenius equations (like equation 2). The rates are then expressed in their respective activation energies (E_b for breakup, E_f for forming) and the temperature. Combining this proposed temperature dependence with the proposed concentration dependence, the equilibrium constant K would scale as

$$K \sim e^{\left(E_b - E_f\right)/kT} \tag{4.10}$$

The dependence of the relaxation time upon the molecular weight (in terms of the model: N_{st}) cannot be chosen but is defined by the model. This dependence is qualitatively an increasing convex function. Figure 4.15 shows a typical result of this dependence. It can be seen that the local slope depends strongly on the number of stickers per chain.

Comparing these predictions to our experimental data, we see in both cases two storage modulus plateau zones together with the broad relaxation spectrum. Also the dependence of $\tau_{G'=G''}$ upon the number of stickers per chain (figure 4.15), matches qualitatively with its experimental counterpart (in figure 4.9): increasing and slightly convex. Assuming that 6 free backbone units are needed to form a stable weak bond (Goycoolea *et al.* 1995)) and that the Galactose units are placed randomly on the backbone chain, the number of stickers on the chain is of order 10, but is difficult to pinpoint precisely. The local scaling power of roughly 3.0 for 10 stickers per chain is obviously low compared to the observed 6.7, but as mentioned above the slope depends strongly on the number of stickers which could only be roughly estimated.

The found scaling power with concentration of 1.8 for the experimental high frequency G' plateau lies in predicted range and is close to 2.0 as predicted from equation 9: $G' \sim N^2$ for $x \ll 1$.

The scaling of the low frequency G' plateau with concentration and temperature is
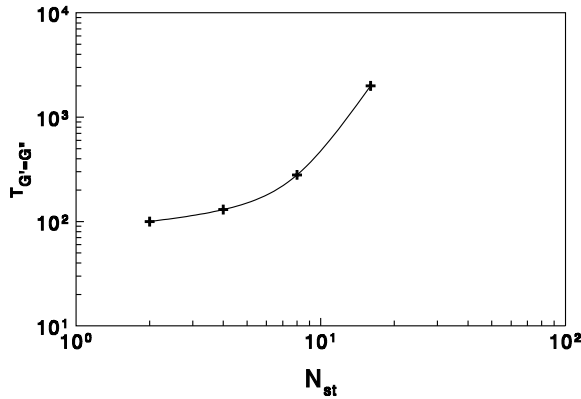
Figure 4.15: Typical result of the dependence of the mean relaxation time on the number of stickers per chain, according to the model of Jongschaap *et al.* in the case that $K = 1$.

less satisfactorily described by the model supplemented with the afore mentioned description for chemical equilibrium. The weak concentration dependence as evidenced by table 4.4 lies below the lower limit predicted by eq 4.9, *i.e.* $G \sim N$ for $x \approx 1$. To explain the strong temperature dependence of the low frequency G' with eqs 4.9 and 4.10, it would be required that $E_b^{strong} > E_f^{strong}$, in other words the bonded state should have a higher energy than the free state. This is qualitatively different for the weak bonds.

Perhaps a more plausible assumption would be, to consider the weak and strong bonds to have a different nature. For example the weak bonds may be hydrogen bridges whereas the strong bonds could be of a hydrophobic nature. Hydrophobic bonds can not be characterized by an activation energy that is more or less independent of temperature, but instead they may a show a strongly increased tendency to bonding when the temperature is raised[16].

Summarizing, the two sticker model of stickers is capable of successfully describing several observations, like the two storage modulus plateau zones and the temperature dependence. The flexibility of the model with respect to the choice for the creation and annihilation rates makes it both versatile, and more difficult to corroborate or falsify. The concentration dependence of the storage modulus plateau at low frequencies remains difficult to understand.

4.6 Discussion

In this paper we presented the linear rheological behavior of Guar gum solutions. Comparing our experimental results to earlier work, no discrepancies are found.

However since we investigated the moduli down to 10^{-4} Hz, we were able to observe the second storage modulus plateau zone at low frequencies. The extensive mapping of the concentration and molecular weight dependence allowed us to compare the experimental results with microrheological models. In this section two subjects that arise from this comparison are discussed. First we discuss some (not yet worked out) model concepts, that may lead to comparable predictions. Secondly, we make some remarks about Guar gum as a model system and comment on the need to obtain additional information about the mesoscopic structure.

4.6.1   Other model concepts

Comparison our experimental data on Guar gum with different microrheological models has shown that existing models can predict qualitatively only parts of the observed behavior. This was not unexpected, since the models are based upon idealizations that are needed for simplicity which do not apply to Guar gum solutions. However, from this comparison it became clear that not even a part of the frequency behavior is described by the reptation model and that physical bonds are needed most likely for explaining the complex overall behavior.

From the predictions of the different associative polymer models we can conclude that the picture of having two types of stickers with a clearly different bonding behavior (different energies needed for breakup and forming) leads to the closest match with the experiments. Sticking to the concept of having two different relaxation mechanisms, determined by different physical bonds, we can also think of other (not yet developed) model ideas. An important difference between these ideas and the model presented in section 4.5.4 is that only a few strong bonds (and no weak bonds) are assumed to be present per chain.

Assuming a few strong bonds would lead to lead to large polymer structures, more or less comparable to star-polymers. For star-polymers also two storage modulus plateau zones have been reported by Pakula *et al.*[25], Vlassopoulos *et al.*[33] and Kapnistos *et al.*[18]. They compared their experimental results to predictions from Milner and McLeish[22] for starlike polymers and found an extra storage modulus plateau at low frequencies. To explain this, a mesoscopic structuring of the star-polymers was proposed, similar to that of dense colloidal particle systems. The central parts of stars with a high number of arms are then considered as cores occupying a volume excluded for elements of neighboring stars. Because of this, the centers of mass of these stars show distinct positional correlations in the sense of a configurational distribution function. The free energy stored in this configuration then causes the storage modulus plateau at low frequencies.

When we assume that in our experimental system, polymer chains form a few strong physical bonds with a very long lifetime, these bonds will cause the formation of large structures, similar to polymer stars but with non-linear and non-monodisperse

polymer arms. These structures will also show slow structural rearrangements on a long timescale, caused either by the breakup of strong bonds or via a diffusive relaxation of the mass centers of these "stars". On a short timescale the classical arm retraction mechanism will be observed (reptation of stars) which causes the storage modulus plateau at high frequencies. Figure 4.16 shows an example of such a starlike polymer structure.
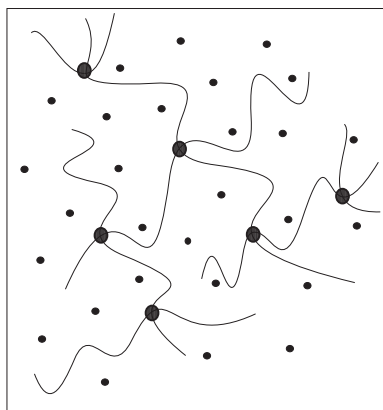
Figure 4.16: Large starlike reptating structures, formed by physical bonds. The dots present the surrounding polymer chains.

This model idea would predict two storage modulus plateau zones and a very broad relaxation spectrum (belonging to the arm retraction mechanism), since the distribution of starlike arms will clearly be polydisperse. When we assume that the via strong physical bonds formed stars do have only a few arms (4-6) we can predict a strong molecular weight dependence for the relaxation time and the zero shear viscosity since they already show an exponential behavior upon the molecular weight for 'normal' starlike polymers[7]. In fact, Lusignan *et al.*[21] measured in 1999 the viscosity of randomly branched polymers as a function of the molecular weight of the linear polymer chain arms. They found a scaling of 6.0 where we found a scaling of 5.8 ± 0.2. In the case that the long timescale process is caused by the breakup of strong (hydrophobic) bonds, the found temperature dependence for the storage modulus plateaus at low frequencies can be predicted qualitatively (see section 4.5.4).
So, although the two sticker model (discussed in section 4.5.4) predicts qualitatively many of the observed phenomena, other model concepts which predict qualitatively the same behavior are also conceivable. At present we can not make a sharp distinction between these. A very suitable experiment for getting a sharper focus would be to remove part of the Galactose sidegroups by means of enzymatic modification (and study the rheological consequences). In case the relaxation between 0.1 and 10 Hz would involve the breakup of hydrogen bridges, modest changes in $G(\omega)$ are

expected. But in the case of starlike reptation of loose ends, the length distribution of these ends may change significantly, giving rise to more noticeable changes in $G'(\omega)$. These experiments will be done in a future study.

4.6.2   The mesoscopic structure

Although the frequency spectrum between 0.1 and 10 Hz is easily characterized regarding the dependencies on experimental variables (time-temperature and time-concentration superposition), the shape of the spectrum and the relaxation strengths can be only qualitatively mapped with existing microrheological models. The behavior at lower frequencies is more difficult to understand and describe, since here the relaxation times are difficult to probe.

Our primary goal was, however, to understand and describe the linear rheological behavior of Guar gum. Our systematic investigation of the dependencies on T, c and M have made it possible to rule out classical relaxation mechanisms. However, pinpointing alternative mechanisms that are in agreement with all observations is difficult. The identification of associative sites as the mechanism responsible for stress relaxation at low frequencies was made on the basis of exclusion of other possibilities, combined with chemical information. And it is the models with the lowest specificity that best survive the comparison with experimental data. On one hand, this reflects that the state of art in modeling has not proceeded far enough for covering the complex and diverse behavior of associative polymers. On the other hand it underlines the need for information in addition to rheological data.

Additional experiments aimed at understanding the chemistry or elucidating the structure may further guide interpretation and modeling. It is however difficult to find suitable techniques for characterizing the Guar. However, scattering experiments like SANS may help to obtain more information about the internal structure and to understand the mesoscopic structure.

4.7   Conclusions

From our extensive investigation of the rheological behavior we can conclude that at high frequencies Guar gum ($>$ 100 Hz) solutions show Rouse behavior. At lower frequencies Guar gum shows two storage modulus plateau zones and a very broad relaxation spectrum (at the high storage modulus plateau) which is not caused by polydispersity.

Guar gum shows very strong scaling behavior with molecular weight and polymer concentration as can be seen in table 4.3. Recent investigations demonstrate that associative polymer systems generally show strong scaling behavior, comparable to our

observations. The exception from these strong scalings is the scaling of the storage modulus plateau zones. The plateau at high frequencies scales as predicted by reptation. Still, the scaling lies also in the range of what can be expected by assuming physical bonds. The plateau at low frequencies however scales very weak with the concentration and the molecular weight and it is not clear what causes this weak dependence.

Comparison with different microrheological models showed that two or more relaxation mechanisms are needed for explaining this complex behavior. The classical reptation model can not even predict a part of the observed frequency behavior, and at least one type of physical bonds is needed for obtaining qualitatively correct predictions. However it was not possible to discriminate between the model ideas of two types of associations (section 4.5.4) and starlike structures caused by strong physical bonds (section 4.6). For a better understanding of the relaxation mechanisms that cause the rheological behavior of Guar gum solutions, more information would have to be obtained about the *in situ* mesoscopic structure. This could make a more specific modeling both feasible and appropriate.

4.8 List of Symbols

a = parameter of the reptation model
a_T = frequency multiplication factor
c = polymer concentration [g/l]
c^* = critical concentration [g/l]
c_g = gel concentration [g/l]
c_g^0 = value of c_g at reference molar mass M_o [g/l]
$\tilde{c} = c/c_g^0$
E_{ap} = apparent activation energy [kT]
E_b = activation energy for breakup [kT]
E_f = activation energy for forming [kT]
f = frequency [Hz]
G' = storage modulus [Pa]
G'' = loss modulus [Pa]
G_0 = storage modulus plateau [Pa]
g = forming rate [1/s]
h = breakup rate [1/s]
h_c = Huggins coefficient
k = Boltzmann constant
k_{MH} = Mark Houwink constant [l/g]
K = chemical equilibrium constant

L = contour length of the primitive chain [m]
M_w = weight average molecular weight [D]
M_0 = reference molar mass [D]
$\tilde{M} = M/M_0$
$n_{\bullet\bullet}$ = number density of closed sticker pairs [m^{-3}]
$n_{\circ}$ = number density of open stickers [m^{-3}]
N = number density of association sites [m^{-3}]
N_{st} = number of stickers per chain
N_c = number of chains per unit volume [m^{-3}]
T = temperature [K]
T_{ref} = reference temperature [K]
x = fraction of bonded stickers
$z = 0.225$
α = Mark Houwink constant
$\dot{\gamma}$ = shear rate [1/s]
η = steady shear viscosity [Pa s]
η^* = complex viscosity [Pa s]
η' = dynamic viscosity [Pa s]
η_0 = zero shear viscosity [Pa s]
η_s = solvent viscosity [Pa s]
$[\eta]$ = intrinsic viscosity [l/g]
η_{red} = reduced viscosity [l/g]
$\nu = 0.59$
τ = relaxation time [s]
$\tau_{G'=G''}$ = characteristic relaxation time [s]
ω = angular frequency [rad/s]

4.9   References

[1]   de Belder, A.N.; Granath, K. *Carbohydrate Research* **1973**, 30, 375-378.

[2]   Blom, C.; Mellema, J. *Rheol. Acta* **1984**, 23, 98-105.

[3]   Bromberg, L. *Macromolecules* **1998**, 31, 6148-6156.

[4]   McCleary, B.V.; Nurthen, E.; Taravel, F.R.; Joseleau, J.P. *Carbohydr. Res.* **1983**, 118, 91-109.

[5]   Cox, W.P.; Merz, E.H. *J. Polym. Sci.* **1958**, 28, 619-622.

[6]   Dea, C.M.; Morrison, A. *Adv. Carbohydr. Chem. Biochem.* **1975**, 31, 241-312.

[7]   Doi, M.; Edwards, S.F. In *The theory of polymer dynamics*, Clarendon, Oxford, 1986.

[8]   Doublier, J.L.; Launay, B. *Proc. Int. Congr. Rheology, Gothenburg, 7th* **1976**, 532-533.

[9]   Doublier, J.L.; Launay, B. *J. Text. Stud.* **1981**, 12, 151-172.

[10] Van den Ende, D.; Blom, C.; Mellema, J. *Proc. Eur. Congr. Rheology, Sevilla, 4th* **1992**, 525-527.

[11] English, R.J.; Gulati, H.S.; Jenkins, R.D.; Khan, S.A. *J. Rheol.* **1997**, 41, 427-444.

[12] English, R.J.; Gulati, H.S.; Jenkins, R.D.; Khan, S.A. *J. Rheol.* **1999**, 43, 1175-1194.

[13] Gidley, M.J.; Eggleston, G.; Morris, E.R. *Carbohydr. Res.* **1992**, 231, 185-196.

[14] Goff, H.D.; Ferdinando, D.; Schorsch, C.*Food Hydrocolloids* **1999**, 13, 353-362.

[15] Goycoolea, F.M.; Morris, E.R.; Gidley, M.J. *Carbohydr. Polym.* **1995**, 27, 69-71.

[16] Haque, A.; Jones, A.K.; Richardson, R.K.; Morris, E.R. In *Gums and stabilisers for the food industry 7*; Philips, G.O.; Willams, P.H.; Wedlock, D.J., Eds.; Oxford University Press Inc., New York, 1994, 291-300.

[17] Jonschaap, R.J.J.; Wientjes, R.H.W.; Duits, M.H.G.; Mellema, J. submitted.

[18] Kapnistos, M.; Semenov, A.N.; Vlassopoulos, D.; Roovers, J. *J. Chem. Phys.* **1999**, 111, 1753-1759.

[19] Lapasin, R.; Pricl, S. In *Rheology of industrial polysaccharides*, Blackie Academic & Professional, London, 1995.

[20] Leibler, L.; Rubinstein, M.; Colby, R.H. *Macromolecules* **1991**, 24, 4701-4707.

[21] Lusignan, C.P.; Mourey, T.H.; Wilson, J.C.; Colby, R.H. *Phys. Rev. E* **1999**, 60, 5657-5669.

[22] Milner, S.T.; Mcleish, T.C.B. *Macromolecules* **1997**, 30, 2159-2166.

[23] Morris, E.R.; Cutler, A.N.; Ross-Murphy, S.B.; Rees, D.A. *Carbohydr. Polym.* **1981**, 1, 5-21.

[24] Oosterbroek, M.; Waterman, H.A.; Wiseall, S.S.; Altena, E.G.; Mellema, J.; Kip, G.A.M. *Rheol. Acta* **1980**, 19, 497-506.

[25] Pakula, T.; Vlassopoulos, D.; Fytas, G.; Roovers, J. *Macromolecules* **1998**, 31, 8931-8940.

[26] Richardson, R.K.; Ross-Murphy, S.B. *Int. J. Biol. Macromol.* **1987**, 9, 250-256.

[27] Robinson, G.; Ross-Murphy, S.B.; Morris, E.R. *Carbohydr. Res.*, **1982**, 107, 17-32.

[28] Ross-Murphy, S.B. *J. Rheol.* **1995**, 39, 1451-1463.

[29] Rouse, P.E., *J. of Chem. Phys.* **1953**, 21, 1272-1280.

[30] Rubinstein, M.; Dobrynin, A.V. *Curr Opin Colloid Interface Sci.* **1999**, 4, 83-87.

[31] Semenov, A.N.; Rubinstein, M. *Macromolecules* **1998**, 31, 1373-1385.

[32] Semenov, A.N.; Rubinstein, M. *Macromolecules* **1998**, 31, 1386-1397.

[33] Vlassopoulos, D.; Fytas, G.; Roovers, J.; Pakula, T.; Fleischer, G. *Faraday Discuss.* **1999**, 112, 225-235.

[34] Wientjes, R.H.W.; Jongschaap, R.J.J.; Duits, M.H.G.; Mellema, J. *J. Rheol.* **1999**, 43, 375-391.

[35] Fetters, L. J.; Graessley, W.W.; Hadjichristidis, N.; Kiss, A.D.; Pearson, D.S.; Younghouse, L.B. *Macromolecules* **1988**, 21, 1644-1653.

Chapter 5

The Relaxation Mechanisms of Modified Guar Gum Solutions

5.1 Synopsis

We investigated the effect of enzymatic modifications (using α-D-Galactosidase) and solvent modifications (adding Urea and Na_2CO_3) on the linear viscoelastic properties of aqueous Guar Gum solutions. These experiments were done to gain more insight into the mechanisms of stress relaxation in different regions of the frequency domain. All modifications were performed on a 1% w/w solution of a Guar with a molar mass of 1 MD. Via enzymatic modifications, Galactose sidegroups were removed in different fractions f of the available amount, up to f = 0.57. Moduli were measured as a function of frequency (0.003-10 Hz) and temperature (283-323 K). On increasing f, a sharp transition from a liquid to a gel was found at f = f_c. Different values for f_c were found for samples stored at 277 K or at 248 K (and thawed), indicating kinetically controlled structure formation at least for part of the samples. Below f_c the changes in the relaxation behavior were very modest. In the Hz range, the characteristic relaxation time and strength, and the time temperature superposition remained much alike that of unmodified Guar. Changing the solvent quality neither had significant effect. Therefore interchain bonding could be ruled out as the origin for the high frequency relaxation behavior. Instead, it was proposed that the fast relaxations involve diffusion processes of multi chain structures. Above f_c gels were formed, i.e. the storage moduli became much higher than the loss moduli, and almost frequency independent. The low frequency storage moduli strongly increased whereas the high frequency moduli remained essentially unchanged. This corroborated that interchain bonds are directly or indirectly involved in the stress relaxation in the mHz range. Further mechanistic information is hard to obtain. Yet we propose a microscopic picture that can explain most of our observations. It would merit a further study with other techniques. The possibility to make weak gels of α-D-Galactosidase treated Guar was demonstrated, and also this deserves further study.

5.2   Introduction

Guar Gum is a Galactomannan polysaccharide originating from the seed endosperm of the guar plant (Cyamopsis tetragonolobus), also known as cluster bean. Galactomannans consist of a (1→4)-linked β-D-mannopyranosyl backbone partially substituted at O-6 with α-D-galactopyranosyl side-groups[1]. Guar has a molecular Mannose/Galactose ratio of approximately 2. (Measured value for the batch used in this project is 1.59). Related Galactomannans are Tara Gum and Locust Bean Gum (LBG), with M/G ratios of respectively 3 and 4. Galactomannans are known to have a higher solubility in water when a larger fraction of the Mannose units is covered with a Galactose side group. For M/G ratios larger than 5 the polymer is no longer soluble. Related to this solubility issue, it is also easier to make a gel from a Galactomannan with a higher M/G. For example, whereas LBG forms a gel after freeze-thawing[2,3], Guar Gum does not. However, Guar Gum is still interesting for industrial applications because of its availability at lower cost, its use as a food thickener and its potential to replace LBG after enzymatic modification (to increase M/G). In the present paper we shall study the linear rheological behaviour of solutions of Guar Gum, as well as enzymatic modifications thereof. Our aim was to gain more insight in the mechanisms underlying the rheology, and to explore the potential use of modified Guar.
Several research groups have investigated the rheology of Guar Gum solutions[5−10]. Comparing the different studies, it becomes clear that the rheological behaviour of Guar Gum solutions is still incompletely understood and that specific polymer-polymer interactions might play a role in the observed rheological behaviour as well as reptation phenomena. This motivated us to perform a systematic study on the frequency, temperature, concentration and molecular weight dependence of the linear visco-elastic moduli. The results were analysed via comparison with mesoscopic models[4]. The main findings are summarized here. We found two storage modulus plateau zone's; one at high frequencies (> 10 Hertz) and one at low frequencies (<0.03 Hz). The storage modulus plateau at low frequencies was in the dPa range, and appeared to be sensitive to strain. Its magnitude increased reversible with temperature, while it was insensitive to concentration. The storage modulus plateau at high frequencies was followed by a broad relaxation spectrum, which was not related to polydispersity. The mean relaxation time of the spectrum showed an Arrhenius-like temperature dependence, and strong concentration dependence. The magnitude of the modulus increased with concentration while it was insensitive to temperature. From comparisons with existing micro rheological models, it was concluded that a recently developed transient network model[12,13] in which the chains are supposed to contain two different types of stickers (weak and strong), gave the best consistency with experimental results. In this model, all stickers are supposed to be regularly distributed along the chain. Chains are supposed to assemble into a transient network, containing both weak and strong bonds, each associated with a certain relaxation

time. In the calculation of the stress tensor, all network strands that are enclosed between two bonded stickers make a contribution. By allowing these bonded stickers to come from any of the association sites located on the same chain, the connectivity of the chains is taken into account. Supplementing this model with a "chemical equilibrium" description for the formation and annihilation of bonds, a predicted relaxation spectrum featuring two $G'(\omega)$ plateau's was obtained. The observed temperature dependencies of the plateau's could be reproduced within the model by inserting suitable numbers for the bond (activation) energies. Dependencies on molecular weight were qualitatively confirmed. In this interpretation, the weak bonds (apparent activation energy 10 k_BT) were associated with hydrogen bridges. The strong bonds would be due to hydrophobic interactions between the free backbone parts[20,21].

To further investigate the validity of these concepts we shall consider in the present paper three issues:

1. Thermodynamic equilibrium. To what extent this is the case, was studied by considering the dependence of the visco-elastic moduli on the thermal treatment of the samples.

2. Weak physical bonds as the origin for the high frequency behaviour. In the case of Guar, the only conceivable weak physical bonds would be hydrogen-bridges. Exploiting the sensitivity of these bonds to their chemical environment, we have investigated this issue by changing the solvent quality.

3. Strong hydrophobic bonds as the origin for the low frequency behaviour. The local hydrophobicity of Galactomannan chains is generally believed to be related to the number of adjacent bare Mannose backbone units. We have investigated the role of hydrophobicity by enzymatically removing Galactose sidegroups.

This chapter is further organized as follows: The experimental details of the chemical modifications as well as the rheological experiments are given in section 5.3. In section 5.4 the experimental results are given. The consequences of these results are discussed in section 5.5 and in section 5.6 the conclusions are shown.

5.3   Experimental

5.3.1   Materials

Guar Gum [Meyhall] was purified by adding 10.0 g to 400 g acetate buffer of pH 4.66 [Merck]. The slurry was homogenised for 75 seconds with a foodblender (500 W) and centrifuged at 22000 g for 5 hours at room temperature. The supernatant, containing 80 % of the suspended mass, was diluted by a factor of two, thus yielding a 1 % w/w stock solution. This solution was stored in a refrigerator. The molecular weight was determined earlier[4] as 910 kD. Galactose side groups were removed from the Guar chains by using α-D-galactosidase [Megazyme]. The activity of the enzyme was specified as 47 U/mg, with 1 U defined as the amount of enzyme that releases

one mmol of p-nitrophenol per minute (substrate: p-Nitrophynyl-α-galactoside) at pH 4.5 and 313 K. The activity of the enzyme for cleaving the sidegroups of Guar was optimized by setting the temperature at 310 K and the pH at 4.7. All modifications were done in 1 % w/w Guar stock solution. For our enzymatic modifications of Guar, a suitable protocol had to be developed. Preliminary modification experiments in which the enzyme was used at low concentration (order: 1 U/g Guar) and without terminating its activity, showed a phase separation after a few hours. Following the visco-elastic moduli in time, a strong decrease was observed, leading to immeasurably small signals after two hours. Visual inspection of the solution afterwards confirmed the phase separation. This phenomenon was not mentioned in another study[22], where similar degrees of modification (i.e. the fraction of side groups removed) had been reached, but using higher galactosidase concentrations (order: 10 U/g Guar). Assuming that α-D-galactosidase treated Guar chains are adequately characterized by their degree of modification, this would suggest that the structure built up by the modified Guar chains is not an equilibrium structure. We think that the phase separation is the result of two interfering processes: the ongoing creation of (hydrophobic) stickers on the chains, and the aggregation of the chains themselves via the formation of bonds. It is conceivable that distinguishable aggregates are formed in the early stages of the modification, which subsequently consolidate via an increase in the number of intra-aggregate bonds. Such a consolidation will only be favored by the ongoing creation of stickers. Then if the number of inter-aggregate bonds is sufficiently small, a phase separation will result. This consideration led us to adapt our protocol. By choosing enzyme concentrations now of order 10^3 U/g Guar Gum and killing the enzyme after a well-defined short reaction time, we aimed to complete the molecular modification before any mesoscopic restructuring (i.e. aggregation) could occur. To estimate the time needed for mesoscopic restructuring, we have used our previous observation that the low frequency elastic modulus needs about 15 minutes to rebuild after being destroyed by shear[4]. In the final protocol, the degree of modification was varied by changing the enzyme concentration, while keeping the reaction time constant. The required amount of enzyme was added to 50 ml of the 1 % w/w Guar Gum solution. The solution was mixed for 30 s by using a handblender (Braun, MR 500 CA, 300 W). The thus obtained homogeneous solution was poured in a pre-heated glass bottle at 310 K, and kept at this temperature under stirring for 15 minutes. Hereafter the modification was stopped instantly by putting the sample in a microwave oven [Sharp R222] at 240 W for 40 s. Subsequently the solution was placed for 15 minutes in a waterbath at 365 K to ensure inactivation of all the enzyme. Any boiling of the sample was avoided: preliminary experiments with Guar solutions had shown that boiling could cause irreversible aggregation. In the end samples were stored either at 277 K, or at 248 K, or placed directly in a rheometer, depending on the type of experiment. The amount of Galactose liberated by the enzyme was deter-

mined using a Lactose/D-Galactose test kit [Boehringer Mannheim]. This procedure establishes the Galactose concentration in a solution by reacting with the Galactose to form NADH, which has a strong absorption peak at 240 nm. Absorption's were quantitatively measured in a [Shimadzu UV-2102] UV spectrophotometer and converted to concentrations using the Lambert-Beer law.
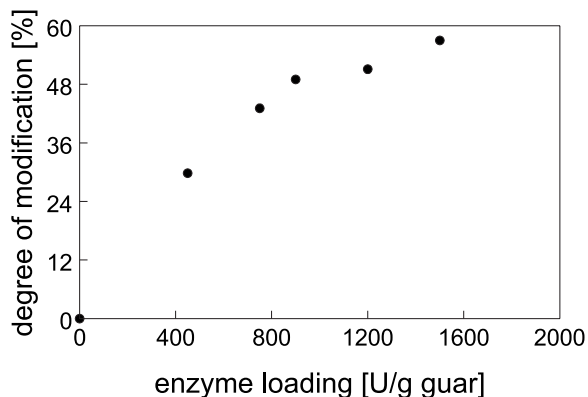
Figure 5.1: Degree of modification as a function of the enzyme loading.

To verify that only Mannose-Galactose bonds had been cleaved by the enzyme, and no Mannose-Mannose bonds (as has been reported[22]), the intrinsic viscosity of a strongly modified Guar Gum (50 % Galactose removal) was determined. The results are shown in figure 5.2.
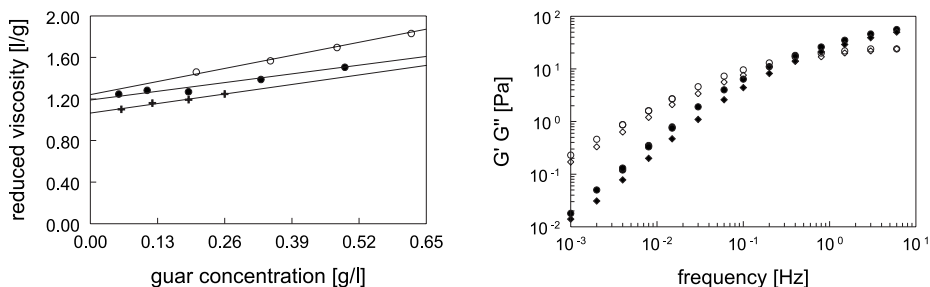
Figure 5.2: Left: Change of the intrinsic viscosity (y-axis value) caused by the modification. ●, ○: unmodified Guar, +: modified Guar. Right: Change of the linear viscoelastic properties caused by the modification procedure: ●,○: stock solution, ◆,◇: reference solution.

The intrinsic viscosity corresponds fairly well to that of the unmodified Guar. The small decrease in [η] could be seen as a confirmation that the chains have become slightly more compact due to intrachain bonding[26]. Further on we checked the influence of the thermal and mechanical treatments of the procedure by taking a sample

through the protocol as described above, but without adding enzyme. The moduli of the thus obtained "reference solution" are compared with those of the original stock solution in figure 5.2. Although a detectable offset between supposedly coinciding moduli was found, the differences are still very small and the shapes of the relaxation spectra are unchanged. In the following, all presented results will be compared to the reference solution.

5.3.2 Rheological measurements

Linear visco-elastic moduli measurements between 10^{-3} and 20 Hz and as a function of the temperature were performed using a Bohlin VOR with a cone and plate geometry (cone angle of 1 degree and 60 mm plate diameter). A Haake RS 150 with a plate- plate geometry (60 mm plate diameter) was used to measure the elasticity of systems that had formed gels. Measurements were conducted at temperatures between 274.5 K and 323 K. With the Bohlin, a correction was made for the temperature dependence (-19 μm/10 K) of the gap width between cone and plate. To avoid effects of solvent evaporation, home made vapor locks, filled with paraffin oil, were used for both rheometers. Solutions were inserted in the Bohlin by using a 10 ml syringe. After insertion, the sample was presheared at 80 1/s for 1 minute to obtain a homogeneously filled gap and to define the mechanical history of the sample. Then the sample was allowed to relaxate for 30 minutes before the measurements were started. Gels were cautiously placed upon the lower plate of the Haake RS150 geometry at a temperature of 278 K. The gap was then set to 2 mm with exponentially decreasing speed. This was done to keep the gel structure intact. For the stronger gels that showed syneresis, the expelled acetate buffer was collected and measured in order to quantify the extent of syneresis. Before measurements were started, moduli measurements were performed between 0.1 and 0.5 Pa at 1 Hz in order to check the limits of linearity. It turned out that all gels showed linear behaviour up to the highest stress.

5.4 Results

5.4.1 Enzymatic Modifications

Unless stated otherwise, samples were stored at 277 K for one week to equilibrate before the rheological behaviour was investigated. In figure 5.3 the storage moduli as a function of frequency are shown for the different degrees of modification (0, 30, 43, 49, 51 and 57 % of available Galactose sidegroups removed).
The measurement temperature for all these samples was set at 283 K in order to allow comparison with earlier obtained results[4]. The results show clearly two regimes as a function of the degree of modification.
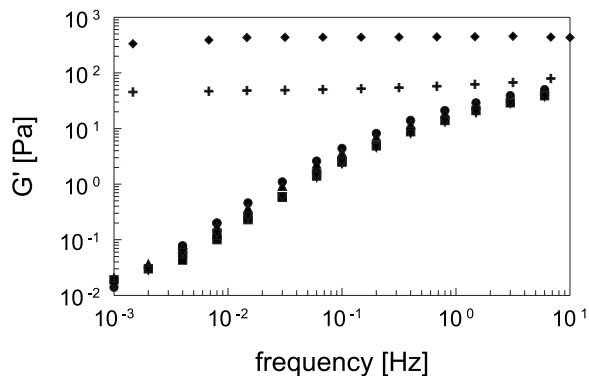
Figure 5.3: The storage moduli as a function of frequency for different degrees of modification. ●: 0, ▲: 30, ■: 43, ▼: 49, +: 51 and ◆: 57 % removal of Galactose

Non-gelling systems

At modifications up to 50 % removal of the Galactose, only minor changes in the linear rheological behaviour are observed. In the high frequency regime, the shapes of the $G'(\omega)$ and $G''(\omega)$ curves remain unchanged. The mean relaxation time (defined as the time corresponding to the frequency where $G = G$") changes less than a factor of two. Also the temperature dependence of this time does not change: Arrhenius plots showed again a good linearity, with activation energies of 13 ± 1 k_BT (with T = 283 K) for both modified and unmodified Guar gum solutions. These values differ from earlier determined energies[4] of 10 k_BT, but we have checked that this can be attributed to small differences in the preparation and measuring procedures. Further on, the magnitude of the elastic modulus at high frequencies does not change at all. Also in the low frequency regime the changes in $G^*(\omega)$ are modest, as is shown in figure 5.4.

Gelling systems

Gel formation
When more than 50% of the available Galactose side-groups was removed, gel formation occurred, as evidenced by the frequency independent moduli in figure 5.3. In a side-experiment, an enzyme-treated Guar solution was introduced in the rheometer directly after the modification, so that gel formation could be observed on-line. The result is shown in figure 5.5.
It makes clear that the gel formation manifests itself by a gradual increase of the low
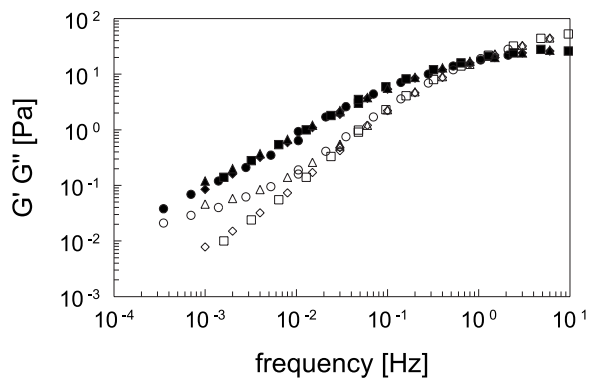
Figure 5.4: Low frequency behaviour of modified samples. The curves have been shifted on top of each other. $G' =$ open symbols, $G'' =$ filled symbols, △: reference solution, ○: 43 % Galactose removal, ◇: pH 10 solution, □: 8 M Urea solution.
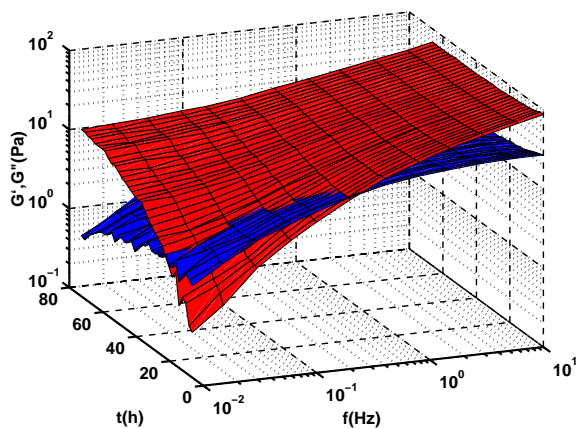

Figure 5.5: Gel formation measured on line. G': grey, G'': black

frequency elasticity. Note that the elastic modulus at high frequencies is conserved in this process. These observations corroborate our previous assumption that the low frequency elasticity in unmodified Guar solutions is related to strong (i.e. long living) reversible bonds. Creating more and longer bare Mannose backbone parts leads to an increased bonding and hence a higher elastic modulus. The finding that the relaxation processes associated with these bonds only play a role at the lowest frequencies is new. It indicates that there is not a strong coupling between the relaxation mechanisms at low and high frequencies.

Melting Behaviour

The gelled systems showed a distinct temperature dependence in their rheology. In figure 5.6 the temperature dependence of the moduli at a frequency of 0.0316 Hz is shown and in figure 5.7 the storage modulus as a function of the frequency is shown for three different temperatures (that were increased with time).
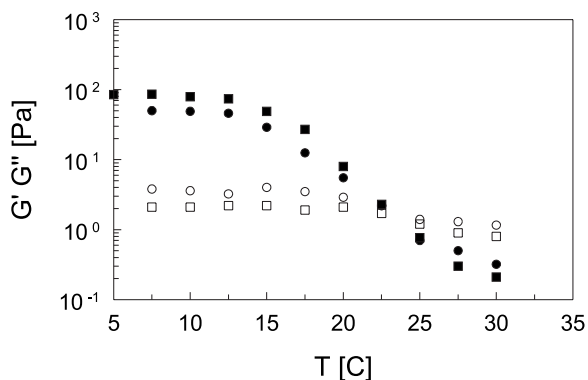
Figure 5.6: Temperature dependence of the moduli at a frequency of 0.0316 Hz. ($\blacksquare$,$\square$)=G',G'' of 51 % modified sample; ($\bullet$,$\circ$)=G',G'' reproducibility check of this sample

It can be seen from figure 5.6 that the gel starts to melt at 288 K (15°C) and becomes fluidlike (i.e. $G' = G''$) at 296 K. This behaviour turned out to be thermoreversible: lowering temperature from 296 K to 278 K resulted after a few hours in a gel showing the very same temperature dependent behaviour. The reproducibility of the initial gel formation was also investigated, by redoing the enzymatic modification with a different sample. The melting curve for this system is also presented in figure 5.6, and shows that reproducibility is fairly good. Changing the degree of enzymatic modification resulted only in slight differences in the melting behaviour. For all gels, it was observed that melting starts at 288 K.
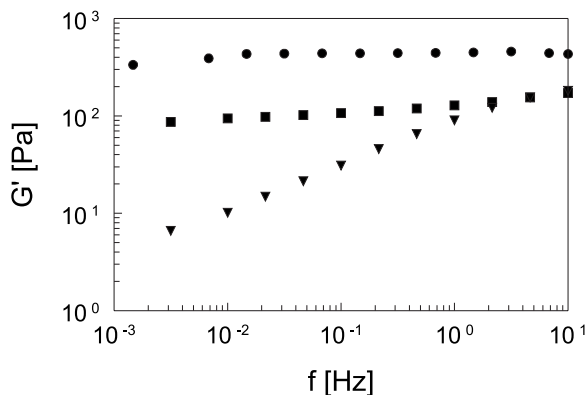
Figure 5.7: Storage modulus of the 51 % modified Guar sample, as a function of the frequency at different temperatures. ●= 283 K, ■=295 K, ▼=305 K.

Influence of Storage Temperature

The dependence on the thermal history of the sample was investigated by changing the storage temperature. Besides samples that were stored at 277 K for one week, also a series was stored at 248 K for six days and subsequently placed at 277 K for one day to allow thawing. The rheological behaviour of these freeze-thawed samples was similar, in that a transition from a liquid to a gel was observed above a certain degree of modification. However, in a quantitative sense there was an important difference: now the required degree of modification amounted approximately 40 % instead of 50 %. (see figure 5.8). This corresponds with results from McCleary et al.[28] who also found qualitatively that the storage temperature influences gel formation of modified Guar gum solutions.
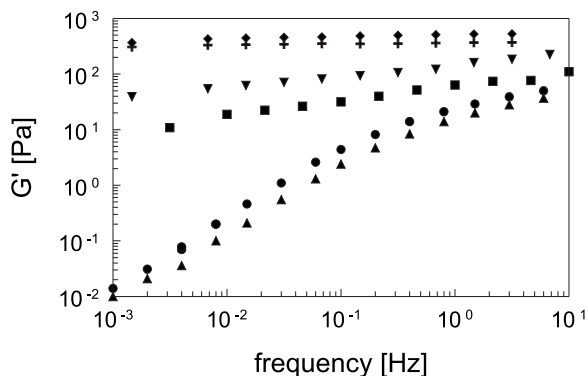
Figure 5.8: The storage moduli for different degrees of modification. Sample storage temperature 248 K instead of 277K. ●: 0, ▲: 30, ■: 43, ▼: 49, +: 51 and ♦: 57 % removal of Galactose

This clear influence of freeze-thawing on the gelation behaviour illustrates that the obtained mesoscopic structure (as reflected via the moduli curves) depends on the aggregation kinetics. Apparently, during freeze-thawing different aggregation processes are favored than during storage at 277 K. This will lead to correspondingly different aggregate structures, that will presumably grow until they become kinetically trapped in some state.

In all cases, the final state (i.e. after a week) of the gel was attained via a syneresis process. Freeze-thawing also turned out to have an influence on the degree of syneresis. The comparison between freeze-thawed and non freeze-thawed gels is summarized in table 5.1. The different concentrations after syneresis for samples with 51 % degree of modification, confirm the presence of non-equilibrium structures in the gels.

Table 5.1: Properties of modified 1 % (w/w) Guar Gum gels.

Modification degree (%)	$T_{storage}$ (K)	$C_{after\ syneresis}$ (% w/w)	$G'_{after\ syneresis}$ (Pa)
51	277	1.0	52
57	277	1.6	450
43	248	1.2	23
49	248	1.3	80
51	248	1.4	350
57	248	1.5	400

5.4.2 Solvent Modification

To investigate what is the contribution to the rheological behaviour of interchain hydrogen bonding, we have solved the Guar Gum also in an 8M Urea solution and in an aqueous 0.1 M Na_2CO_3 buffer with pH=10. Urea is well known as a depressant of hydrogen bonds. This functionality is ascribed to the energetically more favorable hydrogen bonding of water with Urea than with other compounds. In solutions of Guar Gum, the addition of Urea should therefore produce a decreased chance of hydrogen bridging between Mannose backbone units[14,15]. To maximize its influence, we added the Urea to a concentration of 8 moles per liter. The effect on the viscoelastic properties at high frequencies is shown in figure 5.9.
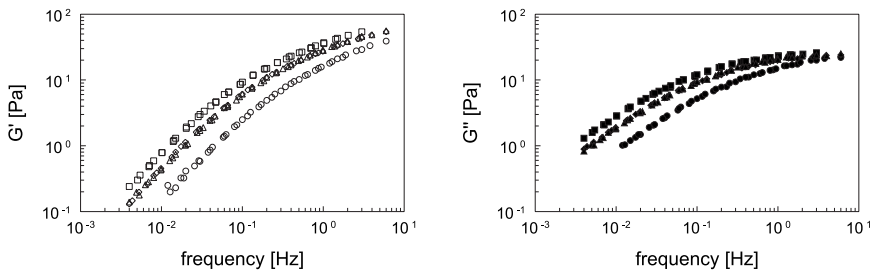
Figure 5.9: Influence of different sample modifications on the high frequency behaviour of Guar gum. G' = open symbols, G'' = filled symbols, $\triangle$: reference solution, $\circ$: 43 % Galactose removal, $\diamond$: 0.1 M Na_2CO_3 pH 10 solution, $\square$: 8 M Urea solution.

A marked decrease in the magnitude of the high frequency elastic modulus should occur if thermal break-up of Guar-Guar hydrogen bonds would be responsible for the stress relaxations. In contrast, only a small frequency shift to the lower frequencies (multiplication factor 0.6) was observed. This finding indicates that hydrogen bonds

between polymers do not play a role in the high frequency regime. The small change in characteristic relaxation frequency might be due to the increased solvent viscosity. The effect of adding Urea on the visco-elastic behaviour at low frequencies was already shown in figure 5.4. The decrease of the elastic modulus in the low frequency range is probably caused by the bare Mannose backbone units becoming less lyophobic. In a recent paper[25] it was mentioned that for protein-protein interactions, Urea diminishes the hydrophobic effect by displacing water in the solvating shell. This might also apply for Guar Gum. A second experiment was done to influence the hydrogen bonding affinity between the Guar chains. Here the acetate buffer at pH 4.7 was replaced by a 0.1 M Na_2CO_3 solution, titrated with HCl to obtain a buffer with pH 10. At this higher pH the number of hydrogen bonds should drop due to the decreased availability of hydrogen species. The effects on the high and low frequency relaxation behaviour are demonstrated in figures 5.4 and 5.9, and are seen to be small like in the case of Urea. The characteristic relaxation time at high frequencies is now completely unaffected, in line with the unchanged solvent viscosity. This finding again indicates that hydrogen bonding does not play a role in the stress relaxation at high frequencies. We believe that more generally it can be said that these relaxations are not related to physical interchain bonding. In a more general sense, replacing the acetate buffer with Urea or Na_2CO_3 can be seen as experiments in which the solvent quality is changed. Removing Galactose sidegroups from the Guar chains could be regarded as an "inverse method" for changing the solvent quality: here the molecular properties of the polymer are changed, while the solvent remains essentially the same (neglecting the influence of small amounts of inactivated enzyme and liberated Galactose). Hence measurements on enzymatically modified Guars can be seen as a third way to study the influence of solvent quality. In figures 5.4 and 5.9 the relaxation behaviour is shown for Guar with 43 % of its Galactose sidegroups removed. Only a slight shift towards higher frequencies is observed, while the magnitudes of the moduli remain unchanged. We take this outcome as another confirmation that interchain bonding does not play a role in the relaxation behaviour at high frequencies.

5.5   Discussion

5.5.1   Relaxation behaviour of native Guar

One of the main findings of this study is that new insight into the origins of stress relaxation of Guar Gum solutions was obtained after measuring the influence of enzymatic and solvent modifications. Below we shall discuss what are the implications of our experimental results for our understanding of the relaxation mechanisms at low and high frequencies.

Fast relaxation mechanism

The insensitivity of the relaxation behaviour at high frequencies to the various modifications has made it clear that this behaviour is not related to the break-up of weak physical bonds between polymer chains. As already argued in our previous investigation[4], this leaves only one other conceivable origin for visco-elastic behaviour in this frequency range, that is, topological constraints. Considering the possible relaxation mechanisms associated with such constraints, classical reptation by individual chains[11] was already ruled out, in view of the magnitude of the storage modulus and the scalings of several rheological quantities[4]. We therefore think that more complex diffusion processes play a role, involving multi chain structures. One finding which was previously taken as an indication that Guar-Guar hydrogen bridges might play a role, was the excellent time-temperature superposition at high frequencies using Arrhenius' law, from which an activation energy of 10 k_BT (with T = 283 K) was found. Now the H-bonding hypothesis has been rejected, the question arises what is the physical meaning of this apparent activation energy. We could imagine that the diffusion time of large complex structures (and therefore the relaxation time) would be inversely proportional to the viscosity of the solvent. Making an Arrhenius plot of the viscosity of water between 283 and 333 K, we found a very good linearity, and an apparent activation energy of 7 k_BT. As an alternative approach, we have also attempted a scaling of the frequency multiplication factors according to the WLF equation. Also here an excellent fit was obtained. However, in contrast to the Arrhenius scaling, the WLF scaling is based upon the concept of excluded volume. These findings illustrate that analyzing the temperature dependence of the characteristic relaxation time is not always a suitable tool for assessing the role of weak interchain bonds in the relaxation behaviour.

Slow relaxation mechanism

It has in this study been corroborated that the relaxation behaviour at low frequencies originates from interchain bonds. Both the enzymatic and the solvent modification experiments point in this direction. Improving the solvent quality causes a decrease in the number and strength of hydrophobic bonds, which is at the macroscopic level reflected in a lowering of the elastic modulus at low frequencies. In the enzymatic modifications, the number and strength of the bonds is increased, resulting in a strong increase of the elastic plateau beyond a certain M/G ratio. Whether the stress relaxation is also *triggered* by the break-up of the bonds is a question, which remains to be addressed. In any case, the relaxation mechanism must involve timescales of 10^3 s or longer. This can be seen from figure 5.10, where the limiting relaxation behaviour ($G' \propto \omega^2$ and $G'' \propto \omega$) is not yet reached at the lowest frequency of 3 mHz.
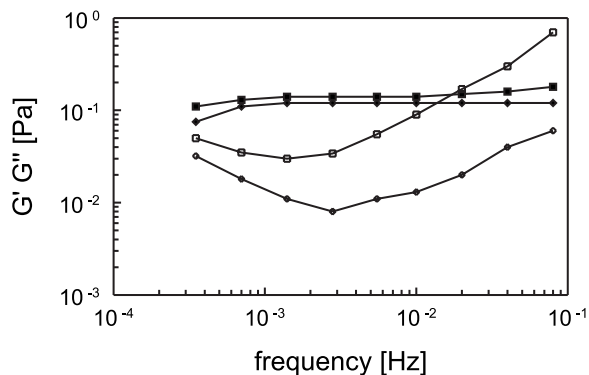
Multi Chain Structures

Figure 5.10: Onset of the slow relaxation spectrum for two different samples. G''=open symbols, G'=filled symbols, ■=1 % (w/w) Guar gum solution 910 kD, ♦= 4 % (w/w) Guar gum solution 270 kD.

Some statements about the structure of native Guar solutions can also be made, now the relaxation mechanisms have been clarified to a certain extent. Interchain bonding will inherently lead to multi chain structures. The presence of such structures was already expected on rheological grounds: an elastic modulus at low frequencies generally involves large length scales. Since the Guar chains themselves are just linear and not very large, the formation of (long living) multi chain structures is needed to obtain these large length scales. Let us now consider the number of bonds per chain. Obviously, this quantity will be related to the number of stickers (sites available for bonding) per chain. This number can be estimated on molecular grounds. Since most of the Galactose side groups in Guar are arranged in pairs and triplets[27], a free backbone part will on average consist of two Mannose units. Assuming that more than five neighboring free Mannose units are needed to form a sticker, as was suggested in literature[23,10], a typical chain of 10^6 Dalton will contain 375 free backbone parts, but only a few ($\bigcirc$(1-10)) stickers. Still, this is a high enough number to create multi chain structures from the stickers.

Formation of the Structures: Kinetically driven or Thermodynamic Equilibrium?

The presence of large length scales in Guar Gum solutions raises the question, to what extent kinetics and equilibrium thermodynamics play a role in the structure formation. The answer is likely to depend on the considered length scale. Structures that are not in thermodynamic equilibrium will most probably be found at the largest lengthscales, and the stress relaxations associated with these structures at the lowest

frequencies of the measurements. Already in our previous study[4] it was observed that the storage modulus plateau at low frequencies showed a much weaker dependence on the Guar concentration, than would be consistent with a thermodynamic equilibrium. Remarkably enough, the dependence of the moduli curves on temperature showed to be reversible. Together these findings point in the direction of a localized thermodynamic equilibrium. In this situation, bonds can break up and re-form in a reversible manner, but with formation kinetics that depends on the local configuration around the stickers. In figure 5.11 we illustrate how we imagine this dependence.
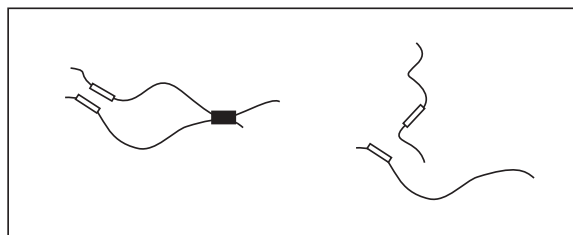
Figure 5.11: Influence of the local configuration on the formation kinetics.

All break-up and bonding events are described with probabilities. The break-up chance of a bond solely depends on temperature. The probability for bonding depends not only on the temperature, but also on the local environment of the stickers. This environment constrains each sticker to a certain volume (or domain), which makes that bonding can only take place in volumes that are shared by two or more stickers. The typical size of the domains is supposed to be of the order of a few Kuhn segments long. Yet it will be related to the structure at large (mesoscopic) length scales, which is formed under kinetic influences in the beginning of the experiment. When the temperature is changed this mesoscopic structure is supposed to remain more or less intact, while locally the environment of the stickers will change. This picture would explain the concentration- and temperature dependence of the low-frequency elasticity (see below).

5.5.2 Tentative Model for Structure and Relaxations in Native Guar Solutions.

In section 5.5.1, statements about the relaxation behaviour were made at an abstract level. In our opinion, drawing more specific conclusions about the structure and relaxations in Guar Gum solutions is not feasible on the basis of our experimental results. Yet to obtain a focus for further research, it is useful to consider which detailed microscopic picture would be the most probable on the basis of our findings. This will be discussed in the present subsection.

Proposed Structure and Relaxations

We think that the presence of a few ◯(1-10) interchain bonds per chain will lead
to a variety of structures, which can be classified as follows:
- Linear structures involving one or a few bonded chains.
- Branched (treelike) structures involving several chains.
- Large aggregated structures involving many chains.

These structures may occur both as free units (figure 5.12 A-C), and as part of a space
filling network (figure 5.12 D-F).
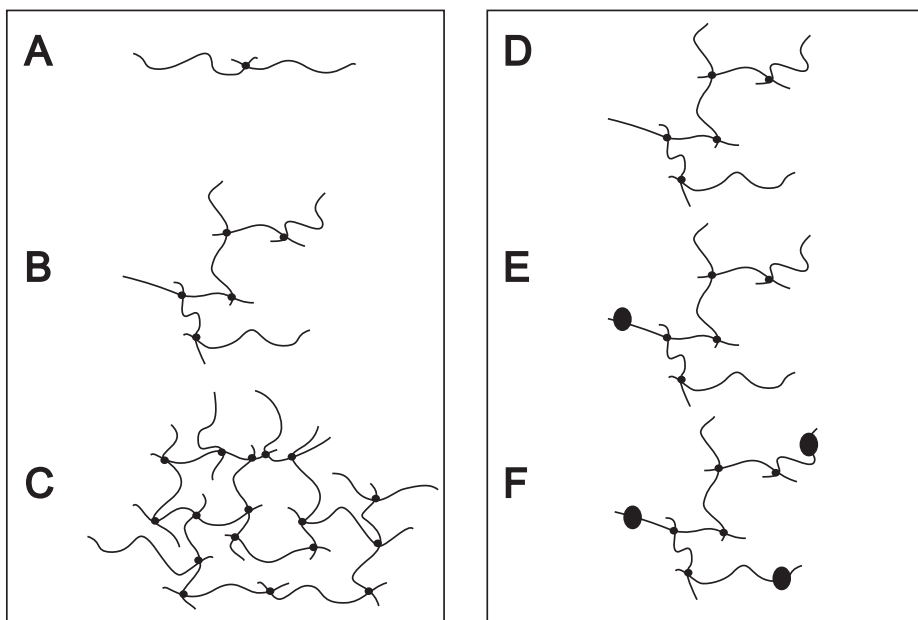
Figure 5.12: Impression of the different multichain structures that may occur in
Guar gum solutions. A=linear structure, B=branched structure, C=large aggregated
structure, D=free structure, E=structure connected at one point to a space filling
network, F=structure connected at more points to the network.

Above the critical overlap concentration (where individual chains start to hinder each
other), these structures will be intra- and intertwined via entanglements. The rhe-
ological behaviour will depend on the number density distribution of the different
structures. Structures that are physically connected via bonds at two or more points
to a space-filling network, will contribute to this network. For the relaxation of the
stress stored in the network, the break-up of bonds is needed. We assume that this
will involve a long relaxation time. Structures that are free or only connected at one
point to a space filling network, can in principle release their stress via diffusion pro-

cesses. The pertaining relaxation times can vary from short to long, depending on the structure size and complexity. For complex structures like in figure 5.12-C, it is possible that they will break-up via the bonds before the diffusion process is completed. In that case the relaxation time is not determined by the diffusion time, but by the bond break-up time. This leaves for the low frequency regime, two possible origins for stress relaxation: 1. the break-up of bonds, and 2. the diffusion of large aggregated structures. In our opinion the latter process will not likely play a role. If this diffusion were to be the dominant relaxation mechanism, then the polydisperse size distribution of the aggregates should have given rise to a very broad low-frequency relaxation spectrum that would go over smoothly into the high-frequency spectrum. In contrast, our observations show that the relaxations at high and low frequencies are well separated in the frequency domain. Therefore, instead of large diffusing structures we think of a space-filling network.

Proposed Kinetics of Structure Formation

The formation of the complex network structure will be kinetically driven. We imagine that it is formed via a two-stage process. Right after the Guar Gum solutions have been subjected to mechanical treatment, distinguishable entities ranging from free chains to small aggregated structures will be present in the solution. A small fraction of these structures will assemble into a space filling primary (or skeleton) network if the number of potential bonds per chain is small. This will occur on a relatively short timescale, since it involves a more or less free diffusion of small entities. Once the primary network has been formed, the second stage sets in. Now the structures will experience a hindrance in their diffusion, from their entanglements with others and from the network. As a consequence further aggregation will only take place locally, between structures that are confined to the same neighborhood. This limited aggregation will lead to a thin network in which structures of different size (from single to multiple chains) are arrested, via connecting bonds and/or topological constraints.

Qualitative Predictions for the Linear Rheological Behaviour

Elastic modulus at high frequencies
In the proposed structure model (discussed above), the polymer solutions will be homogeneous down to the length scale of a few Kuhn segments. The elasticity associated with the diffusion relaxation of multi-chain structures will be determined mainly by the entanglement concentration, provided that the typical distance between two entanglements is small compared to the size of the diffusing structures. The entanglement concentration is independent of molecular weight and temperature but increases with polymer concentration. In our experiments[4] the elastic modulus at

high frequencies showed qualitatively the same dependencies.

Relaxation time at high frequencies
The diffusion of the multi-chain structures will bear a certain resemblance to arm retraction (or starlike reptation) mechanisms. But it will be more complicated in our case, since branched structures are now involved instead of just linear arms. Moreover there will be distributions for the sizes and shapes of the multi-chain structures. In any case, the relaxation spectrum can be predicted to be very broad. Indeed this was observed in our experiments. The temperature dependence of the characteristic relaxation time can be fairly well described by assuming an inverse proportionality to the solvent viscosity (as in the case of simple diffusion processes). In this approach, thermally induced structural changes are neglected, which is a simplification even at the relatively short length-scales probed at high frequencies. The dependencies of the typical relaxation time on concentration and molecular weight cannot be predicted. This is because the relaxation time is not only determined by the entanglement concentration, but also by the characteristics (size, shape, branching) of the multi chain structures. These properties are influenced by the initial formation kinetics, which depends on the concentration and molecular weight in an unknown way.

Elastic modulus at low frequencies
The magnitude of this modulus is determined by the number density of network strands, i.e. polymer strands connected to the space-filling network via two points. This number density is hard to predict, since especially at the long length scales probed by the low frequencies, the structure will be determined by kinetics rather than by thermodynamic equilibrium. On changing the concentration or the molecular weight the kinetics may become different, which makes it rather difficult to predict the influence of these experimental variables on the elastic modulus. We recall here that the unusually weak concentration dependence of the low frequency elasticity in our previous experiments[4] leads us to think of non-equilibrium structures. The temperature dependence of the elastic modulus is less difficult to predict, since here it is not required that the structure is determined by thermodynamic equilibrium. Assuming that the thermally induced structural changes at mesoscopic length scales are modest, we only need to consider localized equilibria (as discussed in section 5.5.1). Adopting the suggestion that the hydrophobicity of free Mannose backbone parts increases with temperature[20,21], the number of stickers will also increase with temperature, since also a fraction of the smaller free backbone parts (less than six Mannose units) will start to act as stickers. Thus, a network hardening can occur without the need for diffusion. The pertaining increase in elasticity corresponds well to our observations.

Relaxation time at low frequencies
This quantity was outside the range of our measurements. Some qualitative predictions concerning the dependencies on experimental variables are possible. In a thin network, co-operative bonding effects will play a minor role and therefore the relaxation time will be determined by the break-up time of bonds directly. Obviously, a relaxation time associated with such a highly local process will not depend on the molecular weight or the concentration.

From the above discussion it becomes clear that qualitative predictions for the linear rheological behaviour as a function of experimental variables are possible in a number of cases. Also, there are dependencies that cannot be predicted due to insufficient knowledge about the structures and kinetics. At least all qualitative statements that can be made on the basis of our tentative picture, are consistent with our experimental observations.

5.5.3   Related Research on Structure and Relaxations

From small angle scattering (USALS and SANS) results[16] it was concluded that the observed scattering behaviour of Guar Gum solutions was in accordance with large fractal aggregates, with no strong positional correlations between the aggregates. Some chains and aggregates were supposed to exist freely in solution, whereas loosely connected aggregates were also presumed present. A few chains may also belong to more aggregates. These findings are not in contradiction with the structure model discussed in section 5.5.2. They could imply that the species of figure 5.12 C are dominantly present, and that the structure of these species is Fractal-like. Besides the research on Galactomannans, another investigation is also worth mentioning: Vlassopoulos et al.[17−19] investigated the linear rheological behaviour of large multiarm polymer stars (of up to 128 arms of 47 kD per arm) and they also found a low frequency storage modulus plateau zone. They attributed this plateau to the structural rearrangements of the stars within their liquidlike order. These rearrangements can occur when the whole aggregate diffuses through the solution or when the break-up of bonds causes a break-up of the aggregate. This indicates that multi chain structures may contribute to a low frequency plateau.

5.5.4   Behaviour of Modified Guar Gels

Tentative mechanisms of gelation and melting

Gelation
For gel formation of modified Guar gum solutions many stickers per chain are needed. Then diffusion over appreciable distances is no longer needed for bond formation,

and many bonds per chain can be formed which will result in a strong network. During the gel formation the network will become more compact thereby causing the observed syneresis.

Influence of freeze-thawing on gelation

In the range between 40 and 50 % Galactose removal, a gel is only formed after the sample has been frozen. A possible explanation for the effect of a freeze-thaw cycle may be related to the temperature dependence of the bonds: During the freezing step, the temperature decreases, causing fewer and weaker stickers and therefore fewer bonds in line with our tentative model of section 5.5.2. Therefore diffusion of aggregates through the solution becomes easier and the mesoscopic structure evolves more towards a thermodynamic equilibrium which means that the network becomes more dense. Reaching a true equilibrium state would involve a phase separation, but this process is hindered because of excluded volume. In the thawing step, the temperature is increased again and bonds will form again. From the more dense starting state more interchain bonds are formed and this can cause the observed gel formation.

Melting behaviour

When the temperature is increased further, micro phase separation may occur: Then even more stickers are placed on the chain causing extra bond formation. This will cause local syneresis, and forces will start to act on the interchain bonds leading to their breakup. The breakup of these bonds causes the observed decrease of the gel-strength with increasing temperature (the melting behaviour).

Sharp sol-gel transition

One of the remaining questions, is why the transition from a liquid to a gel depends so sharply on the degree of enzymatic modification. Such drastic changes might be expected in polymer solutions when a thermodynamic phase transition is involved. However, in the case of Guar, we should think of a kinetically controlled structure. Perhaps a drastic increase in the number of stickers above a certain modification level could explain the sharp transition to a gel. To investigate this point, we performed some simple simulations in which the number of stickers (defined by ≥ 6 adjacent bare Mannose units) is calculated as a function of the degree of modification. Various possible cases were considered: both the placement of Galactose sidegroups and the action of the enzyme were taken to be either random or non-random. In all cases it showed that although the number of stickers per chain increased more than linearly with the degree of modification, a sharp transition was not found. Our explanation for the sharp sol-gel transition is that at the onset of gelation, structural changes occur also at the smallest length scales, causing an increased bonding probability per sticker. Thus a recursive process could be triggered, resulting in a sharp transition to

a gel.

From the discussion above it shows that with the same concepts that were used to model the linear visco-elasticity of Guar gum solutions (increase of hydrophobicity with increasing temperature and kinetically determined mesoscopic structures) also the behaviour of modified Guar gum gels can be rationalized.

Comparison with Locust bean gum gels

The fact that modified Guar gum solutions only form a gel after a freeze-thawing cycle, in the range between 40 and 50 % Galactose removal, is comparable with the behaviour of Locust Bean Gum which also forms gels after a freeze-thaw cycle[2,3]. Compared to modified Guar Gum, Locust Bean Gum (with a M/G ratio of 3.9) lies clearly beyond the M/G limit of 3.27 (50 % Galactose removal) where Guar Gum forms a gel without freeze-thawing cycle. So in that sense, modified Guar Gum forms a gel more easily. This might be caused by the difference in molecular weight (Locust Bean Gum has a molecular weight of 370 kD, whereas modified Guar Gum still has a molecular weight of about 730 kD). The lower molecular weight in the case of Locust Bean Gum will lead to less bonds per chain which makes gel formation more difficult. Another reason might be a possible difference in the fine structure of Guar gum and Locust bean gum (the length distribution of adjacent bare backbone units). This will also influence the number of hydrophobic stickers per chain and therefore the number of bonds per chain.

Besides this difference, also the temperature dependence of the elasticity of Locust Bean Gum gels differs from that of modified Guar Gum gels: For Locust Bean Gum it is reported[3] that formed gels start to melt above 317 K, whereas for modified Guar Gum we have observed that the melting starts at 288 K. The melting itself might be caused by local phase separation as explained above, but it is not *a priori* clear what causes the difference in melting temperature. Again differences in the free backbone length distribution as well as in molecular weight might play a role.

5.5.5 Recommendations for Further Research

From the results and the discussion it has become clear that although more light has been shed on the relaxation mechanisms, the complete behaviour of Guar Gum in solution is still not understood. In order to achieve this goal quantitative modeling of the presented model concept is needed or more generally: microrheological models are needed based on aggregated structures formed via long living bonds and excluded volume (entanglements). Rubinstein and Semenov[29,30] presented in 1998 a model in which the rheological behaviour of aggregates (kinetically formed via bonds) is predicted, but there excluded volume was not taken into account for simplicity reasons.

However they mentioned that in future work, the effect of excluded volume would be accounted. Besides theoretical modeling also experimentally obtained additional structure information is needed. By an investigation of the molecular fine structure of modified Guar Gum[27,24,25] as a function of the degree of modification, the relation between the number of stickers per chain and the obtained gel may become more clear. It could also provide information about the dependence of the bond formation kinetics on the mesoscopic structure. More indirect structure information can be obtained via the relaxation time of the slow relaxation process. If this time is concentration and molecular weight independent it indicates that the relaxation process is the break-up of individual bonds as is predicted by our presented model concept. With the used equipment it was not possible to determine the relaxation time of the slow relaxation spectrum, but the results show (figure 5.10) that this spectrum lies still in a frequency regime that is accessible to other rheometers. Therefore by using for example a very sensitive creep rheometer it should be possible to measure this spectrum.

5.6   Conclusions

From the in this chapter presented results the following can be concluded for the linear rheology of Guar gum, and enzymatic modifications thereof:
1. Bonds cause the rheological behaviour at low frequencies. These bonds are likely to have a hydrophobic origin since the gelstrength increases with an increasing M/G ratio.
2. Weak physical bonds do not cause the rheological behaviour at high frequencies. Instead, the independence of this behaviour on the solvent quality indicates that diffusion processes, which are not exactly known, cause it.
3. The history dependence of the samples that show gel formation proves that at least for these samples the thermodynamic equilibrium is not reached.
4. Combining the various observations, a tentative picture for the structure and relaxations could be constructed. This picture is complex but internally consistent. So far no quantitative model is able to predict the observed rheological behaviour.
5. Via enzymatic modifications it is possible to induce gel formation. The formed gels show a melting trajectory which starts at 288 K.

From these results, it follows that future models should focus on frozen structures that have not reached thermodynamic equilibrium yet. Further on a study on the molecular fine structure of modified Guar gum may provide information that explains the sharp gel transition as a function of the degree of modification. More information about the mesoscopic structure should also be obtained. Investigation of the slow relaxation process may provide this.

5.7   References

[1]   Dea, I.C.M.; Morrison, A. *Adv. Carbohydr. Chem. Biochem.* **1975**, 31, 241-312.

[2]   Tanaka, R.; Hatakeyama, T.; Hatakeyama H. *Polymer Int.* **1998**, 45, 118-126.

[3]   Richardson, P.H.; Norton, I.T. *Macromolecules* **1998**, 31, 1575-1583.

[4]   Wientjes, R.H.W.; Duits, M.H.G.; Jongschaap, R.J.J.; Mellema, J. *Macromolecules* **2000**, 33, to be published.

[5]   Doublier, J.L.; Launay, B. *Proc. Int. Congr. Rheology, Gothenburg 7th* **1976**, 532-533.

[6]   Doublier, J.L.; Launay, B. *J. Text. Stud.* **1981**, 12, 151-172.

[7]   Morris, E.R.; Cutler, A.N.; Ross-Murphy, S.B.; Rees, D.A. *Carbohydr. Polym.* **1981**, 1, 5-21.

[8]   Richardson, R.K.; Ross-Murphy, S.B. *Int. J. Biol. Macromol.* **1987**, 9, 250-256.

[9]   Robinson, G.; Ross-Murphy, S.B.; Morris, E.R. *Carbohydr. Res.* **1982**, 107, 17-32.

[10]   Goycoolea, F.M.; Morris, E.R.; Gidley, M.J. *Carbohydr. Polym.* **1995**, 27, 69-71.

[11]   Doi, M.; Edwards, S.F. *The theory of polymer dynamics* **1986**, Clarendon, Oxford.

[12]   Wientjes, R.H.W.; Jongschaap, R.J.J.; Duits, M.H.G.; Mellema J. *J. Rheol.* **1999**, 43, 375-391.

[13]   Jongschaap, R.J.J.; Wientjes, R.H.W.; Duits, M.H.G.; Mellema J. *Macromolecules* to be published.

[14]   Li, H.; Zhang, W.; Xu, W.; Zhang, X. *Macromolecules* **2000**, 33, 465-469.

[15]   Zou, Q.; Habermann-Rottinghaus, M.; Murphy, K.P. *Proteins: structure, function and genetics* **1998**, 31, 107-115.

[16]   Gittings, M.R.; Cipelletti, L.; Trappe, V.; Weitz, D.A.; In, M.; Marques, C. *J. Phys. Chem. B* **2000**, 104, 4381-4386.

[17]   Pakula, T.; Vlassopoulos, D.; Fytas, G.; Roovers, J. *Macromolecules* **1998**, 31, 8931-8940.

[18]   Vlassopoulos, D.; Fytas, G.; Roovers, J.; Pakula, T.; Fleischer, G. *Faraday Discuss.* **1999**, 112, 225-235.

[19]   Kapnistos, M.; Semenov, A.N.; Vlassopoulos, D.; Roovers, J. *J. Chem. Phys.* **1999**, 1753-1759.

[20]   Haque, A.; Jones, A.K.; Richardson, R.K.; Morris, E.R. *Gums and stabilisers for the food industry 7* **1999**, eds. Phillips, G.O.; Williams, P.H.; Wedlock, D.J., Oxford University Press Inc, New York, 291-300.

[21]   Shirakawa, M.; Uno, Y.; Yamatoya, K.; Nishinari, K. *Gums and stabilisers for the food industry 9* **1998**, eds. Williams, P.H.; Phillips, G.O., Royal Society of Chemistry, Cambridge, 94-103.

[22]   Bulpin, P.V.; Gidley, M.J.; Jeffcoat, R.; Underwood, D.R. *Carbohydr. Polym.* **1990**, 12, 155-168.

[23]   Richardson, P.H.; Clark, A.H.; Russell, A.L.; Aymard, P.; Norton, I.T. *Macromolecules* **1999**, 32, 1519-1527.

[24]   Dea, I.C.M.; Clark, A.H.; McCleary, B.V. *Carbohydr. Res.* **1986**, 147, 275-294.

[25]   McCleary, B.V. *Carbohydr. Res.* **1979**, 71, 205-230.

[26]   Molyneux, P. *Water-soluble polymers: Synthesis, solution properties and applications* **1991**, eds. Shalaby, S.W.; McCormick, C.L.; Butler, G.B., ACS Symposium Series 467, Washington CD, 232-248.

[27]   McCleary, B.V.; Clark, A.H.; Dea, I.C.M.; Rees, D.A. *Carbohydr. Res.* **1985**, 139, 237-260.

[28]   McCleary, B.V.; Amado, R.; Waibel, R.; Neukom, H. *Carbohydr. Res.* **1981**, 92, 269-285.

[29]   Rubinstein, M.; Semenov, A.N. *Macromolecules* **1998**, 31, 1366-1397.

[30]   Rubinstein, M.; Semenov, A.N. *Macromolecules* **1998**, 31, 1373-1385.

Summary

An ingredient which is often used as a thickener in food and cosmetic products is Guar gum. Guar gum is a polymer that consist of a Mannose backbone partially covered with Galactose side groups. Adding only a small amount of Guar gum in water causes a drastic increase in the solution viscosity. In industry this effect is used to improve the product properties. This is mostly done via a trial and error process, since the relation between macroscopic and microscopic properties is not yet understood. By understanding this, further improvement of products like ice-creams, salad dressings and dairy products becomes possible. In this thesis work is presented that was done in order to understand the relation between macroscopic rheological and microscopic molecular quantities of Guar gum solutions.

Therefore, the rheological behaviour of Guar gum was investigated intensively as a function of several variables. The results of this investigation were compared with different microrheological models. From this comparison, it followed that no quantitative falsifiable model predicts the observed rheological behaviour. Besides these models, certain not elaborated concepts might predict this behaviour. Especially the field of models based on entanglements and physical bonds is still open. Previous work showed that both, entanglements and physical bonds might play a role in the rheology of Guar gum solutions. Therefore in this study a model has been developed in which the polymer system is described as a network of spring segments connected via sticky points (as in the Lodge model). An important extension (with respect to previous models) was that chain connectivity is taken into account. All segments that are located in between connected stickers are supposed to carry stress due to the presence of entanglements. The attachment and detachment of stickers is described with kinetic equations in which activation energies play a role. Simultaneous transitions involving groups of stickers are allowed. Model predictions showed a strong dependence on the number of segments per chain and broad relaxation spectra.

Changing the model assumption that chain segments carry stress if they are located between two physical bonds, to the assumption that chain segments carry only stress if they are located between two physical bonds and never have lost their stress in the past led to different model predictions. The difference of these two assumptions can be understood by thinking of a G(t) experiment. If a step strain is performed, the active segments (segments that are located directly or via other segments between two

physical bonds) start to carry stress. Due to the breakup of bonds, these segments will become inactive and therefore they will loose their stress. Due to the forming of bonds, some inactive segments will also become active. In the first of the two assumptions, these segments will not only become active, but they will also carry new stress. In the second assumption, they only become active and remain free of stress. Besides this difference in assumptions, also the model was extended so that different types of physical bonds (strong and weak) can be taken into account. This model predicts broad smooth relaxation spectra in the case of chains with many stickers of one type. In case different stickers are assumed, more plateau regions in the dynamic moduli may appear.

In order to short out the importance of different relaxation mechanisms like Rouse like diffusion, diffusion hindered by topological constraints or the breakup of bonds, the linear viscoelastic behaviour of Guar gum solutions was investigated as a function of frequency, temperature, polymer concentration and molecular weight. In the kiloHertz regime, Rouse behaviour was observed. At lower frequencies, two storage modulus plateau zones were found, indicating two additional types of relaxation processes (slow and fast). One is operative between 1 and 100 Hz, and gives rise to a very broad relaxation spectrum, even for monodisperse Guar. Describing the dependencies of the relaxation time and low-shear viscosity on concentration and molecular weight with power laws resulted in unusually high coefficients. The second type of relaxation process becomes manifest below 0.01 Hertz and was not reported before. Here the temperature dependence is very strong whereas all other dependencies are weak. Analyzing the experiments with existing models revealed that at best a partial description of the experimental dependencies can be obtained. It was concluded that at least two different types of relaxation mechanisms must play a role, classical reptation not being one of these. Best overall predictions were obtained with the former mentioned model assuming two types of bonds (strong and weak one's).

In order to check the important assumptions of that model (two types of physical bonds and having thermodynamic equilibrium), the effects of enzymatic modifications (using α-D-Galactosidase) and solvent modifications (using an 8M Urea and a 0.1 M Na_2CO_3 pH 10 solvent) on the linear viscoelastic properties of Guar gum solutions were investigated. Via enzymatic modifications, Galactose sidegroups were removed in different fractions f of the available amount, up to $f = 0.57$. Storage and Loss moduli were measured as a function of both frequency (0.003-10 Hz) and temperature (283-353 K). On increasing f, a sharp transition in the rheology was found above a critical fraction f_c. Its magnitude turned out to depend on whether the modified Guar solution had been stored above or below its freezing point. This indicates that at least not always thermodynamic equilibrium is reached. Below f_c the changes

in the relaxation behavior were very modest. In the Hertz range, the characteristic relaxation time and strength, and the Time Temperature Superposition remained much alike that of unmodified Guar. Changing the solvent quality neither had significant effect. Therefore interchain bonding could be ruled out as the origin for the high frequency relaxation behavior. Instead, it was proposed that the belonging relaxation process is the diffusion process of multi chain structures. Above f_c gels were formed, i.e. the storage moduli became and much higher than the loss moduli, and almost frequency independent. The low frequency storage moduli strongly increased whereas the high frequency moduli remained essentially unchanged. This corroborated that interchain bonds are directly or indirectly the physical origin of the stress relaxation in the mHz range.

Finally, this led to the following microscopic picture: Chains form a few bonds with each other. Because of these bonds, aggregated structures are formed. A part of these structures will subsequently assemble into a primary (or skeleton) space filling network. With the formation of the network, the mesoscopic structure is frozen because diffusion through the solution becomes impossible. Therefore the hardening of the network will occur on a infinite timescale. Here the slow relaxation process is the breakup of the network, whereas the fast relaxation process is the diffusion of the formed aggregated structures.

Samenvatting

Een ingredint wat vaak gebruikt wordt als verdikkingsmiddel in voedingsmiddelen en cosmetische producten is Guar gum. Guar gum is een polymeer dat bestaat uit een Mannose hoofdketen welke gedeeltelijk bezet is met Galactose zijgroepen. Toevoegen van een kleine hoeveelheid Guar gum aan water veroorzaakt een drastische viscositeitstoename van de oplossing. In de industrie wordt dit effect gebruikt om producteigenschappen te verbeteren. Dit gebeurt meestal via de 'trial' en 'error' methode, omdat de relatie tussen macroscopische en microscopische eigenschappen nog onbegrepen is. Verdere optimalisatie van producten zoals ijs, dressings en zuivelproducten is mogelijk door het verkrijgen van inzicht in deze relatie. In dit proefschrift zijn de resultaten gepresenteerd van onderzoek dat erop gericht was om het verband te begrijpen tussen macroscopische reologische en microscopische moleculaire eigenschappen van Guar gum oplossingen.

Teneinde dit doel te bereiken is Guar gum uitvoerig onderzocht als functie van verschillende variabelen. De resultaten van dit onderzoek zijn vervolgens vergeleken met verschillende microreologische modellen. Daaruit bleek dat geen bestaand kwantitatief model in staat is het geobserveerde gedrag te voorspellen. Naast deze modellen bestaan er ook onuitgewerkte modelconcepten die dit gedrag wel zouden kunnen voorspellen. Met name op het gebied van modellen die gebaseerd zijn op 'entanglements' (verstrengelingen van polymeren) en fysische bindingen zijn er nog veel onuitgewerkte model concepten. Omdat reeds bekende resultaten lieten zien dat zowel 'entanglements' als ook fysische bindingen aanleiding zouden kunnen geven tot het reologische gedrag van Guar gum oplossingen, is een van de concepten uit dit gebied uitgewerkt tot een model. Dit is gedaan om de mogelijkheden te onderzoeken om met een dergelijk model wel het geobserveerde gedrag te voorspellen. In dit model is het polymeersysteem beschreven als een netwerk van veer segmenten die via stickerpunten met elkaar verbonden zijn, hetgeen vergelijkbaar is met het Lodge model. Een belangrijke uitbreiding aangaande het Lodge model is dat hier rekening gehouden wordt met ketenconnectiviteit: alle segmenten die zich bevinden tussen twee punten die verbonden zijn met het netwerk worden verondersteld spanning te dragen door de aanwezigheid van 'entanglements'. Het vasthechten en loslaten van stickers is beschreven met kinetische vergelijkingen die gebaseerd zijn op activeringsenergie afhankelijkheden. Simultane overgangen waarbij meerdere stickers betrokken zijn, zijn toegestaan. De modelvoorspellingen laten een breed relaxatiespec-

trum en een sterke afhankelijkheid zien van het aantal segmenten per polymeerketen.

Het beperken van de aanname dat ketensegmenten spanning dragen als ze zich tussen twee punten bevinden die verbonden zijn met het netwerk, met de toevoeging dat deze segmenten nooit spanningsloos hebben mogen zijn in het verleden, leidde tot nieuwe model voorspellingen. De invloed van deze beperking kan worden begrepen via de verwachting van een G(t) relaxatie-experiment. Het opleggen van een stapvervorming heeft tot gevolg dat de actieve segmenten (segmenten die zich tussen twee netwerkpunten bevinden) spanning gaan dragen. Ten gevolge van het opbreken van bindingen zullen segmenten inactief worden en daardoor hun spanning verliezen. Echter; ten gevolge van de vorming van nieuwe bindingen tussen stikkers zullen inactieve segmenten ook actief worden. In de oorspronkelijke aanname zullen deze segmenten ook spanning gaan dragen, zonder dat er een extra vervorming opgelegd is. Door de opgelegde beperking zullen deze nieuw gevormde actieve segmenten spanningsloos blijven. Naast deze verfijning, is het model ook uitgebreid zodat er rekening gehouden kan worden met verschillende typen fysische bindingen (sterk en zwak). Dit verfijnde model voorspelt een breed glad relaxatie spectrum mits de ketens veel stikkers van een type bevatten. In het geval van verschillende stikkers worden er meerdere plateaus verwacht in de dynamische moduli.

Teneinde de invloed van de verschillende relaxatie mechanismen (zoals Rouse achtige diffusie, diffusie gehinderd door topologische beperkingen of het opbreken van bindingen) op het lineair visco-elastische gedrag van Guar gum oplossingen te bepalen, is het reologische gedrag van Guar gum oplossingen onderzocht als functie van frequentie, temperatuur, polymeer concentratie en polymeer molgewicht. In het kilo-Hertz regime is Rouse gedrag waargenomen. Bij lagere frequenties zijn twee opslagmodulus plateau zones gevonden wat wijst op twee relaxatieprocessen (langzaam en snel). Een proces werkt tussen 1 en 100 Hz en veroorzaakt een zeer breed relaxatie spectrum, zelfs voor monodispers Guar. Het beschrijven van de afhankelijkheden van de polymeer concentratie en het polymeer molgewicht op de gemiddelde relaxatietijd en de nulviscositeit met behulp van machtswetten leverde ongebruikelijk hoge machtswetcofficinten op. Het tweede proces manifesteert zich onder 0.01 Hz en is nog niet eerder gerapporteerd. In dit regime is de temperatuursafhankelijkheid hoog, terwijl alle andere afhankelijkheden zeer zwak zijn. Een vergelijking van de experimentele resultaten met voorspellingen van verschillende bestaande microreologische modellen toonde aan dat hoogstens een gedeeltelijke beschrijving van de experimenteel gevonden afhankelijkheden kan worden verkregen. Naar aanleiding van deze vergelijking is er geconcludeerd dat er minimaal twee verschillende relaxatiemechanismen (naast Rouse relaxatie) een rol moeten spelen en geen van beide mechanismen klassieke reptatie is. De beste modelvoorspellingen werden verkregen

met een model wat gebaseerd was op twee verschillende fysische bindingen (sterke en zwakke).

Teneinde de belangrijkste aannames van dat model (twee typen fysische bindingen en thermodynamisch evenwicht) te testen, zijn de effecten van enzymatische modificaties (via het gebruik van alpha-D-Galactosidase) en van oplosmiddel modificaties (via het gebruik van een 8 M ureum oplossing en een 0.1 M Na2CO3 pH 10 oplossing) op de lineaire visco-elastische eigenschappen van Guar gum oplossingen onderzocht. Met behulp van enzymatische modificaties zijn verschillende fracties f (tot aan f=0.57) Galactose zijgroepen verwijderd. De dynamische moduli zijn gemeten als functie van frequentie (0.003-10 Hz) en temperatuur (283-353 K). Het verhogen van f leverde een scherpe overgang in het reologische gedrag op boven de kritische fractie fc. Deze kritische fractie bleek af te hangen van het al dan niet invriezen en ontdooien van de gemodificeerde Guar oplossing. Dit duidt erop dat er in ieder geval niet altijd sprake is van thermodynamisch evenwicht. Bij het afsplitsen van fracties kleiner dan fc bleken de veranderingen in het reologisch gedrag zeer gering te zijn. In het Hertz gebied bleken de gemiddelde relaxatie tijd en sterkte en de temperatuur afhankelijkheid nagenoeg gelijk te zijn aan de waarden voor ongemodificeerde Guar oplossingen. Ook veranderingen van de oplosmiddelkwaliteit hadden geen significante effecten tot gevolg. Daardoor konden interketen-bindingen uitgesloten worden als oorsprong voor het relaxatiegedrag bij hoge frequenties. In plaats daarvan lijkt het relaxatie proces een diffusie proces van multi-keten structuren te zijn. Boven fc werden gelen gevormd, hetgeen wil zeggen dat de opslagmodulus veel hoger werd dan de verliesmodulus en bovendien nagenoeg frequentie onafhankelijk. Het opslagmodulusplateau bij lage frequenties nam toe, terwijl de moduli bij hoge frequenties nagenoeg niet veranderden. Dit bevestigde het idee dat interketen bindingen al dan niet direct de fysieke oorzaak zijn van spanningsrelaxatie in het miliHertz gebied.

Uiteindelijk leidde dit tot het volgende microscopische beeld: Ketens vormen enkele sterke bindingen met elkaar. Door deze bindingen worden geaggregeerde structuren gevormd. Een deel van deze structuren associeert tot een primair ruimte vullend netwerk. Met de vorming van dit netwerk wordt de mesoscopische structuur ingevroren, omdat diffusie door de oplossing onmogelijk wordt. Daardoor vindt de verharding van het netwerk plaats op een oneindig lange tijdsschaal. Het langzame relaxatieproces is in dit beeld het opbreken van het netwerk, terwijl het snelle relaxatieproces de diffusie van de ingesloten geaggregeerde structuren is.

Acknowledgements

Finally after more than four years of work I am writing the last page of my thesis. But although the scientific part is already completed now, I still have to pay attention, because for some this is the most important chapter. And although I do not agree with that, it offers me the opportunity to express my appreciation to the people that contributed (in)directly to the accomplishment of this thesis.

First of all, I want to thank my daily advisors Michel Duits and Rob Jongschaap. Michel and Rob were always available for discussions and they inspired and motivated me within my PhD research. Especially Michel who got busier during those years managed to keep time free for me and my work until the completion of the thesis. I also want to express my gratitude to my promotor Jorrit Mellema, for teaching me (together with Rob and Michel) to think in a scientific way. Besides them, I am also grateful to my two other advisors Wim Agterof and Rob Vreeker who started this project and offered me the possibility to work at Unilever for several month. During the research two undergraduate students Roel Vromen and Jimmy Bakker, made important scientific contributions and also therefore it was possible to finish the research in time. Further on, the many discussions I have had with Theo Barenbrug helped me in finding the right way. Since my work was mainly experimental work, I would like to thank Egbert Altena, Gerrit Beukema and Jacob Lopulissa for their assistance and support during the experiments.

Besides all the persons who were directly involved, also many people contributed indirectly. The different office mates I have had during the years, Victor, Henny, Paul, Berend Jan and Diana provided a good working climate for me. Finally I want to thank my parents who made it possible for me to reach this level of education and my girlfriend who supported me during these years.

Roland Wientjes   Enschede, December 2000.

Curriculum vitae

The writer of this thesis was born on August 8, 1971 in Enschede in the Netherlands. In may 1990, he completed Grammar school at the Thomas a Kempis College in Zwolle. In the same year he started to study Applied Physics at the University of Twente. Within this study he fulfilled a four month practical assignment with Akzo Nobel Central Research in Arnhem, where he investigated the influence of sidechains on the rheological behavior of polymer melts. The final project of his MSc was carried out in the Rheology Group of prof.dr. J. Mellema and concerned creep behaviour of weakly aggregated colloidal suspensions.

After obtaining his MSc in 1996, he worked for two month at the Rheology Group where he developed a program for doing analytical calculations that describe the behavior of living polymers.

Before he started his PhD-research at the Rheology Group, he worked for four month at Unilever Research in Vlaardingen. There, he investigated the influence of several enzymatic modifications on the rheological behavior of biopolymer solutions. The results from this investigation were used in his PhD-work where he focused on the relationship between macroscopic rheological and microscopic molecular quantities of Guar gum solutions in order to understand the important relaxation mechanisms and the mesoscopic structures that are formed in solution.

Publications

Wolthers, W.; vandenEnde, D.; Breedveld, V.; Duits, M.H.G.; Potanin, A.A.; Wientjes, R.H.W.; Mellema, J.
Linear viscoelastic behavior of aggregated colloidal dispersions
Phys Rev E **1997**, 56, 5726-5733.

Bot, A.; Wientjes, R.H.W.; de Haas, K.H.
The transition zone for Gelatin gels as measured by high-frequency rheology
Imaging Sci J **1997**, 45, 191-196.

Wientjes, R.H.W.; Duits, M.H.G.; Jongschaap, R.J.J.; Mellema, J.
A new transient network model applied to guar gum
Progress and trends in rheology V **1998**, Steinkopff, Darmstadt, proceedings of the Fifth European Rheology Conference, 431-432.

Wientjes, R.H.W.; Jongschaap, R.J.J.; Duits, M.H.G.; Mellema, J.
A new transient network model for associative polymer networks
J Rheol **1999**, 43, 375-391.

Wientjes, R.H.W.; Duits, M.H.G.; Jongschaap, R.J.J.; Mellema, J.
Viscoelastic behaviour of modified Guar gum solutions: reptation or stickiness?
XIIth International congress on rheology **2000**, Cambridge, The British Society of Rheology, 1381-1383.

Wientjes, R.H.W.; Duits, M.H.G.; Jongschaap, R.J.J.; Mellema, J.
Linear rheology of Guar gum solutions
Macromolecules **2000**, accepted for publication.

Jongschaap, R.J.J.; Wientjes, R.H.W.; Duits, M.H.G.; Mellema, J.
A generalized transient network model for associative polymer networks
Macromolecules, accepted for publication.

Schmelter, T.; Wientjes, R.; Vreeker, R.; Klaffke, W.
Enzymatic modifications of Pectins and the impact on their rheological properties
submitted for publication.

Wientjes, J.W.P.; Bakker, R.H.W.; Duits, M.H.G.; Jongschaap, R.J.J.; Mellema, J.
The relaxation mechanisms of Guar gum solutions
submitted for publication.